UNIVERSITY OF CALIFORNIA
RIVERSIDE

Endothelial Biology/Homeostasis: The Roles of AMPK and SIRT1 in eNOS Phosphorylation and Deacetylation

A Dissertation submitted in partial satisfaction
of the requirements for the degree of

Doctor of Philosophy

in

Biomedical Sciences

by

Zhen Chen

June 2010

Dissertation Committee:
Dr. John Y-J. Shyy, Chairperson
Dr. Ameae M. Walker
Dr. David D. Lo

The Dissertation of Zhen Chen is approved:

_____

_____

_____

Committee Chairperson

University of California, Riverside

Acknowledgements

This dissertation would not have been possible without the guidance and support from my major professor, Dr. John Y-J. Shyy. I am deeply grateful for all that I have learned from the study and from work in his laboratory for the past 4 years. I am heartily thankful to Drs. Ameae M. Walker and Dr. David D. Lo for their valuable perspectives and suggestions. I am also grateful to all the colleagues I have worked with and for all the help they have given me during my PhD study.

I owe a life-time of appreciation to my parents, for their endless love and care. Special thanks to Mr. Menno Bouman for always being an understanding and supportive life partner.

The material included in Chapters 2 and 3 was originally published in *Circulation Research* (2009;104:496-505) and *Proceedings of the National Academy of Sciences (USA)* (2010;107:10268-10273). Thanks to the publishers for permission to reuse the material.

ABSTRACT OF THE DISSERTATION

Endothelial Biology/Homeostasis:
The Roles of AMPK and SIRT1 in eNOS Phosphorylation and Deacetylation

by

Zhen Chen

Doctor of Philosophy, Graduate Program in Biomedical Sciences
University of California, Riverside, June 2010
Dr. John Y-J Shyy, Chairperson

Despite significant advances in medicine, atherosclerosis and its complications remain the leading causes of morbidity and mortality in most developed countries. Endothelium, lining the first layer of blood vessels, serves as a dynamic interface in maintaining vascular homeostasis. Endothelial dysfunction is a hallmark of atherosclerosis development, signified by impaired nitric oxide (NO) bioavailability derived from endothelial nitric oxide synthase (eNOS). To investigated the molecular mechanisms by which eNOS-NO is regulated under physiological, pathophysiological and pharmacological contexts, I examined the role of two metabolic master molecules, AMP-activated protein kinase (AMPK) and sirtuin 1 (silent information regulator 2 homolog, SIRT1), in eNOS regulation and NO bioavailability.

In the first part of the study, I demonstrated that AMPK directly phosphorylates eNOS Ser-633, in addition to Ser-1177, thus leading to endothelial NO production, in response to hormonal (adiponectin), physical (shear stress), and pharmacological

(atorvastatin) stimuli. Further, I found reduced eNOS phosphorylation in aortas from mice deficient in AMPK α2 (AMPKα2$^{-/-}$), which confirms the AMPK-mediated eNOS regulation *in vivo*. In addition, with the application of nano–liquid chromatography/tandem mass spectrometry (LC/MS/MS), I provided biochemical basis for eNOS phosphorylation by AMPK. These findings suggest that AMPK phosphorylation of eNOS Ser-633 is a functional signaling event for NO bioavailability in endothelial cells (ECs).

In the second part, I focused on SIRT1, a NAD^+-dependent deacetylase, and its modulation on eNOS. First, I found that SIRT1 responds to laminar shear stress with increased protein level and activity in ECs. In parallel to the observation that SIRT1 level was significantly higher in ECs exposed to physiological pulsatile flow than pathophysiological oscillatory flow, SIRT1 level was shown to be higher in the mouse thoracic aorta exposed to athero-protective flow than in the aortic arch under athero-prone flow. Next, I revealed the functional consequences of the shear stress-enhanced level of SIRT1 in ECs, including mitochondrial biogenesis and eNOS deacetylation. Subsequently, I studied the interplay of AMPK phosphorylation and SIRT1 deacetylation on eNOS *in vitro* and *in vivo* and demonstrated that AMPK phosphorylation of eNOS primes eNOS deacetylation by SIRT1. Collectively, my study suggests that AMPK and SIRT1 could synergistically enhance eNOS-derived NO level with physiological cues such as athero-protective flow.

Table of Contents

List of Figures

List of Tables

List of Abbreviations

ACC: acetyl-CoA carboxylase

AICAR: 5'-aminoimidazole-4-carboxamide ribonucleoside

AMP: adenosine monophosphate

AMPK: AMP-activated protein kinase

Ang II: angiotensin II

ApoE: apolipoprotein E

Akt/PKB: protein kinases B

BAEC: bovine aortic endothelial cell

CA: constitutively active

CaMKKβ: Calmodulin kinase kinase beta

Cav-1: caveolin-1

cGMP: cyclic guanosine monophosphate

CR: caloric restriction

DMEM: Dulbecco modified Eagle medium

DMSO: dimethyl sulfoxide

DN: dominant negative

EC: endothelial cell

eNOS/NOS3: endothelial nitric-oxide synthase

GC: guanylate cyclase

HDAC: histone deacetylase

HEK293: human embryonic kidney 293

HMG-CoA: hydroxymethylglutaryl-CoA

Hsp90: heat shock protein 90

HUVEC: human umbilical vein endothelial cell

ICAM: intercellular adhesion molecule

IP: immunoprecipitation

KLF2: Kruppel-like factor 2

KO: knockout

LC/MS/MS: nano–liquid chromatography/tandem mass spectrometry

LDL: low-density lipoprotein

MOI: multiplicity of infection

MEF: murine embryonic fibroblast

mTOR: mammalian target of rapamycin

NAD^+/NADH: nicotinamide adenine dinucleotide (oxidized and reduced)

NAM: nicotinamide

Nampt: nicotinamide phosphoribosyltransferase

NO: nitric oxide

PECAM-1: platelet endothelial cell adhesion molecule 1

PKA: cAMP-dependent protein kinase

PKC: protein kinase C

PPARγ: peroxisome proliferator-activated receptor gamma

PGC1α: PPARg coactivator 1 alpha

RNS: reactive nitrosative species

ROS: reactive oxygen species

RSV: resveratrol

SIRT1: sirtuin 1, silent mating-type induced regulator 2 protein (Sir2p) homolog 1

VCAM: vascular cell adhesion molecule

VEGF: vascular endothelial growth factor

VEGFR: vascular endothelial growth factor receptor

VSMC: vascular smooth muscle cell

Chapter 1

Introduction

1.1 Purpose of study

Cardiovascular disease, particularly atherosclerosis, is a leading cause of morbidity and mortality in the United States and worldwide (http://www.cdc.gov/omhd/AMH/factsheets/cardio.htm#2). Research on epidemiology, prevention, and treatment of atherosclerosis and associated arterial disorders are active fields of biomedical research. Population-based studies have shown that atherosclerosis develops over decades and begins as early as childhood (Strong et al. 1992). Preceding and ongoing studies suggest that both genetic and epigenetic modifications account for the pathogenesis of atherosclerosis. Collective evidence largely supports that obesity, diabetes, stress and a sedentary lifestyle are associated with an increased risk of atherosclerosis. Hence, interventions designed to reduce these risks aim to protect the population against the condition (Grundy 2006). Despite significant progress in these aspects, the molecular basis underlying atherogenesis and proposed preventive/protective interventions remain elusive.

Atherosclerosis is a multifactorial disease that involves functional changes of multiple molecules in several cell types. Endothelial cells (ECs), forming the monolayer lining the arterial lumen, are a major regulator of vascular homeostasis. By sensing mechanical and chemical signals in the circulation, ECs play an important role in maintaining the dynamic balance between vasodilation and vasoconstriction. Nitric oxide (NO), a potent vasodilator, is a key molecule involved in endothelial functions and

has diverse vasoprotective effects. In ECs, NO is mainly produced by endothelial nitric oxide synthase (eNOS) from L-arginine, via a two-step enzymatic reaction (Palmer et al. 1988; Dawson and Snyder 1994). Endothelial dysfunction, signified by impaired NO bioavailability, may be an early marker for atherosclerosis (Davignon and Ganz 2004). Ample studies have shown that various physiological, pathological, and pharmacological stimuli induce endothelial responses, with attendant eNOS-NO modification, via multiple signaling pathways, which may in turn elicit profound consequences in the vasculature.

Among all these stimuli, fluid shear stress, the tangential component of hemodynamic forces acting on the endothelium, would be the most physiologically relevant condition to study endothelial biology (Balligand et al. 2009). *In vivo*, shear stress regulates diverse vascular events, largely through NO bioavailability (Cowan and Langille 1996). Studies of variations in shear stress in the arterial tree imply the steady and laminar flow patterns with high shear stress in the straight parts are atheroprotective, whereas the disturbed flow patterns with low shear stress in the curvatures and bifurcations are atheroprone (Gimbrone et al. 2000). Previous studies by many research groups including ours have demonstrated that ECs respond differently to athero-protective versus athero-prone flow patterns by transducing them to distinct signaling events and functional changes (Dimmeler et al. 1999; Boo et al. 2002; Zhang et al. 2006; Guo et al. 2007).

The goal of this study was to further elucidate the molecular mechanisms by which eNOS and its derived NO bioavailability are regulated in ECs. Specifically, two major aims are proposed: to study the eNOS regulation by AMP-activated protein kinase

(AMPK) and sirtuin 1 (silent mating-type induced regulator 2 homolog 1, SIRT1). Chapter 2 describes the first aim, examining the role of AMPK in eNOS regulation, in particular, phosphorylation of Ser-633 and the functional consequences of this phosphorylation. Experiments with cultured ECs and mouse models demonstrated that AMPK, activated by laminar shear stress, atorvastatin and adiponectin, could phosphorylate eNOS and result in enhanced NO production. In addition, a biochemical basis was provided for AMPK catalysis on eNOS Ser-633 and Ser-1177, two stimulatory phosphorylation sites. Chapter 3 describes the second aim, delineating the role of fluid shear stress-induced SIRT1 in regulating the enzymatic activity of eNOS. Evidence collected both *in vitro* and *in vivo* suggests that laminar or pulsatile shear stress imposed by atheroprotective flow elevated SIRT1, which in turn deacetylated eNOS. Such a modification on eNOS, primed by AMPK phosphorylation at Ser-633 and Ser-1177, leads to augmented eNOS activation. Collectively, these findings indicate that the most physiologically relevant vascular stimulus, shear stress, regulates eNOS-derived NO via a synergistic regulation by AMPK and SIRT1.

1.2 Endothelial biology, NO bioavailability, and atherosclerosis

The endothelium, formed by ECs, lines the entire circulatory system, from the heart to the smallest capillary. If the endothelium of the whole body could be collected, its total weight would be equal to that of the liver, and likely, it would be the largest endocrine organ in the human body (Higashi et al. 2009). Despite its nature as a simple squamous epithelium, the endothelium has evolved to assume highly specialized functions because of its unique localization. The foremost function of ECs is its major

contribution to maintenance of vascular tone, accomplished by the release of vasodilatory and vasoconstrictive substances. A major vasodilator released by the endothelium is NO, originally termed endothelium-derived relaxing factor (EDRF) by Furchgott (Furchgott and Zawadzki 1980). ECs also produce other endothelium-derived vasodilators, such as prostacyclin and bradykinin (Drexler 1998). As well, ECs release vasoconstrictive agents, including endothelin and angiotensin II (Ang II) to balance the vessel tone.

The normal and healthy endothelium contributes to maintenance of homeostatic vascular tone and structure. Moreover, as a major regulator of vascular biology, the endothelium also exerts diverse vasoprotective effects, including anti-inflammation as well as suppression of vascular smooth muscle cell (VSMC) proliferation and migration (Davignon and Ganz 2004; Libby et al. 2006). When this homeostasis is upset, EC-dependent vasodilatory effects, especially those mediated by NO, are compromised, whereupon the vasoconstrictive effects become dominant, which constitute the molecular components of endothelial dysfunction, a concept coined in 1983 (Catravas et al. 1983). Endothelial dysfunction then leads to imbalanced vascular tone, increased endothelial permeability, platelet aggregation, leukocyte adhesion, and release of inflammatory cytokines, all of which contribute to development of atherosclerotic lesions (Ross 1999). In fact, endothelial dysfunction, manifested by an impaired endothelium-dependent vasodilation, is one of the earliest markers of atherosclerosis, preceding clinical angiography or ultrasonography detection (Luscher and Barton 1997). Therefore, an understanding of endothelial (dys)function in vascular health and diseases has generated tremendous research interest. Accordingly, the possible mechanisms that prevent or slow

down endothelial dysfunction have rendered great promise for designing treatments for vascular disorders such as atherosclerosis.

The study of NO, the most potent endogenous vasodilator released by ECs (Lowenstein et al. 1994), is an important field in endothelial biology. Upon synthesis mainly by endothelial nitric oxide synthase (eNOS), NO diffuses into the sub-endothelial space and causes VSMC relaxation by activating guanylate cyclase (GC), thereby increasing intracellular cyclic guanosine monophosphate (cGMP). The functional outcome of this process is defined as endothelium-dependent vasodilation (Furchgott and Zawadzki 1980; Ignarro et al. 1987; Palmer et al. 1987) (Fig. 1-1), which counteracts the effects of endothelium-derived vasoconstrictors (i.e. Ang II and endothelin). Besides exerting this vasodilatory effect, NO is involved in the maintenance of healthy endothelium, including prevention of oxidative modification of low-density lipoprotein (LDL), a major mechanism of the atherosclerotic process (Rubbo et al. 2002; Steinberg 2009). NO is also required for protecting the endothelium against platelet adherence/aggregation and leukocyte adhesion/infiltration (Palmer et al. 1987; Moncada and Higgs 1993; Nathan and Xie 1994). These functions largely depend on the inhibitory effects of NO on endothelial adhesion molecules, such as vascular cell adhesion molecule-1 (VCAM-1) and intercellular adhesion molecule-1 (ICAM-1) (Khan et al. 1996), as well as on the release of pro-inflammatory chemokines, such as monocyte chemoattractant protein-1 (MCP-1) (Zeiher et al. 1995). In addition, the endothelial production of NO also inhibits VSMC migration and proliferation, in part by regulating matrix metalloproteinase (MMP) activity (Gurjar et al. 1999). Several other molecular

signaling pathways have also been proposed as underlying mechanisms, including the nuclear factor kappa B (NF-κB) (Hoshi et al. 2000; Mehrhof et al. 2005), mitogen-activated protein kinase (MAPK) (Koyama et al. 1998; Che et al. 2001), and phosphatidylinositol-3-kinase (PI3K) pathways (Duan et al. 2000).

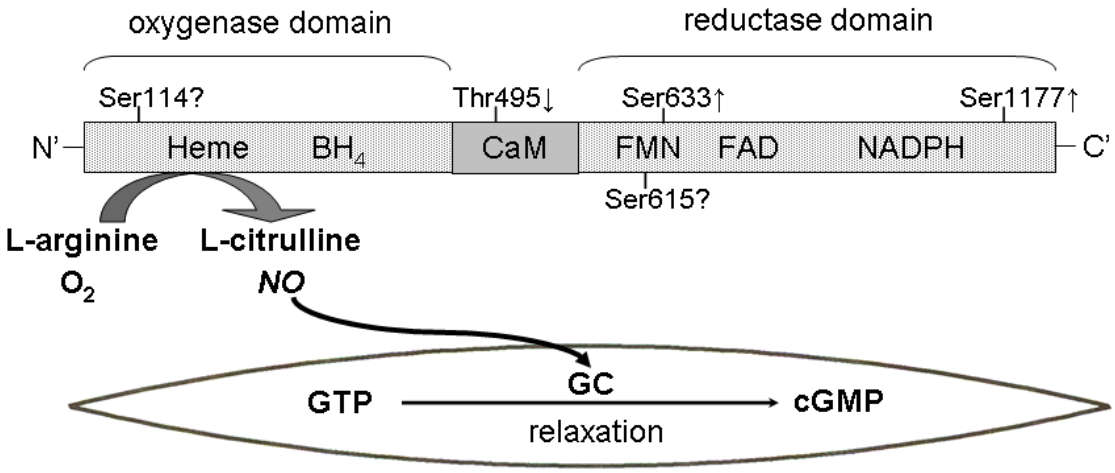

Fig. 1-1 The structure and function of eNOS. NO is produced by eNOS in ECs from L-arginine and then diffuses to VSMCs and activates GC, thereby increasing intracellular cGMP and causing vasodilation. eNOS consists of an oxygenase and a reductase domain, with an interposed CaM binding domain. A number of cofactors, including tetrahydrobiopterin (BH_4) and NADPH, are required to bind to the indicated domains and facilitate the reaction catalyzed by eNOS. Phosphorylation sites are numbered according to the human eNOS sequence. Phosphorylation of Ser-633 and/or Ser-1177 increases, whereas that of Thr-495 inhibits eNOS activity. The effects of Ser-114 and Ser-615 phosphorylation remain unclear.

Collectively, eNOS-catalyzed NO production plays a crucial role in control of vascular homeostasis. In fact, impaired eNOS-derived NO bioavailability has become a synonym for endothelial dysfunction (Yetik-Anacak and Catravas 2006). Yet without a unified definition, this impairment may be caused/signified by insufficient production and/or attenuated eNOS activity, decreased sensitivity of VSMCs to NO, and increased

degradation of NO by reaction with superoxide, all of which could result in compromised vasodilation and loss of the vasoprotection, thus initiating atherogenesis and the development of various vascular disorders (Harrison 1997; Yetik-Anacak and Catravas 2006).

Diverse physiological, pathophysiological, and pharmacological stimuli have been found to modulate endothelial NO bioavailability. Many detrimental or risk factors, (e.g., hypertension, hypercholesterolemia, smoking, insulin resistance) may cause oxidative stress and inactivate NO bioactivity, possibly through AngII and tumor necrosis factor-alpha (TNF-α) pathways (Hadi et al. 2005; Higashi et al. 2009). In contrast, a number of physiological and pharmacological stimuli have been shown to benefit endothelial NO bioavailability, among which exercise training has become one of the promising interventions. A large body of evidence from animal models and human subjects has shown that both short-term and chronic exercises induce adaptive responses in the vasculature (Delp et al. 1993; Sun et al. 1994; Koller et al. 1995; Kingwell et al. 1997; Sun et al. 1998). A major mechanism underlying such effects is augmented blood flow-associated shear-stress-mediated NO release (Chen and Li 1993; Tronc et al. 1996; Tuttle et al. 2001; Hambrecht et al. 2003).

Pharmacological treatments, such as the use of statins (a group of cholesterol-lowering HMG-CoA reductase inhibitors), have also been shown to have pleotropic effects because of their upregulation and/or activation of the eNOS-NO pathway (Laufs et al. 1998; Sun et al. 2006). Although the negative or positive outcomes of various perturbations or interventions in terms of overall vascular function have become clear,

the underlying molecular mechanisms through which the eNOS-NO axis are modified remain incompletely understood. To address the mechanisms by which NO is regulated, the abovementioned stimuli were included in this study to elicit endothelial responses and then dissect the underlying molecular mechanisms.

1.3 Hemodynamic forces, shear stress and endothelial biology

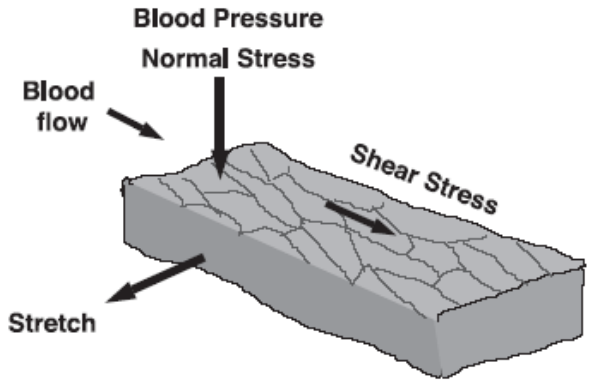

Fig. 1-2 Hemodynamic forces imposed on endothelium. Adapted from Chien 2006.

The arterial tree, consisting of large elastic and muscular vessels, arterioles, and precapillaries, is constantly exposed to hemodynamic forces with wide variation in direction, magnitude, and frequency of pulsatility. These forces include hydrostatic pressures, cyclic strains/circumferential stretch, and frictional wall shear stresses (Fig. 1-2) (Chien 2006). Lining the luminal surface of blood vessels, endothelium serves as an interface immediately exposed to these forces, and it dynamically regulates vascular homeostasis. Among various hemodynamic parameters, wall shear stress, the tangential component of hemodynamic forces resulting from blood flow (Benson et al. 1980; Malek et al. 1999), has been closely associated with the development and progression of atherosclerosis. The first evidence implicating shear stress in atherosclerosis was

described in 1969 (Caro et al. 1969), where the theory was invoked as "local shear stress, affecting local supply and removal rate may control the rate of accumulation of material constituting atheromatous lesions". Concurrently, the hypothesis that "physical exercise involving increase of cardiac output, and hence increased shear rate, might retard the development of atheroma" was also proposed 40 years ago, without much mechanistic insight into the molecular and cellular basis.

In the following decades, facilitated by more advanced approaches, from laser doppler velocimetry, intravascular ultrasound (IVUS), to magnetic resonance imaging (MRI) combined with computational fluid dynamic simulations, the association among plaque localization, flow velocity and wall shear stress was quantitatively established (Zarins et al. 1983; Ku et al. 1985; Asakura and Karino 1990; Wentzel et al. 2001; Stone et al. 2003; Cheng et al. 2005; Wentzel et al. 2005). With evidence collected by bench scientists and clinical investigators, the consensus is that atherosclerotic lesions frequently occur in regions of curvature, bifurcation, and branching of the vessels, termed "athero-prone regions", in contrast to the rare development of atherosclerosis in "athero-protected regions," the unbranched, straight segments of arteries (Cornhill and Roach 1976; Glagov et al. 1988; Nakashima et al. 1994). Related to wall shear stress, the athero-prone regions are associated with turbulent or disturbed flow patterns, signified by an unsteady, low mean shear stress, whereas the athero-protected areas are dominated by steady laminar and pulsatile flow patterns, featuring high, unidirectional mean shear stress (Davies et al. 1995; Gimbrone et al. 2000; Resnick et al. 2000). Great effort has been expended to explain these flow-dependent phenomena. Considering the strategic

location of endothelium and the critical role of ECs in maintaining vascular homeostasis, the shear stress-induced EC responses have been identified as a key underlying mechanism. Consistently, in the athero-protected areas, ECs are elongated and aligned parallel to the direction of blood flow, displaying a quiescent phenotype, whereas ECs lining the athero-prone segments are much rounder in shape, do not have a uniform orientation and feature high turnover rates and pro-inflammatory characteristics (Ando and Yamamoto 2009).

The hemodynamics of blood flow is extremely complex *in vivo* considering that the blood flow is pulsatile (because of heart beats) at any given time and the shear stress would be generated distinctively under the systolic and diastolic cycles. Also, any change in the shape or curvature of a vessel would alter the hemodynamic determinants. For example, at a curvature, blood flow velocity is greater along the outside wall than along the inside wall (Anderson et al. 1993). In addition, the chemical properties of local blood flow may vary greatly throughout the whole circulation. To formulate a simplified model, in the large arteries, blood can be considered a Newtonian fluid (a fluid whose stress at each point is linearly proportional to its strain rate at that point). The constant of proportionality is the viscosity. This is defined by the equation below:

$$\textbf{Wall shear stress } (\tau) = \mu \, (\delta \upsilon / \delta r)$$

where υ is the velocity along the vessel axis, and r is the distance perpendicular to and away from the wall (Brands et al. 1995; Oyre et al. 1998). Hence, the wall shear stress (τ) is linearly correlated to the velocity gradient, and can be deduced by:

$$\textbf{Wall shear stress } (\tau) = 4\mu Q / \pi r^3$$

where μ is the viscosity, Q is the flow rate and r is the vessel radius (Cunningham and Gotlieb 2005). Typically, wall shear stresses of large conduit arteries range between 5 and 20 dyn/cm^2 (Gotlieb 2001).

To assess the effects of different flow patterns on endothelial biology and to further elucidate the underlying mechanisms, several *in vitro* flow systems have been established. Of note, because of the focus of this study, the flow systems introduced herein aim to mimic shear stress, rather than other hemodynamic forces such as cyclic strain/stretch. The greatest advantage of the *in vitro* flow systems is precisely controlled shear stress parameters and EC culture conditions. The two most commonly used *in vitro* systems are a cone-plate apparatus and a parallel-plate flow channel system. The cone-plate apparatus was first introduced by Bussolari and Dewey (Bussolari et al. 1982), followed by several modifications, which are described elsewhere (Ohno et al. 1993). The major disadvantage of this device is the small scale of experiments, which generate a limited amount of sample each time. Recently, a rocking "see-saw" system was developed with the advantages of easy operation, low cost, and high throughput. Unfortunately, the spatiotemporal pattern of shear stress in the system has not been thoroughly quantified (Zhou et al. 2009). Therefore, the use of such a system in a shear stress study needs to be further justified. In this study, a well-established, parallel-plate flow channel system was used (as shown in Fig. 1-3).

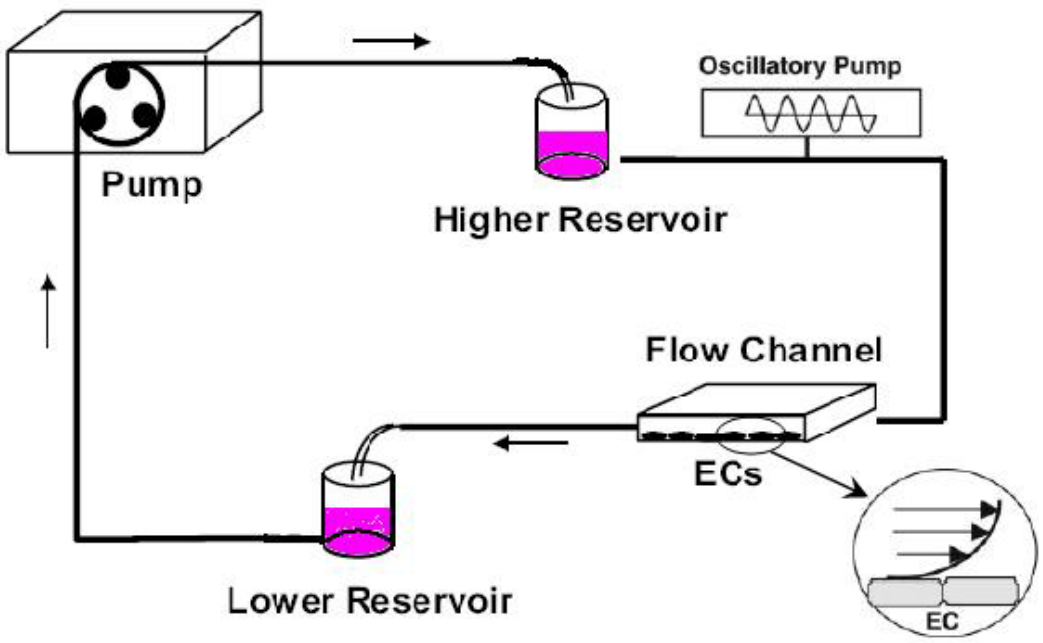

Fig. 1-3 Side view of the parallel-plate flow channel system. The flow condition can be either steady without oscillations (generating laminar shear stress) or superimposed with sinusoidal oscillation by using the oscillatory pump (generating pulsatile or oscillatory shear stress). Round inset shows an enlarged view of two ECs and the velocity gradient due to the applied shear stress. Adapted from Chien 2007 and Zhang 2006.

This system is composed of a glass slide, a silicone gasket, and an acrylic plate chamber. A confluent monolayer of ECs is seeded onto the glass slide, and the flow channel space is created by sandwiching the gasket between the ECs and the chamber base. This assembly is then connected to a high reservoir, a low reservoir, and a peristaltic pump, thus mimicking circulation (Fig. 1-3). The magnitude of applied shear stress (τ) in such a flow system is governed by:

$$\tau = 6\eta Q/(h^2 w)$$

where η is the viscosity of perfusing media, h and w represent the height and width of the channel space, respectively, and Q is the flow rate, which is determined by the height difference between the high and low reservoirs (Frangos et al. 1985). The flow pattern generated by this setup is defined as laminar flow (with steady, laminar shear stress), which has been used as the most simplified flow pattern *in vitro* to assess the effects of atheroprotective flow in endothelial biology. In the studies documented in this dissertation, laminar flow was applied to different types of cells at 3 dyn/cm^2 for 6-hr pre-exposure, followed by a step increase to a magnitude of 12 dyn/cm^2 for various times (Fig. 1-4A). During the flow experiments, the medium was maintained at 37°C and equilibrated with 5% CO_2-95% air.

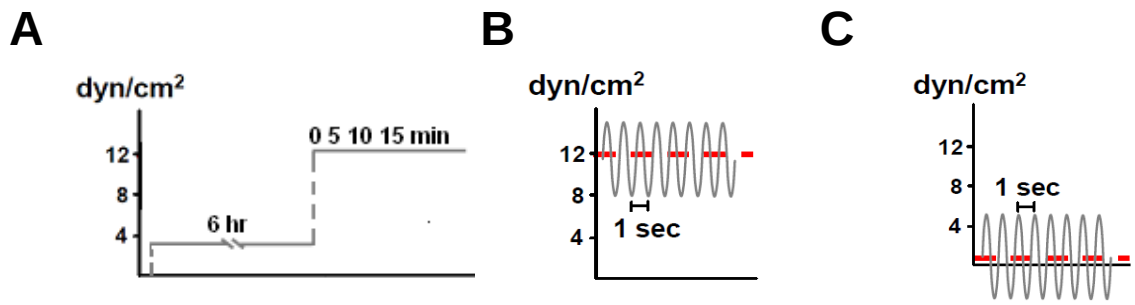

Fig. 1-4 Different flow patterns applied using the flow channel system. (A) Steady laminar shear stress. (B) Pulsatile shear stress. (C) Oscillatory shear stress. (Courtesy of Dr. John Shyy)

To mimic more physiological conditions *in vitro*, pulsatile flow or oscillatory flow can be generated with the flow channel system described above (Fig. 1-4 B,C). The distinctive features between these two flow patterns are that the pulsatile flow generates a uni-directional, high mean shear stress, whereas the oscillatory flow creates a bi-directional, low mean shear stress. These exemplify the flow patterns in the athero-

protected and athero-prone regions, respectively, in the vasculature (Chien 2007). Experimentally, a reciprocating syringe pump is connected to the circulating system as depicted in Fig. 1-3 to introduce a sinusoidal component with a frequency of 1 Hz (mimicking the pulse in the human body) onto the laminar shear stress, and the magnitude of oscillation can also be precisely controlled by adjusting the pump setup. In the studies presented in Chapter 3, pulsatile shear flow or oscillatory shear flow was applied to ECs with a shear stress of 12 ± 4 dyn/cm^2 or 1 ± 4 dyn/cm^2, respectively.

It is worthwhile to discuss here how these *in vitro* flow conditions were selected and tested during the last decades to reflect the *in vivo* athero-protective or athero-prone environments. This development can be traced back to early studies defining the shear stress parameters in carotid arteries. In 1985, Ku et al. associated the magnitude of shear stress with intimal thickening, a marker of atherogenesis. In the inner wall of the human internal carotid sinus, where the intimal thickening is minimal, the mean shear stress was approximately 17 dyn/cm^2 and unidirectional. On the opposite side, in the outer wall of the carotid sinus, where the intimal plaques were thickest, the mean shear stress is as low as 0.5 dynes/cm^2, with an oscillation between -7 and +4 dyn/cm^2 (Ku et al. 1985).

From the *in vivo* data, pioneering research attempting to mimic (patho)physiological shear stress on ECs *in vitro* was initiated by applying a series of flow conditions to elicit endothelial responses, which were then associated with the cellular phenotypes observed in the athero-protective and athero-prone regions *in vivo*. For example, in one of these studies, ECs were exposed to 1.0, 2.0, 3.8, 7.6 and 14.8 dyn/cm^2 shear stress generated by the flow channel system, and the detachment of

leukocytes from ECs was monitored as the readout. A rate of 7.6 dyn/cm^2 was shown to be sufficient to cause leukocyte detachment (Gallik et al. 1989). In a similar manner, various endothelial functions, including cell morphology, proliferation, apoptosis, and angiogenesis, were examined in response to flow conditions (Cunningham and Gotlieb 2005; Chien 2008). More recently, alterations associated with distinctive flow patterns have been characterized at the molecular level. Steady laminar or pulsatile flow with a mean shear stress of 12 dyn/cm^2 downregulated genes involved in endothelial proliferation and inflammation (e.g., Ras, MAPKs and MCP-1) but upregulated those involved in EC survival and angiogenesis (e.g., Tie2 and Flk-1). In contrast, an oscillatory flow pattern (i.e., shear stress of 0.5 or 1 ± 4 dyn/cm^2) has been shown to exert opposite effects on the expression of these genes (summarized in Chien 2008). Importantly, these molecular and cellular characteristics have been found associated with the *in vivo* athero-protected areas (e.g., straight part of the aorta) and athero-prone areas (e.g., the inner curvature of the aortic arch) (Chatzizisis et al. 2007; Dancu and Tarbell 2007).

With these currently applied flow parameters well characterized, a remaining question is whether a definitive threshold of magnitude of shear stress distinguishes "athero-protective" and "athero-prone" flows. Several studies have been conducted to define this threshold, but the answer remains undetermined. A threshold value of steady shear stress around 5 to 6 dyn/cm^2 was defined: endothelin was downregulated below the value and upregulated above the value (Malek and Izumo 1992; Kuchan and Frangos 1993). A later study suggested a threshold of 3 to 6 dyn/cm^2, below which bovine aortic

ECs (BAECs) elongate and align (Zhao et al. 1995), whereas a shear stress of 4 dyne/cm^2 was not sufficient to induce eNOS expression as compared with static conditions (Ranjan et al. 1995). Part of the hindrance in defining a universal threshold to demarcate the "good" and "bad" flow is because of variations in EC responsiveness from different sources. Because of individual variations in human umbilical vein ECs (HUVECs) from donors, BAECs, the other typically used cell model in EC study, might respond to shear stress with subtle, if not large, differences. Another difficulty is that individual studies usually focus on one molecular or cellular response in ECs exposed to flow. Even if a threshold could be defined for a specific modulation, this condition may not be applicable to the regulation of other molecules or cellular functions. After all, the experimental conditions used to study shear stress-induced endothelial responses have been selected to represent those in a typical athero-protected or athero-prone region in the aortic tree and have been tested to elicit athero-protective or athero-prone effects accordingly.

In ECs, a panel of mechano-sensors has been identified to mediate the shear stress-induced EC responses. Many of these sensors are membrane proteins such as receptor tyrosine kinase (e.g., the vascular endothelial growth factor receptor (VEGFR or Flk-1) (Chen et al. 1999; Wang et al. 2002), the integrins (Jalali et al. 2001; Schwartz 2001; Liu et al. 2002), G proteins and G protein-coupled receptors (Olesen et al. 1988; Traub et al. 1999) and Ca^{2+} channel (Yamamoto et al. 2006). Intercellular junction proteins, including platelet endothelial cell adhesion molecule (PECAM) 1, vascular endothelial cell cadherin (VE-cadherin) and VEGFR 2, have also been shown to transduce the shear stress-triggered signals by comprising a mechanosensory complex

(Tzima et al. 2005). More recently, Nauli et al. proposed that primary cilia, the mechanosensory organelles located on the endothelial apical membrane, may play a crucial role in sensing and transducing extracellular fluid shear stress into intracellular signaling and biochemical responses. Such mechanosensory function of cilia depends on two key components: polaris molecule and polycystin-1 protein (Nauli et al. 2008; Poelmann et al. 2008). In addition, membrane lipids and membrane glycocalyx have been shown to participate in this mechanosensing process (Butler et al. 2002; Weinbaum et al. 2003). However, how these mechanosensors are connected to the intracellular pathways remains unclear.

1.4 Multi-level regulation of eNOS

Two decades ago, ECs were found to express a cytosolic enzyme that is Ca^{2+} activated, converts L-arginine into a compound that stimulates soluble GC and acts as an endothelial-derived relaxing factor (Mayer et al. 1989). This enzyme was isolated and defined as eNOS, or NOS3 (Pollock et al. 1991) and the vasorelaxing compound was found to be NO. eNOS is encoded by the *NOS3* gene, and its expression is subjected to transcriptional and post-transcriptional regulation. At the mRNA level, eNOS can be induced by stimuli such as shear stress and atorvastatin, largely through the transcription factor Kruppel-like factor 2 (KLF2) (SenBanerjee et al. 2004; van Thienen et al. 2006). Emerging evidence suggests that eNOS mRNA stability may also be regulated through microRNA (Suarez et al. 2007; Yin et al. 2009). At the post-translational level, eNOS is regulated by a complex but highly coordinated network, including phosphorylation,

(de)acetylation and subcellular localization, all of which directly or indirectly affect its enzymatic activity, that is, NO production.

Structurally, eNOS consists of an oxygenase domain and a reductase domain, interposed by a Ca^{2+}/calmodulin (CaM) binding domain. Since the original model showing that eNOS activation depends on CaM binding, a tightly regulated multi-site phosphorylation has been identified. There are 5 known eNOS Ser/Thr phosphorylation sites: two stimulatory sites, Ser-1177 and Ser-633; one inhibitory site, Thr-495; and two other sites, Ser-114 and Ser-615, the function of which are still controversial (Mount et al. 2007). The two positive regulatory sites, Ser-1177 and Ser-633, reside in two autoinhibitory sequences of eNOS, one in the reductase domain close to the carboxy-terminus and the other in the flavin monomucleotide (FMN) binding domain (Michell et al. 2002; Bauer et al. 2003) (illustrated in Fig. 1-1).

The phosphorylation of Ser-1177 may be required for the initial activation of eNOS by Ca^{2+} flux, followed by Ser-633 phosphorylation, which appears to be important for sustained NO production (Boo et al. 2003). Gain- or loss-of function mutants, namely, Ser mutated to Asp or Ala, have been used to investigate the role of specific sites in eNOS regulation. The S1177A mutant, preventing Ser-1177 phosphorylation, was found to reduce both basal and stimulated NO production, whereas the S1177D mutant, mimicking Ser-1177 phosphorylation, increased eNOS activity (Michell et al. 2002; Bauer et al. 2003). A similar approach revealed S633D eNOS to be the most efficacious phospho-mimetic mutant, yielding a 5-fold increase in basal and a 2-fold increase in stimulated NO release from transfected cells (Bauer et al. 2003).

A diverse list of activators, including mechanical, humoral, metabolic and pharmacological stimuli, have been identified to modify eNOS Ser-1177 and Ser-633 phosphorylation and hence NO production, via a panel of protein kinases. One example is fluid shear stress, which has been shown to cause eNOS phosphorylation at Ser-1177 through multiple protein kinases, including protein kinase A (PKA), protein kinase B (Akt), and AMPK (Dimmeler et al. 1999; Boo et al. 2002a; Zhang et al. 2006). Shear stress was also reported to increase Ser-633 phosphorylation via PKA (Boo et al. 2002b). Other stimulators that enhance eNOS activity through phosphorylation include statins and adiponectin, which are also used in this study, as described in Chapter 2.

Recently, eNOS deacetylation has emerged to be an important modification that modulates eNOS activity. Mattagajasingh demonstrated first that caloric restriction (CR) may have salutary effects on endothelial function, in part through SIRT1-induced deacetylation of eNOS (Mattagajasingh et al. 2007). This dissertation aimed to define the major and novel pathways that mediate the beneficial effects of various stimuli that are of physiological or therapeutic significance, in particular, in regulating eNOS phosphorylation and deacetylation.

1.5 AMPK, an energy sensor in vascular biology

Since the identification of AMPK more than 20 years ago (Carling et al. 1987), mounting evidence indicates that AMPK functions as a "metabolic switch" or "fuel gauge" that senses and regulates the balance of cellular energy (Kahn et al. 2005). In principle, AMPK is activated by cellular energy deficit; for example, an increase in the AMP/ATP ratio (Hardie and Carling 1997) is commonly observed in fasting, CR, and

exercise. AMPK can also be activated by changes in the intracellular level of Ca^{2+}, which is independent of elevated AMP/ATP ratio (Woods et al. 2005). To date, LKB1 (encoded by the Peutz-Jegher tumor-suppressor gene) and CaM kinase kinase β (CaMKKβ) have been identified to be two major upstream AMPK kinases (AMPKKs). Both enzymes phosphorylate AMPKα, the catalytic subunit at Thr172, which leads to its activation (Hawley et al. 2003; Hawley et al. 2005).

Upon activation, AMPK switches on energy-producing and catabolic processes such as glycolysis, glycogen breakdown, and fatty acid oxidation, while tuning down ATP-consuming and anabolic events, such as gluconeogenesis and fatty acid and protein synthesis, to restore the energy balance (Hardie 2008). A paradigm exemplifying how AMPK, by sensing cellular energy status, regulates both catabolic and anabolic pathways to govern the whole-body energy metabolism, is its master control on acetyl-CoA carboxylase (ACC), the rate-limiting enzyme in fatty acid synthesis. Activated by energy deficit (e.g., under starvation or exercise), AMPK phosphorylates ACC at Ser-79 and inhibits its catalytic activity. Such an inhibition decreases the formation of malonyl-CoA, the product of ACC-catalyzed reaction and the building block for fatty acid synthesis (Ha et al. 1994). Instead, the reduced level of malonyl-CoA leads to an activation of carnitine-palmitoyl transferase I (CPT-I), which in turn promotes fatty acid breakdown to restore energy balance (McGarry et al. 1978).

The AMPK substrates, rapidly expanding in number, mediate the regulatory effects of AMPK in diverse metabolic pathways in multiple tissues/organs. In the skeletal muscle and the heart, AMPK phosphorylates glucose transporter GLUT4, which

results in increased GLUT4 translocation and increased glucose uptake (Hayashi et al. 1998; Russell et al. 1999). AMPK has also been found to phosphorylate insulin receptor substrate 1 (IRS-1), thus contributing to insulin sensitivity (Jakobsen et al. 2001). In the liver, AMPK has been shown to phosphorylate transcription factor hepatic nuclear factor 4α (HNF-4α), and hence downregulate gluconeogenic gene expression, thus leading to decreased hepatic glucose output (Leclerc et al. 2001). Other than controlling carbohydrate metabolism, AMPK is also pivotal in lipid metabolism by its modification of hormone-sensitive lipase (HSL), ACC, HMG-CoA reductase (HMGR), and in protein synthesis, dependent on its activation of the eukaryotic elongation factor 2 kinase (eEF2K) and inhibition of the mammalian target of rapamycin (mTOR)-signaling pathway (Browne et al. 2004; Gwinn et al. 2008). Notably, AMPK has been proposed to have an integrative role as a regulator of whole-body energy metabolism because of its modulation in the brain. This notion is supported by the effect of adiponectin, an adipocyte-secreted hormone, in activation of AMPK in the hypothalamus, which causes an increase in food intake (Andersson et al. 2004; Kubota et al. 2007). However, the biochemical basis underlying how hypothalamic AMPK controls appetite is currently unclear. Based on this large body of findings, targeting AMPK has become a promising therapeutic strategy to treat metabolic disorders. For example, metformin, the most widely prescribed anti-diabetic drug in the world has been shown to exert its beneficial effects through its activation of AMPK (Zhou et al. 2001; Towler and Hardie 2007).

In addition to tissues involved in metabolism, AMPK also affects cardiovascular functions. AICAR (aminoimidazole carboxamide ribonucleotide), an AMPK-specific

activator, has been shown to stimulate eNOS Ser-1177 phosphorylation in human aortic ECs (Morrow et al. 2003). Several groups demonstrated that AMPK mediates eNOS activation in ECs responding to adiponectin, thrombin, and histamine (Chen et al. 2003; Ouchi et al. 2004; Thors et al. 2004). The studies carried out in our lab have shown that laminar shear stress can activate AMPK, thus leading to increased eNOS activity and NO bioavailability (Zhang et al. 2006; Young et al. 2009). Furthermore, several widely used pharmacological agents, including statins (known to attenuate hypercholesterolemia) and metformin, have been shown to activate AMPK-eNOS signaling in ECs (Davis et al. 2006; Sun et al. 2006). Considering the critical role of AMPK in EC biology, I hypothesized that AMPK may phosphorylate eNOS in response to shear stress. This hypothesis was tested in the first project of this dissertation. The experimental approaches and results are presented in Chapter 2.

1.6 SIRT1 and the interplay with AMPK

SIRT1, a member of the sirtuin family, is classified as the class III histone deacetylase (HDACs). SIRT1 received its name for its homology with the yeast silent information regulator 2 protein (Sir2p), which mediates CR-induced lifespan-extension in yeast. In mammalian cells, SIRT1 was first identified as a histone deacetylase (Imai et al. 2000). The number of other non-histone targets of SIRT1 has increased rapidly, thus revealing its importance in diverse pathways and functions. To name a few functions, SIRT1 deacetylates multiple Lys residues of tumor suppressor p53, consequently inhibiting its transactivation activity and suppressing apoptosis in response to oxidative stress and DNA damage (Luo et al. 2001; Vaziri et al. 2001). SIRT1 can also deacetylate

forkhead O transcription factors (FOXOs) to induce cell-cycle arrest and stress resistance (Brunet et al. 2004; Motta et al. 2004). Besides these nuclear modifications, SIRT1 is present in the cytoplasm, where it deacetylates acetyl CoA synthetase 2 (AceCS2), which is involved in metabolic controls (Hallows et al. 2006).

Studies of mouse models have characterized a prominent role of SIRT1 in mediating the benefits of CR in multiple tissues, and its overall anti-aging effects (Lagouge et al. 2006; Boily et al. 2008). One of the most relevant targets involving SIRT1 is perhaps peroxisome proliferator-activated receptor γ (PPARγ) coactivator 1 α (PGC1α), the master regulator of mitochondrial biogenesis. PGC1α is activated by SIRT1 deacetylation, which leads to enhanced mitochondrial biogenesis in adipose tissues and skeletal muscles. This molecular event is correlated with exercise tolerance and thermogenesis and protection against the onset of obesity and associated metabolic dysfunction (Nemoto et al. 2005; Rodgers et al. 2005; Rodgers et al. 2008).

Recently, Canto et al showed a convergent action of AMPK and SIRT1 on PGC1α. The authors demonstrated that AMPK phosphorylation of PGC1α primes the subsequent PGC1α deacetylation by SIRT1 (Canto et al. 2009). In line with the requirement of NAD^+ for its deacetylase activity, SIRT1 is activated by an increased cellular NAD^+/NADH ratio. By sensing the change of NAD^+/NADH, SIRT1 is another cellular energy indicator involved in the stress response and energy homeostasis. Indeed, several stimuli such as CR and exercise that activate AMPK also enhance SIRT1 activity (Canto and Auwerx 2009).

The protective role of SIRT1 has also been demonstrated in vascular biology. Ota et al. showed that SIRT1 in ECs is sufficient and necessary to prevent oxidative stress-induced endothelial senescence (Ota et al. 2007). Mattagajasingh et al. demonstrated that loss of SIRT1 activity in rat arteries impaired endothelium-dependent vasodilation (Mattagajasingh et al. 2007). By overexpressing SIRT1 in ECs, Zhang et al. observed decreased atherosclerosis in $ApoE^{-/-}$ mice (Zhang et al. 2008). As well, Miyazaki et al. found that SIRT1 activation suppressed Ang II type 1 receptor expression in VSMCs, which blunted Ang II-induced hypertension (Miyazaki et al. 2008). In this dissertation, I explored the effects of shear stress in regulating SIRT1 and examined the functional consequences of such a regulation. Because shear stress can elevate both AMPK and SIRT1, I further tested their role in the synergistic regulation of the eNOS-NO axis. The details of the experimental approaches and results are described in Chapter 3.

1.6 References

Anderson, HV, RL Kirkeeide, Y Stuart, RW Smalling, J Heibig and JT Willerson (1993). "Coronary artery flow monitoring following coronary interventions." Am J Cardiol **71**(14): 62D-69D.

Andersson, U, K Filipsson, CR Abbott, A Woods, K Smith, SR Bloom, et al. (2004). "AMP-activated protein kinase plays a role in the control of food intake." J Biol Chem **279**(13): 12005-8.

Ando, J and K Yamamoto (2009). "Vascular mechanobiology: endothelial cell responses to fluid shear stress." Circ J **73**(11): 1983-92.

Asakura, T and T Karino (1990). "Flow patterns and spatial distribution of atherosclerotic lesions in human coronary arteries." Circ Res **66**(4): 1045-66.

Balligand, JL, O Feron and C Dessy (2009). "eNOS activation by physical forces: from short-term regulation of contraction to chronic remodeling of cardiovascular tissues." Physiol Rev **89**(2): 481-534.

Bauer, PM, D Fulton, YC Boo, GP Sorescu, BE Kemp, H Jo, et al. (2003). "Compensatory phosphorylation and protein-protein interactions revealed by loss of function and gain of function mutants of multiple serine phosphorylation sites in endothelial nitric-oxide synthase." J Biol Chem **278**(17): 14841-9.

Benson, TJ, RM Nerem and TJ Pedley (1980). "Assessment of wall shear stress in arteries, applied to the coronary circulation." Cardiovasc Res **14**(10): 568-76.

Boily, G, EL Seifert, L Bevilacqua, XH He, G Sabourin, C Estey, et al. (2008). "SirT1 regulates energy metabolism and response to caloric restriction in mice." PLoS One **3**(3): e1759.

Boo, YC, J Hwang, M Sykes, BJ Michell, BE Kemp, H Lum, et al. (2002). "Shear stress stimulates phosphorylation of eNOS at Ser(635) by a protein kinase A-dependent mechanism." Am J Physiol Heart Circ Physiol **283**(5): H1819-28.

Boo, YC, G Sorescu, N Boyd, I Shiojima, K Walsh, J Du, et al. (2002). "Shear stress stimulates phosphorylation of endothelial nitric-oxide synthase at Ser1179 by Akt-independent mechanisms: role of protein kinase A." J Biol Chem **277**(5): 3388-96.

Boo, YC, GP Sorescu, PM Bauer, D Fulton, BE Kemp, DG Harrison, et al. (2003). "Endothelial NO synthase phosphorylated at SER635 produces NO without requiring intracellular calcium increase." Free Radic Biol Med **35**(7): 729-41.

Brands, PJ, AP Hoeks, L Hofstra and RS Reneman (1995). "A noninvasive method to estimate wall shear rate using ultrasound." Ultrasound Med Biol **21**(2): 171-85.

Browne, GJ, SG Finn and CG Proud (2004). "Stimulation of the AMP-activated protein kinase leads to activation of eukaryotic elongation factor 2 kinase and to its phosphorylation at a novel site, serine 398." J Biol Chem **279**(13): 12220-31.

Brunet, A, LB Sweeney, JF Sturgill, KF Chua, PL Greer, Y Lin, et al. (2004). "Stress-dependent regulation of FOXO transcription factors by the SIRT1 deacetylase." Science **303**(5666): 2011-5.

Bussolari, SR, CF Dewey, Jr. and MA Gimbrone, Jr. (1982). "Apparatus for subjecting living cells to fluid shear stress." Rev Sci Instrum **53**(12): 1851-4.

Butler, PJ, TC Tsou, JY Li, S Usami and S Chien (2002). "Rate sensitivity of shear-induced changes in the lateral diffusion of endothelial cell membrane lipids: a role for membrane perturbation in shear-induced MAPK activation." FASEB J **16**(2): 216-8.

Canto, C and J Auwerx (2009). "PGC-1alpha, SIRT1 and AMPK, an energy sensing network that controls energy expenditure." Curr Opin Lipidol **20**(2): 98-105.

Canto, C, Z Gerhart-Hines, JN Feige, M Lagouge, L Noriega, JC Milne, et al. (2009). "AMPK regulates energy expenditure by modulating NAD+ metabolism and SIRT1 activity." Nature **458**(7241): 1056-60.

Carling, D, VA Zammit and DG Hardie (1987). "A common bicyclic protein kinase cascade inactivates the regulatory enzymes of fatty acid and cholesterol biosynthesis." FEBS Lett **223**(2): 217-22.

Caro, CG, JM Fitz-Gerald and RC Schroter (1969). "Arterial wall shear and distribution of early atheroma in man." Nature **223**(5211): 1159-60.

Catravas, JD, JS Lazo, KJ Dobuler, LR Mills and CN Gillis (1983). "Pulmonary endothelial dysfunction in the presence or absence of interstitial injury induced by intratracheally injected bleomycin in rabbits." Am Rev Respir Dis **128**(4): 740-6.

Chatzizisis, YS, AU Coskun, M Jonas, ER Edelman, CL Feldman and PH Stone (2007). "Role of endothelial shear stress in the natural history of coronary atherosclerosis and vascular remodeling: molecular, cellular, and vascular behavior." J Am Coll Cardiol **49**(25): 2379-93.

Che, W, J Abe, M Yoshizumi, Q Huang, M Glassman, S Ohta, et al. (2001). "p160 Bcr mediates platelet-derived growth factor activation of extracellular signal-regulated kinase in vascular smooth muscle cells." Circulation **104**(12): 1399-406.

Chen, H, M Montagnani, T Funahashi, I Shimomura and MJ Quon (2003). "Adiponectin stimulates production of nitric oxide in vascular endothelial cells." J Biol Chem **278**(45): 45021-6.

Chen, HI and HT Li (1993). "Physical conditioning can modulate endothelium-dependent vasorelaxation in rabbits." Arterioscler Thromb **13**(6): 852-6.

Chen, KD, YS Li, M Kim, S Li, S Yuan, S Chien, et al. (1999). "Mechanotransduction in response to shear stress. Roles of receptor tyrosine kinases, integrins, and Shc." J Biol Chem **274**(26): 18393-400.

Cheng, C, R van Haperen, M de Waard, LC van Damme, D Tempel, L Hanemaaijer, et al. (2005). "Shear stress affects the intracellular distribution of eNOS: direct demonstration by a novel in vivo technique." Blood **106**(12): 3691-8.

Chien, S (2006). "Molecular basis of rheological modulation of endothelial functions: importance of stress direction." Biorheology **43**(2): 95-116.

Chien, S (2007). "Mechanotransduction and endothelial cell homeostasis: the wisdom of the cell." Am J Physiol Heart Circ Physiol **292**(3): H1209-24.

Chien, S (2008). "Effects of disturbed flow on endothelial cells." Ann Biomed Eng **36**(4): 554-62.

Cornhill, JF and MR Roach (1976). "A quantitative study of the localization of atherosclerotic lesions in the rabbit aorta." Atherosclerosis **23**(3): 489-501.

Cowan, DB and BL Langille (1996). "Cellular and molecular biology of vascular remodeling." Curr Opin Lipidol **7**(2): 94-100.

Cunningham, KS and AI Gotlieb (2005). "The role of shear stress in the pathogenesis of atherosclerosis." Lab Invest **85**(1): 9-23.

Dancu, MB and JM Tarbell (2007). "Coronary endothelium expresses a pathologic gene pattern compared to aortic endothelium: correlation of asynchronous hemodynamics and pathology in vivo." Atherosclerosis **192**(1): 9-14.

Davies, PF, T Mundel and KA Barbee (1995). "A mechanism for heterogeneous endothelial responses to flow in vivo and in vitro." J Biomech **28**(12): 1553-60.

Davignon, J and P Ganz (2004). "Role of endothelial dysfunction in atherosclerosis." Circulation **109**(23 Suppl 1): III27-32.

Davis, BJ, Z Xie, B Viollet and MH Zou (2006). "Activation of the AMP-activated kinase by antidiabetes drug metformin stimulates nitric oxide synthesis in vivo by promoting the association of heat shock protein 90 and endothelial nitric oxide synthase." Diabetes **55**(2): 496-505.

Dawson, TM and SH Snyder (1994). "Gases as biological messengers: nitric oxide and carbon monoxide in the brain." J Neurosci **14**(9): 5147-59.

Delp, MD, RM McAllister and MH Laughlin (1993). "Exercise training alters endothelium-dependent vasoreactivity of rat abdominal aorta." J Appl Physiol **75**(3): 1354-63.

Dimmeler, S, I Fleming, B Fisslthaler, C Hermann, R Busse and AM Zeiher (1999). "Activation of nitric oxide synthase in endothelial cells by Akt-dependent phosphorylation." Nature **399**(6736): 601-5.

Drexler, H (1998). "Factors involved in the maintenance of endothelial function." Am J Cardiol **82**(10A): 3S-4S.

Duan, C, JR Bauchat and T Hsieh (2000). "Phosphatidylinositol 3-kinase is required for insulin-like growth factor-I-induced vascular smooth muscle cell proliferation and migration." Circ Res **86**(1): 15-23.

Frangos, JA, SG Eskin, LV McIntire and CL Ives (1985). "Flow effects on prostacyclin production by cultured human endothelial cells." Science **227**(4693): 1477-9.

Furchgott, RF and JV Zawadzki (1980). "The obligatory role of endothelial cells in the relaxation of arterial smooth muscle by acetylcholine." Nature **288**(5789): 373-6.

Gallik, S, S Usami, KM Jan and S Chien (1989). "Shear stress-induced detachment of human polymorphonuclear leukocytes from endothelial cell monolayers." Biorheology **26**(4): 823-34.

Gimbrone, MA, Jr., JN Topper, T Nagel, KR Anderson and G Garcia-Cardena (2000). "Endothelial dysfunction, hemodynamic forces, and atherogenesis." Ann N Y Acad Sci **902**: 230-9; discussion 239-40.

Glagov, S, C Zarins, DP Giddens and DN Ku (1988). "Hemodynamics and atherosclerosis. Insights and perspectives gained from studies of human arteries." Arch Pathol Lab Med **112**(10): 1018-31.

Gotlieb, S, Ed. (2001). *Cardiovascular Pathology*. New York, NY. Churchill-Livingstone

Grundy, SM (2006). "Drug therapy of the metabolic syndrome: minimizing the emerging crisis in polypharmacy." Nat Rev Drug Discov **5**(4): 295-309.

Guo, D, S Chien and JY Shyy (2007). "Regulation of endothelial cell cycle by laminar versus oscillatory flow: distinct modes of interactions of AMP-activated protein kinase and Akt pathways." Circ Res **100**(4): 564-71.

Gurjar, MV, RV Sharma and RC Bhalla (1999). "eNOS gene transfer inhibits smooth muscle cell migration and MMP-2 and MMP-9 activity." Arterioscler Thromb Vasc Biol **19**(12): 2871-7.

Gwinn, DM, DB Shackelford, DF Egan, MM Mihaylova, A Mery, DS Vasquez, et al. (2008). "AMPK phosphorylation of raptor mediates a metabolic checkpoint." Mol Cell **30**(2): 214-26.

Ha, J, S Daniel, SS Broyles and KH Kim (1994). "Critical phosphorylation sites for acetyl-CoA carboxylase activity." J Biol Chem **269**(35): 22162-8.

Hadi, HA, CS Carr and J Al Suwaidi (2005). "Endothelial dysfunction: cardiovascular risk factors, therapy, and outcome." Vasc Health Risk Manag **1**(3): 183-98.

Hallows, WC, S Lee and JM Denu (2006). "Sirtuins deacetylate and activate mammalian acetyl-CoA synthetases." Proc Natl Acad Sci U S A **103**(27): 10230-5.

Hambrecht, R, V Adams, S Erbs, A Linke, N Krankel, Y Shu, et al. (2003). "Regular physical activity improves endothelial function in patients with coronary artery disease by increasing phosphorylation of endothelial nitric oxide synthase." Circulation **107**(25): 3152-8.

Hardie, DG (2008). "Role of AMP-activated protein kinase in the metabolic syndrome and in heart disease." FEBS Lett **582**(1): 81-9.

Hardie, DG and D Carling (1997). "The AMP-activated protein kinase--fuel gauge of the mammalian cell?" Eur J Biochem **246**(2): 259-73.

Hawley, SA, J Boudeau, JL Reid, KJ Mustard, L Udd, TP Makela, et al. (2003). "Complexes between the LKB1 tumor suppressor, STRAD alpha/beta and MO25 alpha/beta are upstream kinases in the AMP-activated protein kinase cascade." J Biol **2**(4): 28.

Hawley, SA, DA Pan, KJ Mustard, L Ross, J Bain, AM Edelman, et al. (2005). "Calmodulin-dependent protein kinase kinase-beta is an alternative upstream kinase for AMP-activated protein kinase." Cell Metab **2**(1): 9-19.

Hayashi, T, MF Hirshman, EJ Kurth, WW Winder and LJ Goodyear (1998). "Evidence for 5' AMP-activated protein kinase mediation of the effect of muscle contraction on glucose transport." Diabetes **47**(8): 1369-73.

Higashi, Y, K Noma, M Yoshizumi and Y Kihara (2009). "Endothelial function and oxidative stress in cardiovascular diseases." Circ J **73**(3): 411-8.

Hoshi, S, M Goto, N Koyama, K Nomoto and H Tanaka (2000). "Regulation of vascular smooth muscle cell proliferation by nuclear factor-kappaB and its inhibitor, I-kappaB." J Biol Chem **275**(2): 883-9.

Ignarro, LJ, GM Buga, KS Wood, RE Byrns and G Chaudhuri (1987). "Endothelium-derived relaxing factor produced and released from artery and vein is nitric oxide." Proc Natl Acad Sci U S A **84**(24): 9265-9.

Imai, S, CM Armstrong, M Kaeberlein and L Guarente (2000). "Transcriptional silencing and longevity protein Sir2 is an NAD-dependent histone deacetylase." Nature **403**(6771): 795-800.

Jakobsen, SN, DG Hardie, N Morrice and HE Tornqvist (2001). "5'-AMP-activated protein kinase phosphorylates IRS-1 on Ser-789 in mouse C2C12 myotubes in response to 5-aminoimidazole-4-carboxamide riboside." J Biol Chem **276**(50): 46912-6.

Jalali, S, MA del Pozo, K Chen, H Miao, Y Li, MA Schwartz, et al. (2001). "Integrin-mediated mechanotransduction requires its dynamic interaction with specific extracellular matrix (ECM) ligands." Proc Natl Acad Sci U S A **98**(3): 1042-6.

Kahn, BB, T Alquier, D Carling and DG Hardie (2005). "AMP-activated protein kinase: ancient energy gauge provides clues to modern understanding of metabolism." Cell Metab **1**(1): 15-25.

Khan, BV, DG Harrison, MT Olbrych, RW Alexander and RM Medford (1996). "Nitric oxide regulates vascular cell adhesion molecule 1 gene expression and redox-sensitive transcriptional events in human vascular endothelial cells." Proc Natl Acad Sci U S A **93**(17): 9114-9.

Kingwell, BA, PJ Arnold, GL Jennings and AM Dart (1997). "Spontaneous running increases aortic compliance in Wistar-Kyoto rats." Cardiovasc Res **35**(1): 132-7.

Koller, A, A Huang, D Sun and G Kaley (1995). "Exercise training augments flow-dependent dilation in rat skeletal muscle arterioles. Role of endothelial nitric oxide and prostaglandins." Circ Res **76**(4): 544-50.

Koyama, H, NE Olson, FF Dastvan and MA Reidy (1998). "Cell replication in the arterial wall: activation of signaling pathway following in vivo injury." Circ Res **82**(6): 713-21.

Ku, DN, DP Giddens, CK Zarins and S Glagov (1985). "Pulsatile flow and atherosclerosis in the human carotid bifurcation. Positive correlation between plaque location and low oscillating shear stress." Arteriosclerosis **5**(3): 293-302.

Kubota, N, W Yano, T Kubota, T Yamauchi, S Itoh, H Kumagai, et al. (2007). "Adiponectin stimulates AMP-activated protein kinase in the hypothalamus and increases food intake." Cell Metab **6**(1): 55-68.

Kuchan, MJ and JA Frangos (1993). "Shear stress regulates endothelin-1 release via protein kinase C and cGMP in cultured endothelial cells." Am J Physiol **264**(1 Pt 2): H150-6.

Lagouge, M, C Argmann, Z Gerhart-Hines, H Meziane, C Lerin, F Daussin, et al. (2006). "Resveratrol improves mitochondrial function and protects against metabolic disease by activating SIRT1 and PGC-1alpha." Cell **127**(6): 1109-22.

Laufs, U, V La Fata, J Plutzky and JK Liao (1998). "Upregulation of endothelial nitric oxide synthase by HMG CoA reductase inhibitors." Circulation **97**(12): 1129-35.

Leclerc, I, C Lenzner, L Gourdon, S Vaulont, A Kahn and B Viollet (2001). "Hepatocyte nuclear factor-4alpha involved in type 1 maturity-onset diabetes of the young is a novel target of AMP-activated protein kinase." Diabetes **50**(7): 1515-21.

Libby, P, M Aikawa and MK Jain (2006). "Vascular endothelium and atherosclerosis." Handb Exp Pharmacol(176 Pt 2): 285-306.

Liu, Y, BP Chen, M Lu, Y Zhu, MB Stemerman, S Chien, et al. (2002). "Shear stress activation of SREBP1 in endothelial cells is mediated by integrins." Arterioscler Thromb Vasc Biol **22**(1): 76-81.

Lowenstein, CJ, JL Dinerman and SH Snyder (1994). "Nitric oxide: a physiologic messenger." Ann Intern Med **120**(3): 227-37.

Luo, J, AY Nikolaev, S Imai, D Chen, F Su, A Shiloh, et al. (2001). "Negative control of p53 by Sir2alpha promotes cell survival under stress." Cell **107**(2): 137-48.

Luscher, TF and M Barton (1997). "Biology of the endothelium." Clin Cardiol **20**(11 Suppl 2): II-3-10.

Malek, A and S Izumo (1992). "Physiological fluid shear stress causes downregulation of endothelin-1 mRNA in bovine aortic endothelium." Am J Physiol **263**(2 Pt 1): C389-96.

Malek, AM, SL Alper and S Izumo (1999). "Hemodynamic shear stress and its role in atherosclerosis." JAMA **282**(21): 2035-42.

Mattagajasingh, I, CS Kim, A Naqvi, T Yamamori, TA Hoffman, SB Jung, et al. (2007). "SIRT1 promotes endothelium-dependent vascular relaxation by activating endothelial nitric oxide synthase." Proc Natl Acad Sci U S A **104**(37): 14855-60.

Mayer, B, K Schmidt, P Humbert and E Bohme (1989). "Biosynthesis of endothelium-derived relaxing factor: a cytosolic enzyme in porcine aortic endothelial cells Ca2+-dependently converts L-arginine into an activator of soluble guanylyl cyclase." Biochem Biophys Res Commun **164**(2): 678-85.

McGarry, JD, GF Leatherman and DW Foster (1978). "Carnitine palmitoyltransferase I. The site of inhibition of hepatic fatty acid oxidation by malonyl-CoA." J Biol Chem **253**(12): 4128-36.

Mehrhof, FB, R Schmidt-Ullrich, R Dietz and C Scheidereit (2005). "Regulation of vascular smooth muscle cell proliferation: role of NF-kappaB revisited." Circ Res **96**(9): 958-64.

Michell, BJ, MB Harris, ZP Chen, H Ju, VJ Venema, MA Blackstone, et al. (2002). "Identification of regulatory sites of phosphorylation of the bovine endothelial nitric-oxide synthase at serine 617 and serine 635." J Biol Chem **277**(44): 42344-51.

Miyazaki, R, T Ichiki, T Hashimoto, K Inanaga, I Imayama, J Sadoshima, et al. (2008). "SIRT1, a longevity gene, downregulates angiotensin II type 1 receptor expression in vascular smooth muscle cells." Arterioscler Thromb Vasc Biol **28**(7): 1263-9.

Moncada, S and A Higgs (1993). "The L-arginine-nitric oxide pathway." N Engl J Med **329**(27): 2002-12.

Morrow, VA, F Foufelle, JM Connell, JR Petrie, GW Gould and IP Salt (2003). "Direct activation of AMP-activated protein kinase stimulates nitric-oxide synthesis in human aortic endothelial cells." J Biol Chem **278**(34): 31629-39.

Motta, MC, N Divecha, M Lemieux, C Kamel, D Chen, W Gu, et al. (2004). "Mammalian SIRT1 represses forkhead transcription factors." Cell **116**(4): 551-63.

Mount, PF, BE Kemp and DA Power (2007). "Regulation of endothelial and myocardial NO synthesis by multi-site eNOS phosphorylation." J Mol Cell Cardiol **42**(2): 271-9.

Nakashima, Y, AS Plump, EW Raines, JL Breslow and R Ross (1994). "ApoE-deficient mice develop lesions of all phases of atherosclerosis throughout the arterial tree." Arterioscler Thromb **14**(1): 133-40.

Nathan, C and QW Xie (1994). "Regulation of biosynthesis of nitric oxide." J Biol Chem **269**(19): 13725-8.

Nauli, SM, Y Kawanabe, JJ Kaminski, WJ Pearce, DE Ingber and J Zhou (2008). "Endothelial cilia are fluid shear sensors that regulate calcium signaling and nitric oxide production through polycystin-1." Circulation **117**(9): 1161-71.

Nemoto, S, MM Fergusson and T Finkel (2005). "SIRT1 functionally interacts with the metabolic regulator and transcriptional coactivator PGC-1{alpha}." J Biol Chem **280**(16): 16456-60.

Ohno, M, GH Gibbons, VJ Dzau and JP Cooke (1993). "Shear stress elevates endothelial cGMP. Role of a potassium channel and G protein coupling." Circulation **88**(1): 193-7.

Olesen, SP, DE Clapham and PF Davies (1988). "Haemodynamic shear stress activates a K+ current in vascular endothelial cells." Nature **331**(6152): 168-70.

Ota, H, M Akishita, M Eto, K Iijima, M Kaneki and Y Ouchi (2007). "Sirt1 modulates premature senescence-like phenotype in human endothelial cells." J Mol Cell Cardiol **43**(5): 571-9.

Ouchi, N, H Kobayashi, S Kihara, M Kumada, K Sato, T Inoue, et al. (2004). "Adiponectin stimulates angiogenesis by promoting cross-talk between AMP-activated protein kinase and Akt signaling in endothelial cells." J Biol Chem **279**(2): 1304-9.

Oyre, S, S Ringgaard, S Kozerke, WP Paaske, M Erlandsen, P Boesiger, et al. (1998). "Accurate noninvasive quantitation of blood flow, cross-sectional lumen vessel area and wall shear stress by three-dimensional paraboloid modeling of magnetic resonance imaging velocity data." J Am Coll Cardiol **32**(1): 128-34.

Palmer, RM, DS Ashton and S Moncada (1988). "Vascular endothelial cells synthesize nitric oxide from L-arginine." Nature **333**(6174): 664-6.

Palmer, RM, AG Ferrige and S Moncada (1987). "Nitric oxide release accounts for the biological activity of endothelium-derived relaxing factor." Nature **327**(6122): 524-6.

Poelmann, RE, K Van der Heiden, A Gittenberger-de Groot and BP Hierck (2008). "Deciphering the endothelial shear stress sensor." Circulation **117**(9): 1124-6.

Pollock, JS, U Forstermann, JA Mitchell, TD Warner, HH Schmidt, M Nakane, et al. (1991). "Purification and characterization of particulate endothelium-derived relaxing factor synthase from cultured and native bovine aortic endothelial cells." Proc Natl Acad Sci U S A **88**(23): 10480-4.

Ranjan, V, Z Xiao and SL Diamond (1995). "Constitutive NOS expression in cultured endothelial cells is elevated by fluid shear stress." Am J Physiol **269**(2 Pt 2): H550-5.

Resnick, N, H Yahav, S Schubert, E Wolfovitz and A Shay (2000). "Signalling pathways in vascular endothelium activated by shear stress: relevance to atherosclerosis." Curr Opin Lipidol **11**(2): 167-77.

Rodgers, JT, C Lerin, Z Gerhart-Hines and P Puigserver (2008). "Metabolic adaptations through the PGC-1 alpha and SIRT1 pathways." FEBS Lett **582**(1): 46-53.

Rodgers, JT, C Lerin, W Haas, SP Gygi, BM Spiegelman and P Puigserver (2005). "Nutrient control of glucose homeostasis through a complex of PGC-1alpha and SIRT1." Nature **434**(7029): 113-8.

Ross, R (1999). "Atherosclerosis--an inflammatory disease." N Engl J Med **340**(2): 115-26.

Rubbo, H, A Trostchansky, H Botti and C Batthyany (2002). "Interactions of nitric oxide and peroxynitrite with low-density lipoprotein." Biol Chem **383**(3-4): 547-52.

Russell, RR, 3rd, R Bergeron, GI Shulman and LH Young (1999). "Translocation of myocardial GLUT-4 and increased glucose uptake through activation of AMPK by AICAR." Am J Physiol **277**(2 Pt 2): H643-9.

Schwartz, MA (2001). "Integrin signaling revisited." Trends Cell Biol **11**(12): 466-70.

SenBanerjee, S, Z Lin, GB Atkins, DM Greif, RM Rao, A Kumar, et al. (2004). "KLF2 Is a novel transcriptional regulator of endothelial proinflammatory activation." J Exp Med **199**(10): 1305-15.

Shigematsu, K, H Koyama, NE Olson, A Cho and MA Reidy (2000). "Phosphatidylinositol 3-kinase signaling is important for smooth muscle cell replication after arterial injury." Arterioscler Thromb Vasc Biol **20**(11): 2373-8.

Steinberg, D (2009). "The LDL modification hypothesis of atherogenesis: an update." J Lipid Res **50 Suppl**: S376-81.

Stone, PH, AU Coskun, S Kinlay, ME Clark, M Sonka, A Wahle, et al. (2003). "Effect of endothelial shear stress on the progression of coronary artery disease, vascular remodeling, and in-stent restenosis in humans: in vivo 6-month follow-up study." Circulation **108**(4): 438-44.

Strong, JP, GT Malcom, WP Newman, 3rd and MC Oalmann (1992). "Early lesions of atherosclerosis in childhood and youth: natural history and risk factors." J Am Coll Nutr **11 Suppl**: 51S-54S.

Suarez, Y, C Fernandez-Hernando, JS Pober and WC Sessa (2007). "Dicer dependent microRNAs regulate gene expression and functions in human endothelial cells." Circ Res **100**(8): 1164-73.

Sun, D, A Huang, A Koller and G Kaley (1994). "Short-term daily exercise activity enhances endothelial NO synthesis in skeletal muscle arterioles of rats." J Appl Physiol **76**(5): 2241-7.

Sun, D, A Huang, A Koller and G Kaley (1998). "Adaptation of flow-induced dilation of arterioles to daily exercise." Microvasc Res **56**(1): 54-61.

Sun, W, TS Lee, M Zhu, C Gu, Y Wang, Y Zhu, et al. (2006). "Statins activate AMP-activated protein kinase in vitro and in vivo." Circulation **114**(24): 2655-62.

Thors, B, H Halldorsson and G Thorgeirsson (2004). "Thrombin and histamine stimulate endothelial nitric-oxide synthase phosphorylation at Ser1177 via an AMPK mediated pathway independent of PI3K-Akt." FEBS Lett **573**(1-3): 175-80.

Towler, MC and DG Hardie (2007). "AMP-activated protein kinase in metabolic control and insulin signaling." Circ Res **100**(3): 328-41.

Traub, O, T Ishida, M Ishida, JC Tupper and BC Berk (1999). "Shear stress-mediated extracellular signal-regulated kinase activation is regulated by sodium in endothelial cells. Potential role for a voltage-dependent sodium channel." J Biol Chem **274**(29): 20144-50.

Tronc, F, M Wassef, B Esposito, D Henrion, S Glagov and A Tedgui (1996). "Role of NO in flow-induced remodeling of the rabbit common carotid artery." Arterioscler Thromb Vasc Biol **16**(10): 1256-62.

Tuttle, JL, RD Nachreiner, AS Bhuller, KW Condict, BA Connors, BP Herring, et al. (2001). "Shear level influences resistance artery remodeling: wall dimensions, cell density, and eNOS expression." Am J Physiol Heart Circ Physiol **281**(3): H1380-9.

Tzima, E, M Irani-Tehrani, WB Kiosses, E Dejana, DA Schultz, B Engelhardt, et al. (2005). "A mechanosensory complex that mediates the endothelial cell response to fluid shear stress." Nature **437**(7057): 426-31.

van Thienen, JV, JO Fledderus, RJ Dekker, J Rohlena, GA van Ijzendoorn, NA Kootstra, et al. (2006). "Shear stress sustains atheroprotective endothelial KLF2 expression more potently than statins through mRNA stabilization." Cardiovasc Res **72**(2): 231-40.

Vaziri, H, SK Dessain, E Ng Eaton, SI Imai, RA Frye, TK Pandita, et al. (2001). "hSIR2(SIRT1) functions as an NAD-dependent p53 deacetylase." Cell **107**(2): 149-59.

Wang, Y, H Miao, S Li, KD Chen, YS Li, S Yuan, et al. (2002). "Interplay between integrins and FLK-1 in shear stress-induced signaling." Am J Physiol Cell Physiol **283**(5): C1540-7.

Weinbaum, S, X Zhang, Y Han, H Vink and SC Cowin (2003). "Mechanotransduction and flow across the endothelial glycocalyx." Proc Natl Acad Sci U S A **100**(13): 7988-95.

Wentzel, JJ, R Corti, ZA Fayad, P Wisdom, F Macaluso, MO Winkelman, et al. (2005). "Does shear stress modulate both plaque progression and regression in the thoracic aorta? Human study using serial magnetic resonance imaging." J Am Coll Cardiol **45**(6): 846-54.

Wentzel, JJ, R Krams, JC Schuurbiers, JA Oomen, J Kloet, WJ van Der Giessen, et al. (2001). "Relationship between neointimal thickness and shear stress after Wallstent implantation in human coronary arteries." Circulation **103**(13): 1740-5.

Woods, A, K Dickerson, R Heath, SP Hong, M Momcilovic, SR Johnstone, et al. (2005). "Ca2+/calmodulin-dependent protein kinase kinase-beta acts upstream of AMP-activated protein kinase in mammalian cells." Cell Metab **2**(1): 21-33.

Yamamoto, K, T Sokabe, T Matsumoto, K Yoshimura, M Shibata, N Ohura, et al. (2006). "Impaired flow-dependent control of vascular tone and remodeling in P2X4-deficient mice." Nat Med **12**(1): 133-7.

Yetik-Anacak, G and JD Catravas (2006). "Nitric oxide and the endothelium: history and impact on cardiovascular disease." Vascul Pharmacol **45**(5): 268-76.

Yin, C, FN Salloum and RC Kukreja (2009). "A novel role of microRNA in late preconditioning: upregulation of endothelial nitric oxide synthase and heat shock protein 70." Circ Res **104**(5): 572-5.

Young, A, W Wu, W Sun, HB Larman, N Wang, YS Li, et al. (2009). "Flow activation of AMP-activated protein kinase in vascular endothelium leads to Kruppel-like factor 2 expression." Arterioscler Thromb Vasc Biol **29**(11): 1902-8.

Zarins, CK, DP Giddens, BK Bharadvaj, VS Sottiurai, RF Mabon and S Glagov (1983). "Carotid bifurcation atherosclerosis. Quantitative correlation of plaque localization with flow velocity profiles and wall shear stress." Circ Res **53**(4): 502-14.

Zeiher, AM, B Fisslthaler, B Schray-Utz and R Busse (1995). "Nitric oxide modulates the expression of monocyte chemoattractant protein 1 in cultured human endothelial cells." Circ Res **76**(6): 980-6.

Zhang, QJ, Z Wang, HZ Chen, S Zhou, W Zheng, G Liu, et al. (2008). "Endothelium-specific overexpression of class III deacetylase SIRT1 decreases atherosclerosis in apolipoprotein E-deficient mice." Cardiovasc Res **80**(2): 191-9.

Zhang, Y, TS Lee, EM Kolb, K Sun, X Lu, FM Sladek, et al. (2006). "AMP-activated protein kinase is involved in endothelial NO synthase activation in response to shear stress." Arterioscler Thromb Vasc Biol **26**(6): 1281-7.

Zhao, S, A Suciu, T Ziegler, JE Moore, Jr., E Burki, JJ Meister, et al. (1995). "Synergistic effects of fluid shear stress and cyclic circumferential stretch on vascular endothelial cell morphology and cytoskeleton." Arterioscler Thromb Vasc Biol **15**(10): 1781-6.

Zhou, G, R Myers, Y Li, Y Chen, X Shen, J Fenyk-Melody, et al. (2001). "Role of AMP-activated protein kinase in mechanism of metformin action." J Clin Invest **108**(8): 1167-74.

Zhou, X, D Liu, L You and L Wang (2009). "Quantifying fluid shear stress in a rocking culture dish." J Biomech **43**(8): 1598-602.

Chapter 2

AMP-Activated Protein Kinase Functionally Phosphorylates Endothelial Nitric Oxide Synthase Ser-633

2.1 Abstract

Endothelial nitric oxide synthase (eNOS) plays a central role in maintaining cardiovascular homeostasis by controlling NO bioavailability. The activity of eNOS in vascular endothelial cells (ECs) largely depends on posttranslational modifications, including phosphorylation. Because the activity of AMP-activated protein kinase (AMPK) in ECs can be increased by multiple cardiovascular events, we studied the phosphorylation of eNOS Ser-633 by AMPK and examined its functional relevance in the mouse models. Shear stress, atorvastatin, and adiponectin all increased AMPK Thr-172 and eNOS Ser-633 phosphorylations, which were abolished if AMPK was pharmacologically inhibited or genetically ablated. The constitutively active form of AMPK or an AMPK agonist caused a sustained Ser-633 phosphorylation. Expression of gain-/loss-of-function eNOS mutants revealed that Ser-633 phosphorylation is important for NO production. The aorta of AMPK$\alpha 2^{-/-}$ mice showed attenuated atorvastatin-induced eNOS phosphorylation. Nano–liquid chromatography/tandem mass spectrometry (LC/MS/MS) confirmed that eNOS Ser-633 was able to compete with Ser-1177 or acetyl-coenzyme A carboxylase Ser-79 for AMPKα phosphorylation. Nano-LC/MS/MS confirmed that eNOS purified from AICAR-treated ECs was phosphorylated at both Ser-

633 and Ser-1177. Our results indicate that AMPK phosphorylation of eNOS Ser-633 is a functional signaling event for NO bioavailability in ECs.

2.2 Introduction

The endothelium is pivotal in the regulation of vascular tone, which largely depends on endothelial nitric oxide synthase (eNOS)-derived NO bioavailability (Furchgott and Zawadzki 1980; Palmer et al. 1987; Stuehr 1999). In addition to relaxing vessels, NO exerts such pleiotropic effects as anti-inflammation and anti-thrombosis on the vascular wall (Loscalzo 2001; Lerman and Zeiher 2005). Existing as a homodimer, eNOS contains an N-terminal oxygenase domain, an interposed Ca^{2+}/calmodulin (CaM) binding domain, and a C-terminal reductase domain (Andrew and Mayer 1999). Much progress has been made in understanding the regulatory mechanisms of eNOS at transcriptional, translational, and posttranslational levels. The phosphorylation/dephosphorylation of Ser and Thr of eNOS by protein kinases/phosphatases seems to be important for its enzymatic activity in vascular endothelial cells (ECs) (Sessa 2004).

To date, 5 Ser/Thr phosphorylation sites in eNOS have been identified. They are Ser-114, Thr-495, Ser-615, Ser-633, and Ser-1177 in human and mouse eNOS, which correspond to Ser-116, Thr-497, Ser-617, Ser-635, and Ser-1179 in the bovine counterpart (Mount et al. 2007). Functioning as stimulatory phosphorylation sites, Ser-633 and Ser-1177 are located in each of the 2 autoinhibitory sequences (i.e., AIS I and II) (Fulton et al. 1999; Michell et al. 2002; Bauer et al. 2003). The phosphorylation of Ser-1177 appears to eliminate the blockage of electron transfer within the C termini of the 2

eNOS monomers (Lane and Gross 2002). The phosphorylation of Ser-1177 has been suggested to be critical for eNOS activation responding to several stimuli, such as shear stress, adiponectin, and 3-hydroxy-3-methylglutaryl-coenzyme A (HMG-CoA) inhibitors (i.e., statins), known to increase NO bioavailability (Dimmeler et al. 1999; Chen et al. 2003; Harris et al. 2004). These physiological and pharmacological stimuli activate a number of protein kinases, including AMP-activated protein kinase (AMPK), protein kinase (PK)A, PKB (Akt), CaM-dependant protein kinase (CaMK)II, and PKG, which in turn phosphorylate Ser-1177 (Chen et al. 1999; Dimmeler et al. 1999; Fulton et al. 1999; Butt et al. 2000; Fleming et al. 2001; Michell et al. 2001; Boo et al. 2002; Zhang et al. 2006). The Ser-633 residue in eNOS resides in the flavin mononucleotide binding domain (Michell et al. 2002). The gain-of-function phosphomimetic eNOS Ser-635D mutant yielded increased basal and vascular endothelial growth factor or ATP-stimulated NO release in transfected COS-7 cells (Bauer et al. 2003). Such experiments suggested that Ser-633 might be more efficacious than Ser-1177 in augmenting the eNOS-derived NO bioavailability. Furthermore, phosphorylation of Ser-633 may enhance NO production without changing the intracellular calcium level ($[Ca^{2+}]i$) (Boo et al. 2003), and it seems to be a later event than that of Ser-1177 (Boo et al. 2002). Thus, this posttranslational modification of Ser-633 is proposed to maintain persistent eNOS activity after its initial activation by calcium flux. Using the PKA inhibitors H89 and PKI, Boo et al suggested that PKA, rather than Akt, phosphorylates Ser-633 in ECs subjected to shear stress (Boo et al. 2002).

AMPK is an energy sensor/metabolic switch, because AMPK phosphorylates and hence regulates the activity of enzymes such as acetyl-CoA carboxylase (ACC) and HMG-CoA reductase (Carling et al. 1989; Corton et al. 1995). AMPK consists of a catalytic α subunit and regulatory β and γ subunits. The different isoforms of the subunits of AMPK are encoded by distinct genes (α1, α2, β1, β2, γ1, γ2, and γ3) and expressed differentially depending on tissue types (Hardie 2007). Substantial evidence demonstrates that AMPK is not only critical in regulating metabolic homeostasis but also important in cardiovascular biology, attributable in part to AMPK-activating eNOS in ECs and cardiomyocytes (Li et al. 2004; Arad et al. 2007; Levine et al. 2007). By far, the activation of eNOS by AMPK is thought to be mediated through the phosphorylation of Ser-1177 under many physiological conditions and pharmacological stimuli (Chen et al. 1999; Sun et al. 2006; Zhang et al. 2006; Calvert et al. 2008).

Despite the plausible role of Ser-633 phosphorylation contributing to eNOS-derived NO activity, the functional basis of this phosphorylation event is largely unknown. In this study, we addressed whether AMPK is an upstream kinase that phosphorylates Ser-633, whether Ser-633 competes with ACC Ser-79 and eNOS Ser-1177 for catalysis by AMPKα, and whether Ser-633 phosphorylation is required for NO bioavailability.

2.3 Materials and Method

2.3.1 Antibodies and reagents

Antibodies used were anti-pan-AMPKα, anti-AMPK-α1, anti-AMPK-α2, anti-phospho-AMPK Thr-172, anti-phospho-ACC Ser-79, anti-phospho-Akt Ser-473, anti-

eNOS, and anti-α-tubulin, horseradish peroxide (HRP)-conjugated anti-rabbit or anti-mouse antibodies (Cell Signaling Technology), anti-phospho-eNOS Ser-1177/1179, and anti-phospho-eNOS Ser-633/635 (BD Biosciences Pharmingen). Griess reagent and AICAR were from Sigma. Compound C was from Calbiochem and atorvastatin was from Toronto Research Chemicals. Recombinant adiponectin was purchased from Phoenix Pharmaceuticals, Inc.

2.3.2 Cell culture, fluid shear stress experiments, adenoviral infection, and siRNA knocking down

Bovine aortic endothelial cells (BAECs) and human embryonic kidney 293 (HEK293) cells were cultured in DMEM containing 10% FBS. Murine embryonic endothelial fibroblasts (MEFs) were isolated from the wild-type C57BL6 or AMPKα2$^{-/-}$ mouse embryos (E13) and cultured in vitro by a standard protocol (Helgason 2005).

The parallel-plate flow channel was used to conduct shear stress experiments (Zhang et al. 2006). BAECs were exposed to a laminar flow at 5 dyne/cm^2 for 6 h, and then the magnitude of shear stress was increased to 12 dyne/cm^2 for different time intervals.

Ad-AMPK-CA, a recombinant adenovirus expressing an AMPKα2 mutant, was described previously (Foretz et al. 2005). BAECs, HEK293 cells or MEFs seeded on 6-well plates were infected at 70% confluency with Ad-AMPK-CA at different multiplicities of infection (MOI) and incubated for 24 h before further experimentation.

HUVECs were seeded in 6-well plates and allowed to grow to 70% confluence. Transient transfection was performed with Lipofectamine RNAiMAX. In brief, HUVECs

were transfected with AMPKα1, AMPKα2 (Qiagen, SI02622235, SI02758595), or scramble siRNAs at 10 nM in reduced serum medium. Four hours after transfection, the medium was changed to fresh complete medium and cells were kept in culture for 72 h before experimentation.

2.3.3 Western blotting, expression of GST-eNOS proteins and IP kinase activity assays

Lysates from BAECs, HEK293 cells, MEFs, or mouse aortas were resolved on 8% SDS-PAGE, and proteins were transferred to PVDF membrane. The blotting with various antibodies followed a standard protocol as previously described (Sun et al. 2006).

The wild-type bovine eNOS cDNA in a pGEX-4T-1 vector was used as a template and the site-directed mutation at Ser-635 and Ser-1179 were performed using a QuikChange mutagenesis kit (Stratagene). Various recombinant GST-eNOS proteins were expressed in *E. Coli* and purified by glutathione 4B beads.

AMPKα was immunoprecipitated from BAEC lysates by the use of anti-pan-AMPKα. The phosphorylation of GST-eNOS by the immunoprecipitated AMPK was detected by Western blotting.

2.3.4 NO bioavailability assays

The bovine eNOS was subcloned into a pcDNA3 vector. The gain/loss-of-function mutants (i.e., S635A and S635D) were then created by site-directed mutagenesis (34). Plasmids encoding pcDNA3-S635AS1179A and S635DS1179D were provided by Dr. Hanjoong Jo in Department of Biomedical Engineering, Georgia Tech and Emory

University. HEK293 cells and MEFs were transiently transfected with 1 μg of respective DNA and 2.5 μl Lipofectamine 2000 (Invitrogen) per 10^6 cells. The NO production in cells transfected with various plasmids was assessed by using Griess reagent to determine the accumulated nitrite in cell culture media.

2.3.5 Animal Experiments

The animal experimental protocols were approved by the University of California at Riverside Institutional Animal Care and Use Committee. C57BL6 mice were purchased from The Jackson Laboratory. AMPK$\alpha 2^{-/-}$ mice were originally created by Dr B. Viollet (Viollet et al. 2003). Atorvastatin at 50 mg/kg body weight was administered to male mice (8 weeks old) by gastric gavage. Saline was fed to control mice as a vehicle control. After 6, 12, or 24 hours, mice were killed, and abdominal aortas were removed. Proteins from aortic extracts were resolved by 8% SDS-PAGE and underwent Western blotting analysis.

2.3.6 SAMS, eNOS633, and eNOS1177 Binding Assays

eNOS633 and eNOS1177 peptides were synthesized with the sequences PLVSSWRRKRKESSNTDSA and RTQEVTSRIRTQSFSLQER, respectively. BAECs were treated with AICAR for 30 minutes, and AMPK was immunoprecipitated. The phosphorylation of SAMS, eNOS633, and eNOS1177 peptides by AMPK was determined by the incorporation of 32P. The kinase assays were performed in 40 mmol/L HEPES, 0.2 mmol/L AMP, 8 μCi (γ-^{32}P) ATP, 0.2 mmol/L ATP, 80 mmol/L NaCl, 5 mmol/L MgCl2, 8% glycerol, and 0.8 mmol/L dithiothreitol at 37°C for 1 hour. The reaction mixture was spotted onto Whatman P81 filter paper and washed 5 times with 1%

phosphoric acid and once with acetone. After being air-dried, the ^{32}P incorporation was quantified by use of a Beckman liquid scintillation counter.

2.3.7 Nanoliquid chromatography/mass spectrometry

Waters' nano-Acquity UPLC (ultra performance liquid chromatography) and Q-TOF Premier mass spectrometer were used for all LC/MS and LC/MS/MS experiments. The analytical column was a BEH300 C18 column (1.7 μm particle, 75 μm internal diameter, 20 cm long) (PN# 186003544, Waters), whereas the trapping column was a Symmetry C18 column (5 μm particle, 180 μm internal diameter, 2 cm long) (PN# 186003514, Waters). Sample was loaded by the autosampler of the UPLC with a 10 μl sample loop and a partial-fill method. The LC solvents were 0.2% formic acid in water for mobile phase A and 0.2% formic acid in acetonitrile for mobile phase B. The LC gradient was as follows: 100% A at 0-3 minutes; 92% A/8% B at 8 minutes; 60%A/40% B at 70 minutes; 40% A/60% B at 90 minutes; 10% A/90% B at 100-110 minutes; 97% A/3% B at 115 minutes; 100% A at 135 minutes. The duration of the complete LC method was for 140 minutes, and LC flow rate was kept at 0.3 μl/min. A 1 hr blank injection was placed between each sample.

For SAMS and eNOS633 competition assay, SAMS was mixed with eNOS633 in ratios of 1:0, 1:1, or 1:10, and the peptide mixtures were incubated with the immunoprecipitated AMPKα in kinase assay buffer for 24 h at 37ºC. After 30 minutes centrifugation at 14,000 rpm, the supernatants were transferred and diluted (10x) with 0.1% trifluoroacetic acid. Three microliters of the diluted samples were analyzed by a nano-LC/MS system, which consists of Q-TOF Premier mass spectrometer, nano-

Acquity UPLC (ultra-performance liquid chromatography), and a BEH130 C_{18} analytical column (Waters Corp.). Individually extracted ion chromatograms corresponding to SAMS (m/z 465.49, 4+) or eNOS633 (m/z 571.79, 4+) phosphopeptide were manually analyzed to calculate spectral intensities (ion counts) after subtraction of baseline backgrounds. The extracted ion total counts (EITC) obtained were used to quantify the changes of phosphorylation level for each peptide under the competition condition. The competition between SAMS/S1177 and S633/S1177 was analyzed in the same manner.

For eNOS phosphopeptide detection, we used the titanium dioxide (TiO_2) coated magnetic beads provided with the Phos-Trap phosphopeptide enrichment kit (PN# PRT302001KT, Perkin Elmer, Waltham , MA) to purify and enrich phosphopeptides from the trypsin-treated eNOS that was immnoprecipitated from BAECs or HEK-293 cells. eNOS was immunoprecipitated and the beads were washed twice with 1 ml of 50 mM NH_4HCO_3, pH 8.0. eNOS was then digested by adding 100 µl trypsin (20 ng/µl) directly to beads at 37ºC overnight. The buffer solutions contained in the Phos-Trap phosphopeptide enrichment kit were prepared according to manufacturer's instructions. The supernatant of trypsin-treated eNOS was lyophilized by a 4ºC speedvac concentrator and was redissolved in 20 µl trypsin buffer. The remaining beads were washed with 200 µl of the binding buffer, a component of the Phos-Trap phosphopeptide enrichment kit. After centrifugation at 14,000 rpm for 15 minutes, 200 µl supernantent was collected and mixed with 20 µl sample described above. Each sample was then incubated with 40 µl TiO_2-coated magnetic beads for 20 minutes, subjected to 4× wash with binding buffer, and then 1× wash with washing buffer. The bound-phosphopeptides were then eluted

with 30 μl elution buffer. The supernatant was collected and lyophilized. The freeze-dried pellet was dissolved in 12 μl of 0.1% trifluoroacetic acid and subjected to LC/MS/MS analyses. The phosphorylation sites within eNOS phosphopeptides were mapped by a characteristic neutral loss of the phosphate group in the process of collision-induced dissociation (CID).

2.3.8 Statistical Analysis

The significance of variability was determined by Student's *t* test or 1-way ANOVA. All results are presented as means±SD from at least 3 independent experiments. In all cases, $P<0.05$ was considered statistically significant.

2.4 Results

2.4.1 AMPK and eNOS Ser-635 phosphorylation in cultured ECs

AMPK is activated by several physiological and pharmacological stimuli such as shear stress, statins, and adiponectin, and is associated with eNOS phosphorylation at Ser-1177/1179 (Sun et al. 2006; Zhang et al. 2006; Cheng et al. 2007). We examined first the effect of these stimuli on phosphorylation of eNOS Ser-633/635 in cultured ECs. BAECs were treated with laminar flow, atorvastatin, or recombinant adiponectin for up to 2 hours. As shown in Fig. 2-1, these 3 stimuli increased the phosphorylation of eNOS Ser-635 as early as 5 minutes, which was sustained for up to 2 hours. The sustainable increase in phosphorylation was also observed for AMPK Thr-172 and its target ACC Ser-79. However, the phosphorylation of eNOS Ser-1179 was increased only transiently in response to these stimuli, reaching a peak level at 5 or 15 minutes and declining afterward.

2.4.2 AMPK phosphorylates both eNOS Ser-635 and Ser-1179 *in vitro*

The temporal phosphorylation of eNOS Ser-635 and AMPK Thr-172 as seen in Fig. 2-1 suggests that eNOS Ser-635 may be a catalytic target of AMPK. To test whether AMPK can phosphorylate eNOS Ser-635, we treated BAECs with AICAR, an AMPK-specific agonist, or infected BAECs with Ad-AMPK-CA, an adenoviral vector expressing the constitutively active form of AMPK. AICAR treatment increased the phosphorylation of eNOS at both Ser-635 and Ser-1179 in a dose-dependent manner (Fig. 2-2A). Similarly, Ad-AMPK-CA infection increased phosphorylation of eNOS Ser-635 in ECs, as compared with Ad-null infection in control cells (Fig. 2-2B).

Using immunoprecipitation (IP) kinase activity assay, we examined next whether AMPK can directly phosphorylate eNOS Ser-635. As shown in Fig. 2-2C, AMPKα immunoprecipitated from AICAR-stimulated BAECs phosphorylated glutathione *S*-transferase (GST)-eNOS at both Ser-635 and Ser-1179, as revealed by Western blot analysis. Phosphorylation was elevated with increased concentration of AMPK antibody used for IP. GST-eNOS with S/A mutation at either
Ser-635 or Ser-1179 was used in parallel assays. As expected, phosphorylation by AMPK at the mutated site was abolished, but the other site was unaffected. Collectively, these results suggest that AMPK can directly and specifically phosphorylate eNOS at Ser-635.

To determine whether AMPK is necessary for eNOS Ser-635 phosphorylation, BAECs were treated with compound C, an AMPK antagonist, before treatment with laminar flow, atorvastatin, or recombinant adiponectin. As shown in Fig. 2-3A, AMPK and ACC phosphorylation was impaired in ECs treated with compound C, as compared

with that in control cells. With AMPK inhibited by compound C, the phosphorylation of eNOS Ser-635 by laminar flow, atorvastatin, or adiponectin was also greatly attenuated, which suggests that AMPK is required for eNOS Ser-635 phosphorylation. We used siRNA to knock down AMPKα1 or α2 in HUVECs. The isoform-specific AMPK knockdown by siRNA also decreased eNOS Ser-633 phosphorylation caused by atorvastatin (Fig. 2-3B).

2.4.3 AMPK activation mediates eNOS Ser-633 phosphorylation *in vivo*

To correlate the in vitro findings in Fig. 2-1 through Fig. 2-3 with in vivo conditions, we explored whether AMPK regulates eNOS phosphorylation at Ser-633 (rodent and human homolog of bovine eNOS Ser-635) in the mouse vessel wall. C57BL6 wild-type mice were given atorvastatin (50 mg/kg body weight), and eNOS phosphorylation in the aorta was analyzed. Consistent with the results obtained in vitro, AMPK Thr-172 phosphorylation in vivo was increased by atorvastatin for up to 24 hour, a pattern similar to that for phosphorylation of eNOS Ser-633 (Fig. 2-4). In contrast, AMPK and ACC phosphorylation in aortas of AMPKα2$^{-/-}$ mice treated with atorvastatin increased marginally. Furthermore, the phosphorylation levels of eNOS Ser-633 and Ser-1177 in AMPKα2$^{-/-}$ mice were noticeably lower than those in the C57BL6 wild-type mice, with atorvastatin. However, Akt Ser-473 phosphorylation still increased with atorvastatin administration in AMPKα2$^{-/-}$ mice (Fig 2-4).

2.4.4 NO production caused by AMPK phosphorylation of eNOS Ser-635

NO assays were performed to test the functional relevance of AMPK phosphorylating eNOS Ser-633/635. Because HEK293 cells express AMPKα1 and α2 but not eNOS, we transfected these cells with plasmids encoding the wild-type eNOS, 635A, or 635A1179A mutants. The cells were then treated with AICAR to activate AMPK. HEK293 cells were also transfected with phospho-mimetic eNOS mutants 635D or 635D1179D. In eNOS-expressing (wild-type) cells treated with AICAR, the level of NO was elevated, similar to cells transfected with Ad-AMPK-CA (Fig.2-5A). A comparable level of NO production was observed in cells transfected with 635D or 635D1179D. In contrast, NO production was low in cells expressing eNOS 635A or 635A1179A, which mimicked dephosphorylation, with AICAR treatment or with Ad-AMPK-CA infection. The phosphorylation of eNOS Ser-635 and Ser-1179 was increased in cells treated with AICAR (Fig. 2-5B). Phospho-eNOS (S635) antibody could not detect any phosphorylation event in cells transfected with eNOS 635A, which was consistent with the low production of NO. We also compared NO production in murine embryonic fibroblasts (MEFs) isolated from C57BL6 and AMPKα2$^{-/-}$ embryos. As shown in Fig. 2-5C, the ablation of AMPKα2 resulted in impaired NO bioavailability in MEFs expressing eNOS (wild type), at the basal level and under AICAR stimulation. The NO production level was similar in C57BL6 and AMPKα2$^{-/-}$ MEFs transfected with 635D. In addition, supplementing AMPKα2$^{-/-}$ MEFs with Ad-AMPK-CA restored the NO production to the level of that in cells expressing 635D. Taken together, these results suggest that AMPK regulates eNOS function, at least in part, through phosphorylating eNOS Ser-633/635.

2.4.5 AMPK shows comparable activities toward eNOS Ser-633/635 and Ser-1177/1179

Because AMPKα could phosphorylate eNOS Ser-633/635, Ser-1177/1179, and ACC Ser-79, we hypothesized that the 3 substrates might share the same catalytic site(s) within AMPKα, and, therefore, they might be mutually exclusive and compete each other for phosphorylation. To test this, we used synthetic peptides instead of full-length proteins for the kinase activity and substrate competition assays.

Two synthetic peptides with sequences flanking eNOS S633 and S1177 (Fig.2-6A), respectively, showed a phosphorylation level similar to that of SAMS, an ACC homology (Fig. 2-6B). To verify that the 3 peptides bind to the same active site of AMPK with comparable affinities, we performed nano-LC/MS analysis to test the competition between SAMS, S633, and S1177 peptides for AMPKα phosphorylation. The expected mass and *m*/*z* are shown in Table 2-1. A mixture of SAMS and S1177 peptide was included in the AMPKα IP kinase assays. Nano-LC/MS revealed that the phosphorylation of SAMS and S1177 depended on the ratios of peptide mixed (Fig. 2-6C). A similar competition between SAMS and S633 was found (Fig. 2-6D). Furthermore, peptides S633 and S1177 mutually competed with each other for AMPKα (Fig. 2-6E).

Although LC/MS analysis indicated that both S633 and S1177 peptides were phosphorylated by AMPK, the exact amino acids were undetermined. To further elucidate whether Ser-633/635 phosphorylation is physiologically relevant, we immunoprecipitated eNOS from AICAR-treated BAECs for nano-LC/MS/MS analysis.

As shown in Fig. 2-7, phosphorylation of eNOS Ser-635 and Ser-1179 indeed occurred concurrently in ECs with activated AMPK. The phosphorylated Ser within the corresponding tryptic peptides was shown by characteristic neutral loss of the phosphate group (H_3PO_4), which reduced the mass value of Ser from 87 to 69 Da. This result, together with that from peptide competition assay, suggests that Ser-633 and Ser-1177 are comparable AMPK substrates in ECs.

2.5 Discussion

Shear stress, statins, and adiponectin are physiological, pharmacological, and hormonal stimuli that are beneficial for NO bioavailability. All 3 of these stimuli exert positive effects on the phosphorylation of AMPK Thr-172 and eNOS Ser-633/635. In complementary experiments, genetic or pharmacological inhibition of AMPK attenuated phosphorylation of eNOS Ser-633/635, with attendant decrease in NO production. IP kinase assay was previously used to reveal the phosphorylation of Ser-1177/1179 by Akt (Dimmeler et al. 1999; Fulton et al. 1999). Here, we used a similar approach to demonstrate that Ser-633/635 is a direct target site of AMPKα. The hierarchy of AMPK in phosphorylating eNOS Ser-633 in vivo was confirmed in AMPK$\alpha 2^{-/-}$ mice receiving atorvastatin. Because endothelium-dependent vessel dilation is mainly regulated by eNOS-mediated NO release, our data suggest that AMPK-eNOS Ser-633/635 is a major signaling pathway for endothelial biology.

The phosphorylation of Ser-633/635 and Ser-1177/1179 is stimulatory for eNOS activity with increased NO production. The phosphorylation of Ser-635 was more sustained than that of Ser-1179 in BAECs, regardless of type of stimulation (Fig. 2-1).

Among the 4 putative "gain-of-function" eNOS mutants (ie, S116D, S617D, S635D, and S1179D), eNOS S635D was the most efficacious in enhancing NO production (Bauer et al. 2003). Fig. 2-5 indicates that NO production with this mutant was similar to that with 635D1179D, which suggests a possible redundancy of Ser-1179 phosphorylation in regulating NO production. Structurally, Ser-633/635 may be phosphorylated once Ser-1177/1179 is phosphorylated and hence removes the hindrance imposed by AIS II, where Ser-1177/1179 resides.34 IP kinase assay (Fig. 2-2C) showed that Ala mutation of Ser-1177/1179 or Ser-633/635 did not affect the AMPK phosphorylation of either. This finding seems inconsistent with previous observations of Ser-1179 phosphorylation level unchanged with Ser-635 mutated to Ala, whereas Ser-635 phosphorylation was increased with Ser-1179 mutated to Ala (Bauer et al. 2003). This discrepancy might be caused by distinct protein folding of GST-eNOS and endogenous eNOS in living cells.

Several other kinases are implicated in phosphorylating eNOS Ser-633/635 and Ser-1177/1179. PKA, but not Akt, was suggested to phosphorylate eNOS Ser-633/635 (Michell et al. 2001; Boo et al. 2002; Harris et al. 2004). However, PKA, Akt, and CaMKII have been suggested to phosphorylate Ser-1177/1179 (Dimmeler et al. 1999; Fulton et al. 1999; Fleming et al. 2001; Michell et al. 2001; Boo et al. 2002). One major experimental approach in these previous studies was the use of various kinase inhibitors. For example, H89, a PKA inhibitor, when used at 10 μmol/L, also suppressed the AMPK kinase activity by 80% (Davies et al. 2000). We found statin-induced ACC Ser-79 phosphorylation impaired in ECs pretreated with H89 at 10 μmol/L (data not shown). The use of Ad-Akt-DN, H89, KN-93 (a CaMKII inhibitor), and PKA siRNA did not

inhibit the shear stress–induced phosphorylation of AMPK Thr-172 or eNOS Ser-633/635 (Fig. 2-8 and 2-9). Although the atorvastatin-induced eNOS Ser-633 phosphorylation was much attenuated in aortas of AMPK$\alpha 2^{-/-}$ mice, the level of Akt Ser-473 phosphorylation, an indication of Akt activity, remained high (Fig. 2-4). The $\alpha 1$ of AMPK seems to be the major isoform in the endothelium (Schulz et al. 2005). However, knocking out $\alpha 2$ was sufficient to reduce the ACC and eNOS phosphorylation in the ECs and mouse aorta (Fig. 2-3B and 2-4). These results are consistent with a previous finding that the AMPK$\alpha 2$ subunit is more important than $\alpha 1$ in MEFs for the activation of AMPK by hypoxia or glucose deprivation (Laderoute et al. 2006). Previous study by Kemp and colleagues indicated that $\beta 1$ is crucial for the assembly of AMPK heterotrimer (Iseli et al. 2008). Apparently, the aortic expression of $\beta 1$ was slightly affected by the ablation of $\alpha 2$ (data not shown). Thus, the AMPK trimeric complexes consisting of $\alpha 1\beta 1$ in AMPK$\alpha 2^{-/-}$ mice did not seem to exert compensatory activity to phosphorylate eNOS Ser-633.

The SAMS peptide is a modified version of the 15 amino acids flanking ACC Ser-79. AMPK phosphorylates SAMS peptide with a Km of 30±2 μmol/L and Vmax of 8.1±1.5 μmol/min per milligram,(Davies et al. 1989; Weekes et al. 1993) which is about 2.5 times higher than that of ACC. A peptide encompassing HMG-CoA reductase Ser-871, the putative AMPKα phosphorylating site, had a Km of 22±4 μmol/L.41 A 16-aa peptide containing eNOS Ser-1177 was phosphorylated by AMPK, with a Km of 54±6 μmol/L and Vmax of 5.8±0.3 μmol/min per milligram (Chen et al. 1999). We showed

that each of the 19-aa eNOS peptides (i.e., S633 and S1177) could compete with SAMS for AMPKα phosphorylation, and the competition occurred at similar concentrations of the peptides. Thus, AMPKα would phosphorylate eNOS Ser-633/635, eNOS Ser-1177/1179, ACC Ser-79, and HMG-CoA reductase Ser-871 with comparable enzyme kinetics. Such comparability has physiological implications. ACC and HMG-CoA reductase, the rate-limiting enzymes for fatty acid and cholesterol synthesis, are ubiquitously expressed in almost all cell types. Depending on cellular energy level and the ensuing AMPK activation status, ACC, HMG-CoA reductase, and other enzymes involved in metabolism are phosphorylated to regulate energy storage/mobilization. However, eNOS expression is highly restricted to endothelial cells and cardiomyocytes, where NO bioavailability is imperative (Hsieh et al. 2006). AMPK phosphorylates ACC, HMG-CoA reductase, and other AMPK targets in cells where eNOS expression is limited, thereby controlling lipid metabolism. In cardiovascular cells, where eNOS is abundant, eNOS and ACC are competitive substrates for AMPK. Not only energy balance (e.g., lipid synthesis) but also eNOS-mediated NO bioavailability is thus regulated by AMPK in these cells.

The similar enzyme kinetics among eNOS 633, eNOS 1177, HMG-CoA reductase, and SAMS peptides suggests that eNOS, HMG-CoA reductase, and ACC may compete for the same catalytic site(s) of AMPKα. LC/MS/MS analysis showed that both eNOS Ser-633 and Ser-1177 are phosphorylated in AICAR-treated cells (Fig. 2-7). Scott et al suggested that a pseudosubstrate sequence, conserved in the eukaryotic AMPKα, binds to the catalytic groove of AMPKα when AMP does not bind to the γ subunit (Scott

et al. 2007). Because of the resemblance between the peptide sequence of the pseudosubstrate and those flanking AMPK target sites, including ACC Ser-79, HMG-CoA reductase Ser-871, and eNOS Ser-1177, an AMPK consensus recognition motif (~22 aa) was thereby proposed (Towler and Hardie 2007). Interestingly, the deduced hydrophobic and basic residues that are important for AMPK recognition align similarly with those between eNOS Ile-616 and Asp-637.

In conclusion, this study suggests that AMPKα is the primary kinase phosphorylating eNOS Ser-633/635, which is functionally linked to NO bioavailability. The functional and kinetic information reported herein should be useful for future investigation of the structure–function relationship of AMPK catalysis in endothelial biology.

2.6 References

Andrew, PJ and B Mayer (1999). "Enzymatic function of nitric oxide synthases." Cardiovasc Res **43**(3): 521-31.

Arad, M, CE Seidman and JG Seidman (2007). "AMP-activated protein kinase in the heart: role during health and disease." Circ Res **100**(4): 474-88.

Bauer, PM, D Fulton, YC Boo, GP Sorescu, BE Kemp, H Jo, et al. (2003). "Compensatory phosphorylation and protein-protein interactions revealed by loss of function and gain of function mutants of multiple serine phosphorylation sites in endothelial nitric-oxide synthase." J Biol Chem **278**(17): 14841-9.

Boo, YC, J Hwang, M Sykes, BJ Michell, BE Kemp, H Lum, et al. (2002). "Shear stress stimulates phosphorylation of eNOS at Ser(635) by a protein kinase A-dependent mechanism." Am J Physiol Heart Circ Physiol **283**(5): H1819-28.

Boo, YC, GP Sorescu, PM Bauer, D Fulton, BE Kemp, DG Harrison, et al. (2003). "Endothelial NO synthase phosphorylated at SER635 produces NO without requiring intracellular calcium increase." Free Radic Biol Med **35**(7): 729-41.

Butt, E, M Bernhardt, A Smolenski, P Kotsonis, LG Frohlich, A Sickmann, et al. (2000). "Endothelial nitric-oxide synthase (type III) is activated and becomes calcium independent upon phosphorylation by cyclic nucleotide-dependent protein kinases." J Biol Chem **275**(7): 5179-87.

Calvert, JW, S Gundewar, S Jha, JJ Greer, WH Bestermann, R Tian, et al. (2008). "Acute metformin therapy confers cardioprotection against myocardial infarction via AMPK-eNOS-mediated signaling." Diabetes **57**(3): 696-705.

Carling, D, PR Clarke, VA Zammit and DG Hardie (1989). "Purification and characterization of the AMP-activated protein kinase. Copurification of acetyl-CoA carboxylase kinase and 3-hydroxy-3-methylglutaryl-CoA reductase kinase activities." Eur J Biochem **186**(1-2): 129-36.

Chen, H, M Montagnani, T Funahashi, I Shimomura and MJ Quon (2003). "Adiponectin stimulates production of nitric oxide in vascular endothelial cells." J Biol Chem **278**(45): 45021-6.

Chen, ZP, KI Mitchelhill, BJ Michell, D Stapleton, I Rodriguez-Crespo, LA Witters, et al. (1999). "AMP-activated protein kinase phosphorylation of endothelial NO synthase." FEBS Lett **443**(3): 285-9.

Cheng, KK, KS Lam, Y Wang, Y Huang, D Carling, D Wu, et al. (2007). "Adiponectin-induced endothelial nitric oxide synthase activation and nitric oxide production are mediated by APPL1 in endothelial cells." Diabetes **56**(5): 1387-94.

Corton, JM, JG Gillespie, SA Hawley and DG Hardie (1995). "5-aminoimidazole-4-carboxamide ribonucleoside. A specific method for activating AMP-activated protein kinase in intact cells?" Eur J Biochem **229**(2): 558-65.

Davies, SP, D Carling and DG Hardie (1989). "Tissue distribution of the AMP-activated protein kinase, and lack of activation by cyclic-AMP-dependent protein kinase, studied using a specific and sensitive peptide assay." Eur J Biochem **186**(1-2): 123-8.

Davies, SP, H Reddy, M Caivano and P Cohen (2000). "Specificity and mechanism of action of some commonly used protein kinase inhibitors." Biochem J **351**(Pt 1): 95-105.

Dimmeler, S, I Fleming, B Fisslthaler, C Hermann, R Busse and AM Zeiher (1999). "Activation of nitric oxide synthase in endothelial cells by Akt-dependent phosphorylation." Nature **399**(6736): 601-5.

Fleming, I, B Fisslthaler, S Dimmeler, BE Kemp and R Busse (2001). "Phosphorylation of Thr(495) regulates Ca(2+)/calmodulin-dependent endothelial nitric oxide synthase activity." Circ Res **88**(11): E68-75.

Foretz, M, N Ancellin, F Andreelli, Y Saintillan, P Grondin, A Kahn, et al. (2005). "Short-term overexpression of a constitutively active form of AMP-activated protein kinase in the liver leads to mild hypoglycemia and fatty liver." Diabetes **54**(5): 1331-9.

Fulton, D, JP Gratton, TJ McCabe, J Fontana, Y Fujio, K Walsh, et al. (1999). "Regulation of endothelium-derived nitric oxide production by the protein kinase Akt." Nature **399**(6736): 597-601.

Furchgott, RF and JV Zawadzki (1980). "The obligatory role of endothelial cells in the relaxation of arterial smooth muscle by acetylcholine." Nature **288**(5789): 373-6.

Hardie, DG (2007). "AMP-activated protein kinase as a drug target." Annu Rev Pharmacol Toxicol **47**: 185-210.

Harris, MB, MA Blackstone, SG Sood, C Li, JM Goolsby, VJ Venema, et al. (2004). "Acute activation and phosphorylation of endothelial nitric oxide synthase by HMG-CoA reductase inhibitors." Am J Physiol Heart Circ Physiol **287**(2): H560-6.

Helgason, CD (2005). "Culture of primary adherent cells and a continuously growing nonadherent cell line." Methods Mol Biol **290**: 1-12.

Hsieh, PC, ME Davis, LK Lisowski and RT Lee (2006). "Endothelial-cardiomyocyte interactions in cardiac development and repair." Annu Rev Physiol **68**: 51-66.

Iseli, TJ, JS Oakhill, MF Bailey, S Wee, M Walter, BJ van Denderen, et al. (2008). "AMP-activated protein kinase subunit interactions: beta1:gamma1 association requires beta1 Thr-263 and Tyr-267." J Biol Chem **283**(8): 4799-807.

Laderoute, KR, K Amin, JM Calaoagan, M Knapp, T Le, J Orduna, et al. (2006). "5'-AMP-activated protein kinase (AMPK) is induced by low-oxygen and glucose deprivation conditions found in solid-tumor microenvironments." Mol Cell Biol **26**(14): 5336-47.

Lane, P and SS Gross (2002). "Disabling a C-terminal autoinhibitory control element in endothelial nitric-oxide synthase by phosphorylation provides a molecular explanation for activation of vascular NO synthesis by diverse physiological stimuli." J Biol Chem **277**(21): 19087-94.

Lerman, A and AM Zeiher (2005). "Endothelial function: cardiac events." Circulation **111**(3): 363-8.

Levine, YC, GK Li and T Michel (2007). "Agonist-modulated regulation of AMP-activated protein kinase (AMPK) in endothelial cells. Evidence for an AMPK -> Rac1 -> Akt -> endothelial nitric-oxide synthase pathway." J Biol Chem **282**(28): 20351-64.

Li, J, X Hu, P Selvakumar, RR Russell, 3rd, SW Cushman, GD Holman, et al. (2004). "Role of the nitric oxide pathway in AMPK-mediated glucose uptake and GLUT4 translocation in heart muscle." Am J Physiol Endocrinol Metab **287**(5): E834-41.

Loscalzo, J (2001). "Nitric oxide insufficiency, platelet activation, and arterial thrombosis." Circ Res **88**(8): 756-62.

Michell, BJ, Z Chen, T Tiganis, D Stapleton, F Katsis, DA Power, et al. (2001). "Coordinated control of endothelial nitric-oxide synthase phosphorylation by protein kinase C and the cAMP-dependent protein kinase." J Biol Chem **276**(21): 17625-8.

Michell, BJ, MB Harris, ZP Chen, H Ju, VJ Venema, MA Blackstone, et al. (2002). "Identification of regulatory sites of phosphorylation of the bovine endothelial nitric-oxide synthase at serine 617 and serine 635." J Biol Chem **277**(44): 42344-51.

Mount, PF, BE Kemp and DA Power (2007). "Regulation of endothelial and myocardial NO synthesis by multi-site eNOS phosphorylation." J Mol Cell Cardiol **42**(2): 271-9.

Palmer, RM, AG Ferrige and S Moncada (1987). "Nitric oxide release accounts for the biological activity of endothelium-derived relaxing factor." Nature **327**(6122): 524-6.

Schulz, E, E Anter, MH Zou and JF Keaney, Jr. (2005). "Estradiol-mediated endothelial nitric oxide synthase association with heat shock protein 90 requires adenosine monophosphate-dependent protein kinase." Circulation **111**(25): 3473-80.

Scott, JW, FA Ross, JK Liu and DG Hardie (2007). "Regulation of AMP-activated protein kinase by a pseudosubstrate sequence on the gamma subunit." EMBO J **26**(3): 806-15.

Sessa, WC (2004). "eNOS at a glance." J Cell Sci **117**(Pt 12): 2427-9.

Stuehr, DJ (1999). "Mammalian nitric oxide synthases." Biochim Biophys Acta **1411**(2-3): 217-30.

Sun, W, TS Lee, M Zhu, C Gu, Y Wang, Y Zhu, et al. (2006). "Statins activate AMP-activated protein kinase in vitro and in vivo." Circulation **114**(24): 2655-62.

Towler, MC and DG Hardie (2007). "AMP-activated protein kinase in metabolic control and insulin signaling." Circ Res **100**(3): 328-41.

Viollet, B, F Andreelli, SB Jorgensen, C Perrin, A Geloen, D Flamez, et al. (2003). "The AMP-activated protein kinase alpha2 catalytic subunit controls whole-body insulin sensitivity." J Clin Invest **111**(1): 91-8.

Weekes, J, KL Ball, FB Caudwell and DG Hardie (1993). "Specificity determinants for the AMP-activated protein kinase and its plant homologue analysed using synthetic peptides." FEBS Lett **334**(3): 335-9.

Zhang, Y, TS Lee, EM Kolb, K Sun, X Lu, FM Sladek, et al. (2006). "AMP-activated protein kinase is involved in endothelial NO synthase activation in response to shear stress." Arterioscler Thromb Vasc Biol **26**(6): 1281-7.

Fig. 2-1

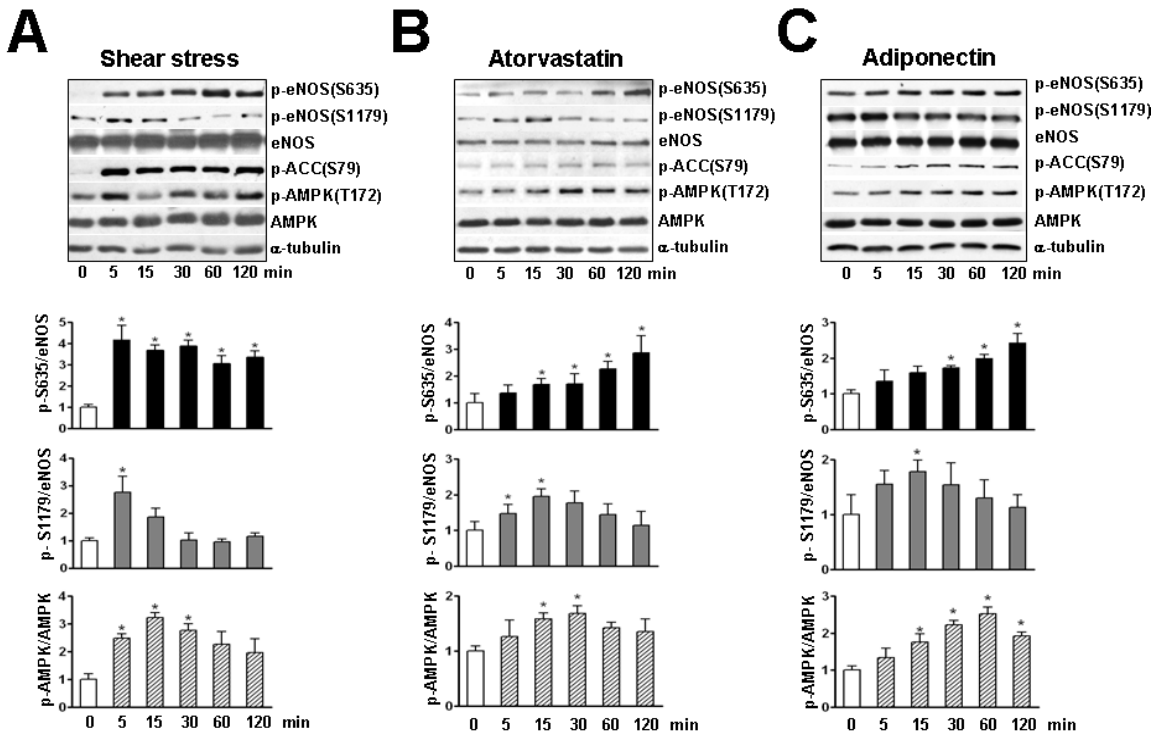

Fig. 2-1 Shear stress, statin, and adiponectin enhance phosphorylation of AMPK Thr172 and eNOS Ser635 in BAECs. Confluent monolayers of BAECs were pre-exposed to laminar shear stress at 5 dyne/cm^2 for 6 hours, which was increased to 12 dyne/cm2 for the durations shown (A), treated with atorvastatin at 1 μmol/L (B), or adiponectin at 30 μg/mL (C) for the indicated times. The cells were then lysed and underwent SDS-PAGE, followed by Western blotting with various primary antibodies. The bar graphs below are densitometry quantifications of the ratios of phospho-eNOS at Ser-635 or Ser-1179 to total eNOS and that of phospho-AMPK Thr-172 to total AMPKα. The data are means±SD from 3 independent experiments, with static cells (A) or untreated controls (B and C) set as 1. **P*<0.05 compared to control groups.

Fig. 2-2

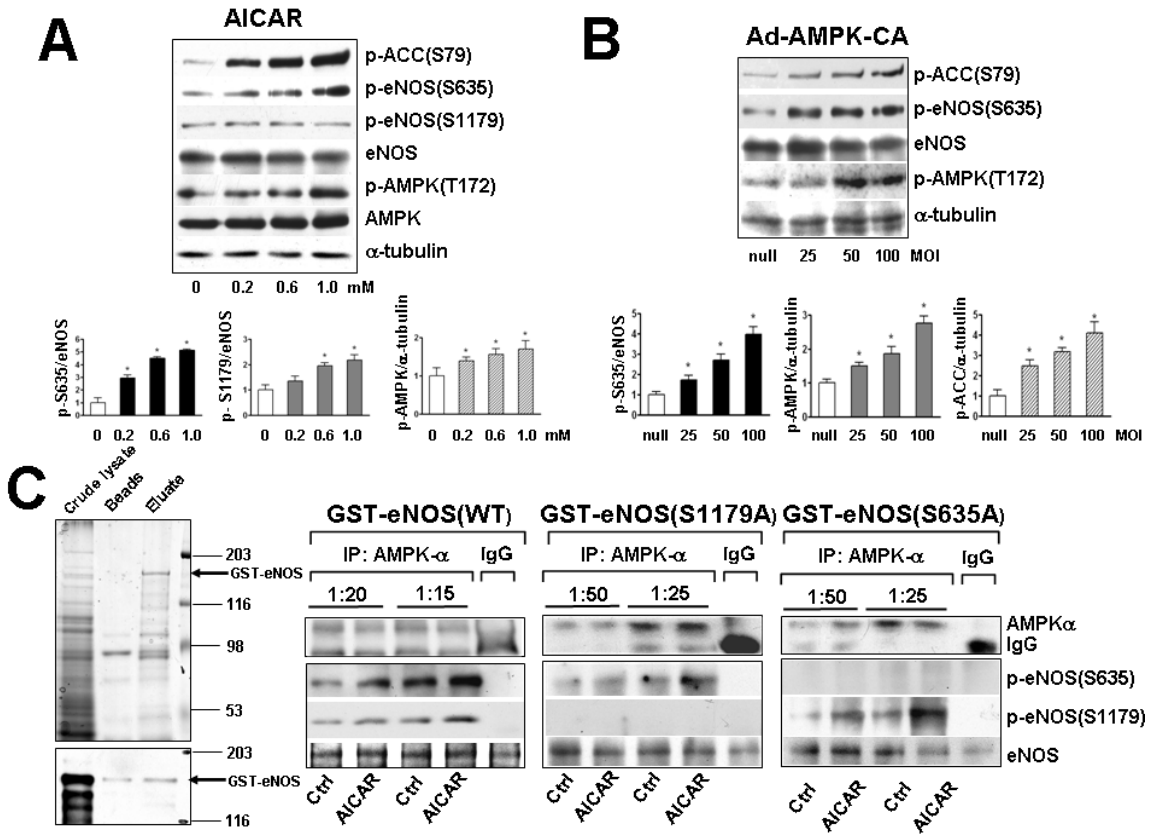

Fig. 2-2 AMPK phosphorylates eNOS Ser-635 in cultured ECs. Confluent BAECs were treated with various concentrations of AICAR for 15 minutes (A) or infected with Ad-AMPK-CA at different multiplicities of infection (MOI) for 24 hours (B). The control cells were infected with Ad-null virus at 50 multiplicities of infection. Cell lysates were analyzed by Western blotting with the indicated antibodies. Bargraphs are densitometry analysis from 3 independent experiments. **P*<0.05 compared to control groups. C, BAECs were treated with AICAR at 1 mmol/L for 15 minutes or left untreated as controls. AMPKα was immunoprecipitated from cell lysates with the use of anti–pan-AMPKα at 1:20 or 1:15 dilution. Rabbit IgG was used as an IP control. The kinase activity of immunoprecipitated AMPKα was assayed with recombinant GST-eNOS (wild type [WT]), GST-eNOS (S1179A), or GST-eNOS (S635A) as substrates. Left, The expressed GST-eNOS is shown by Coomassie blue staining and Western blotting. The phosphorylation of GST-eNOS S1179 and S635 by the immunoprecipitated AMPKα was detected by Western blotting. The level of immunoprecipitated AMPKα and GST-eNOS used in the assays was also shown by immunoblotting. Data represent results from 3 independent experiments.

Fig. 2-3

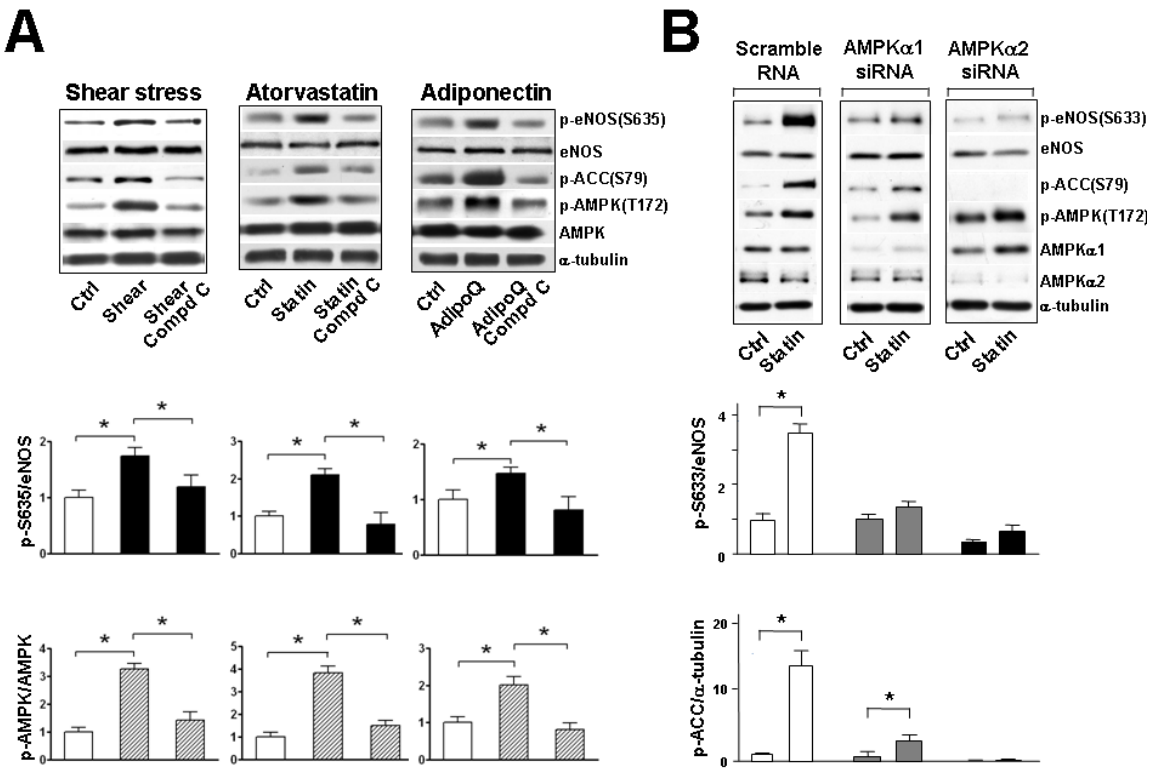

Fig. 2-3 AMPK inhibition attenuates eNOS Ser-635 phosphorylation in ECs. A, BAECs were pretreated with compound C at 20 μmol/L for 30 minutes before undergoing 30-minute treatment with laminar shear stress at 12 dyne/cm^2, atorvastatin at 1 μmol/L, or adiponectin at 30 μg/mL. In B, HUVECs were transfected with AMPKα1siRNA, AMPKα2 siRNA, or scramble RNA (10 nmol/L) before atorvastatin treatment. Phosphorylation of eNOS Ser-635, AMPK Thr-172, and ACC Ser-79 was revealed by Western blotting. The bar graphs represent the densitometry analyses of Western blotting as means±SD of 3 or 4 independent experiments. *P<0.05 between groups as indicated.

Fig. 2-4

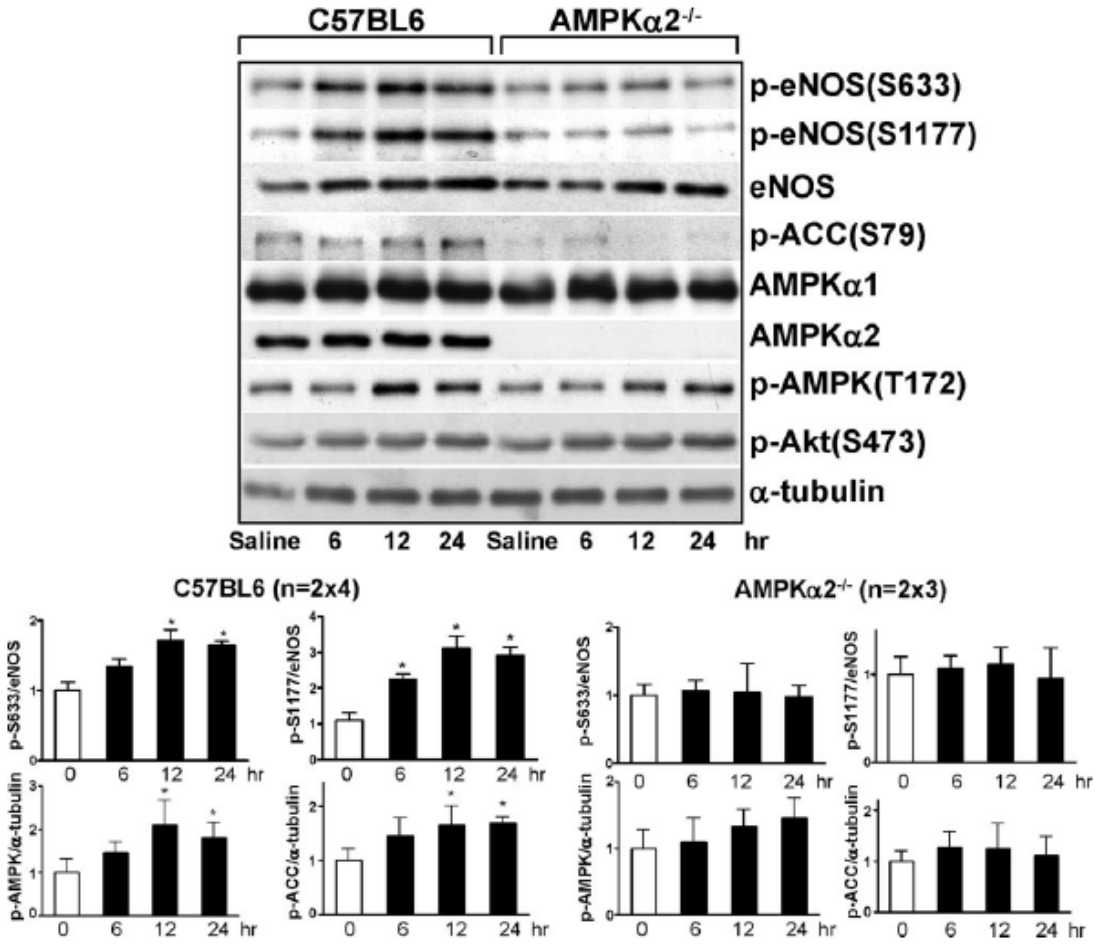

Fig. 2-4 AMPK mediates eNOS Ser-633 phosphorylation in mouse aortas in vivo. C57BL6 (A) or AMPKα2$^{-/-}$ (B) mice were given atorvastatin at 50 mg/kg body weight for the indicated times before euthanasia. In the control group, mice received the same volume (0.5 mL) of saline 6 hours before euthanasia. Tissue extracts from 2 aortas were pooled into 1 sample to be analyzed by Western blotting with various antibodies as indicated. The bar graphs are results of densitometry analyses of the ratio of phospho-eNOS to total eNOS, phospho-AMPK, and phosphor-ACC to α-tubulin. The saline controls were set as 1. Data represent means±SD from 3 independent experiments. **P*<0.05 between atorvastatin-treated and control mice.

Fig. 2-5

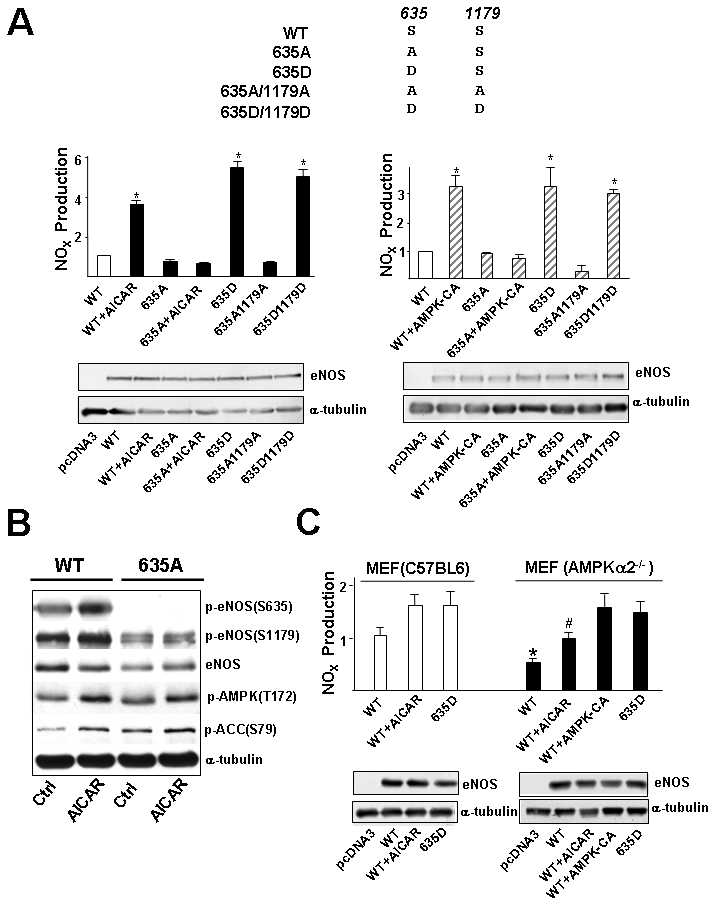

Fig. 2-5 AMPK is necessary for eNOS Ser-635-mediated NO bioavailability.

A, HEK293 cells were transfected with various plasmids expressing the wild-type (WT) and eNOS mutants (i.e.,635A, 635D, 635A/1179A, and 635D/1179D).

One set of cells transfected with WT or 635A was treated with AICAR (1 mmol/L), and in parallel experiments, another set was infected with Ad-AMPKα2-CA (100 MOI). The NO bioavailability from various cells was determined by Griess assay and expressed as NOx. In all experiments, the NOx produced from cells transfected with pcDNA3 was considered background and thus subtracted from total NOx values of all cell groups. On Western blotting, the relative level of expressed eNOS was normalized to that of α-tubulin. NOx production was further normalized to the relative level of eNOS. B, HEK293 cells transfected with WT or 635A eNOS were treated with AICAR (1 mmol/L) for 15 minutes. Cell lysates were resolved on SDS-PAGE and subjected to Western blotting with various antibodies as indicated. C, MEFs isolated from C57BL6 or AMPKα2$^{-/-}$ mice were transfected with various eNOS plasmids in the presence or absence of AICAR or coinfected with Ad-AMPK-CA, as indicated. NOx production was measured accordingly. In A, NOx produced from HEK293 cells transfected with WT-eNOS was set as 1. In C, NOx value corresponding to C57BL6 MEFs transfected with WT-eNOS was set as 1. Data are means±SD from 5 independent experiments. In A, **P*<0.05 compared with HEK293 cells transfected with WT eNOS. In C, **P*<0.05 between C57BL6 MEFs and AMPKα2$^{-/-}$ MEFs transfected with WT-eNOS; #*P*<0.05 between C57BL6 MEFs and AMPKα2$^{-/-}$ MEFs transfected with WT-eNOS and then treated with AICAR.

Fig. 2-6

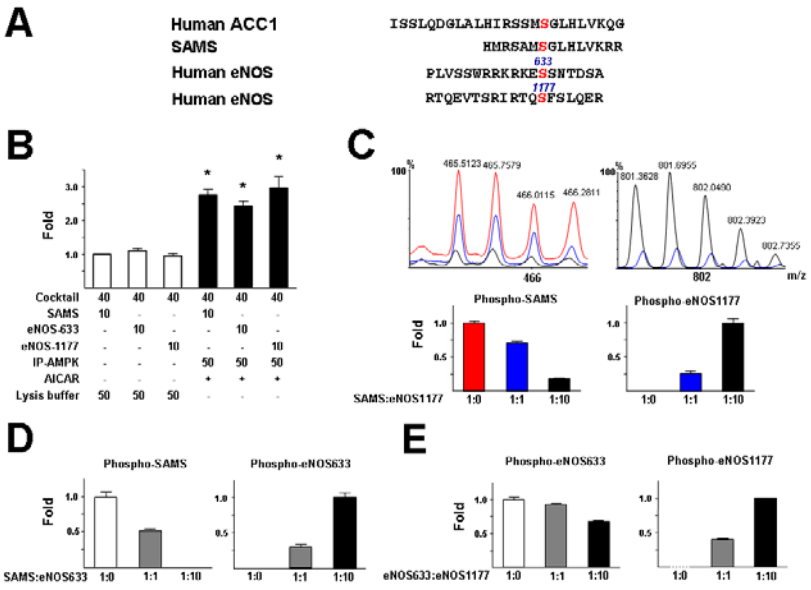

Fig. 2-6 Competition between eNOS Ser-633/635 and Ser-1177/1179 for AMPK phosphorylation detected by LC/MS. Shown in A are peptide sequences of SAMS and those adjacent to human ACC1 Ser-79, human eNOS Ser-633, and human eNOS Ser-1177. The sequences shown indicate the synthesized S633 and S1177 oligopeptides. B, BAECs were treated with AICAR (1 mmol/L) for 15 minutes and lysed. AMPK was immunoprecipitated from BAEC lysates by anti–pan-AMPKα. SAMS, S633, or S1177 (1 mmol/L) together with (γ-32P) ATP (8 μCi) were mixed with the immunoprecipitated AMPKα for IP kinase activity assays. The phosphorylation of SAMS, S633, and S1177 peptides was determined by the incorporation of ^{32}P. The scintillation counts of various samples were normalized to that of control containing reaction cocktail (40 μL), SAMS (10 μL), and lysis buffer (50 μL) set as 1. *P<0.05 compared with control. C, SAMS and S1177 peptides were mixed at ratios of 1:0, 1:1, and 1:10, and the peptide mixture was included in AMPKα IP kinase assays. Nano-LC/MS was performed to detect the phosphorylated SAMS and S1177. The spectra show *m/z* around 466 and 802, with the red, blue, and black lines representing SAMS: S1177 at 1:0, 1:1, and 1:10, respectively. Phosphorylated SAMS and eNOS-633 peptides were detected as positive ions with *m/z* 465.49, 4+, and *m/z* 571.79, 4+, respectively. Quantitation of signal intensity for individual ions was based on the maximal apex–peak height (i.e., ion counts) displayed on the *m/z* spectrum derived from summing all individual scans across the entire retention time of the corresponding ion on the extracted ion chromatogram. The baseline background was subtracted from the above peak height to obtain extracted ion total counts (EITC), which was then used to quantify the changes of phosphorylation level for each peptide, with the highest value set as 1. Data are means±SD from triplicate experiments. Similar analyses were performed to assess the competition between SAMS and S633 (D) or that between S633 and S1177 (E) for AMPKα phosphorylation.

Fig. 2-7

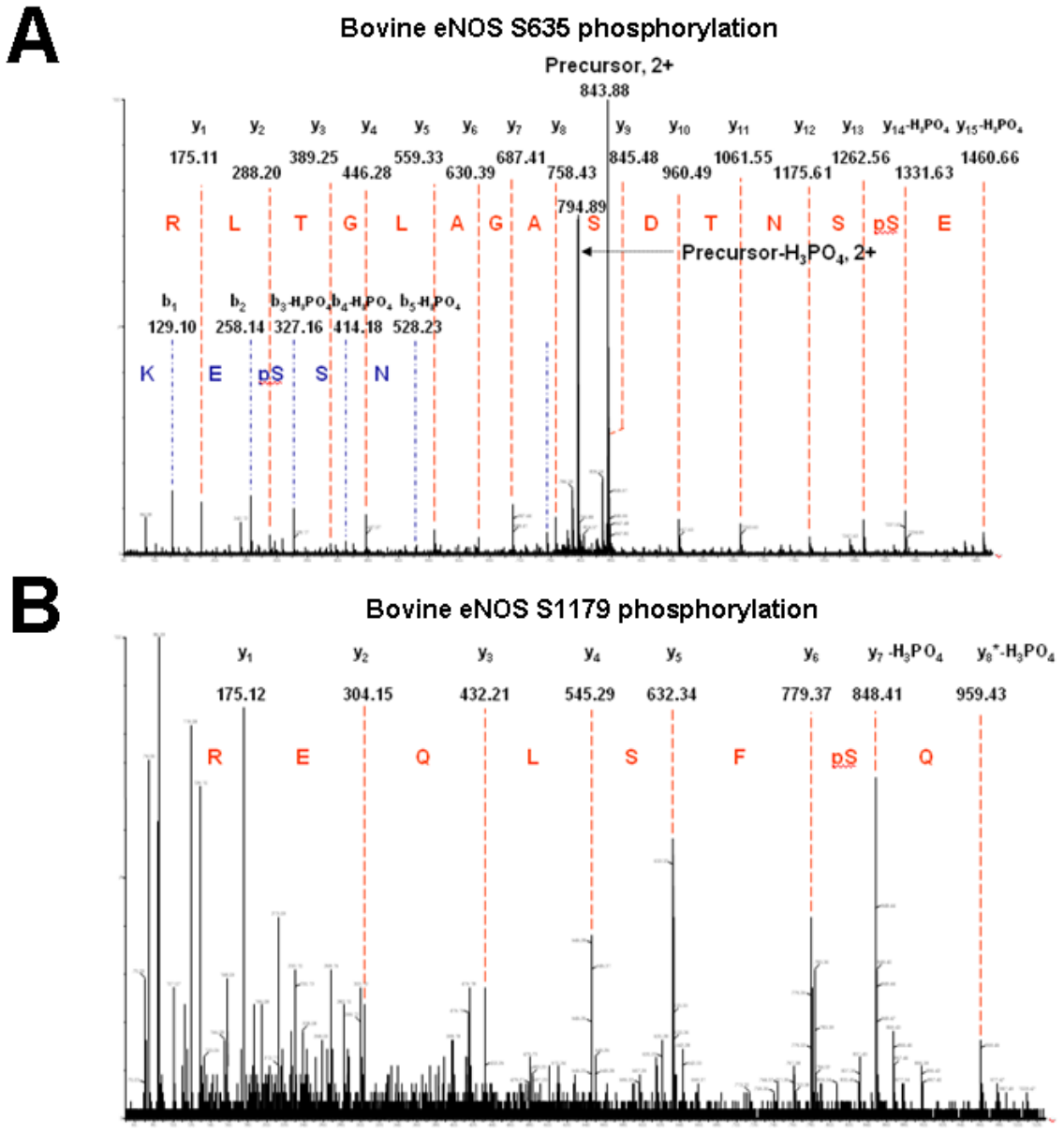

Fig. 2-7 LC/MS/MS analysis of eNOS Ser-635 and Ser-1179 phosphorylation in BAECs. eNOS immunoprecipitated from AICAR-treated BAECs was trypsin-digested and then passed through TiO_2-coated magnetic beads to enrich phosphopeptides. Nano-LC/MS/MS was used to map the phosphorylation site within the peptides containing Ser-635 (A) or Ser-1179 (B).

Fig. 2-8

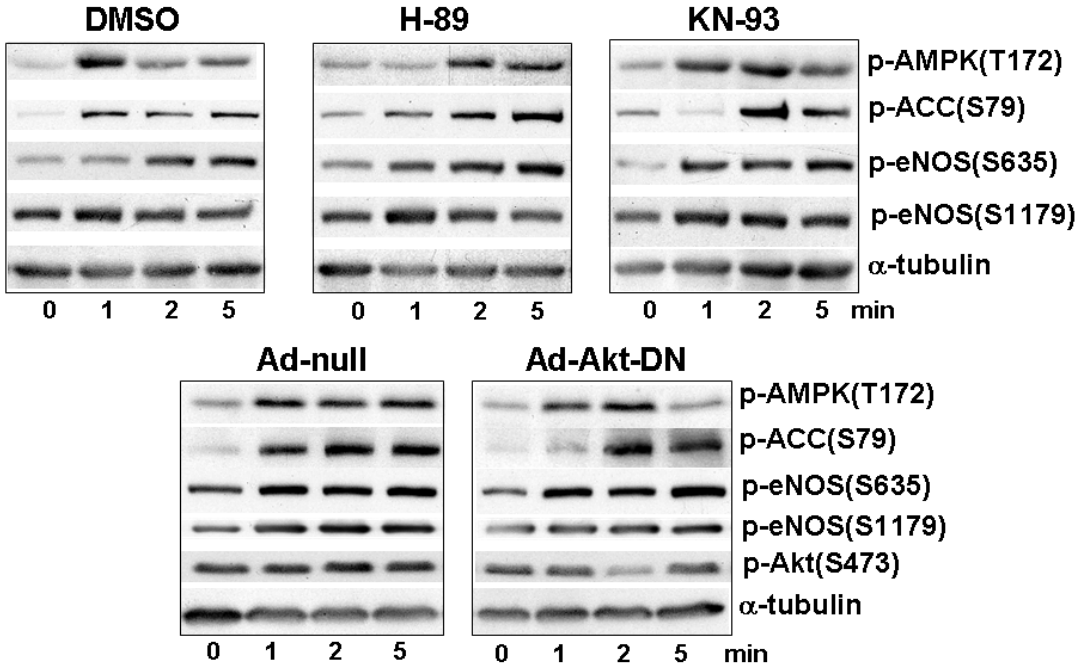

Fig. 2-8 PKA, CaMKII or Akt inhibitors do not inhibit shear stress-increased eNOS Ser-633 phophorylation. BAECs were treated with H89 (50 nM) or KN-93 (1 μM) for 30 minutes or infected with Ad-null control virus (50 MOI) or Ad-Akt-DN (50 MOI) expressing a dominant mutant of Akt. The cells were then subjected to a laminar shear stress at 12 dyne/cm^2 for 1, 2, and 5 minutes. The collected cell lysates were analyzed by Western Blot with various antibodies as indicated.

Fig. 2-9

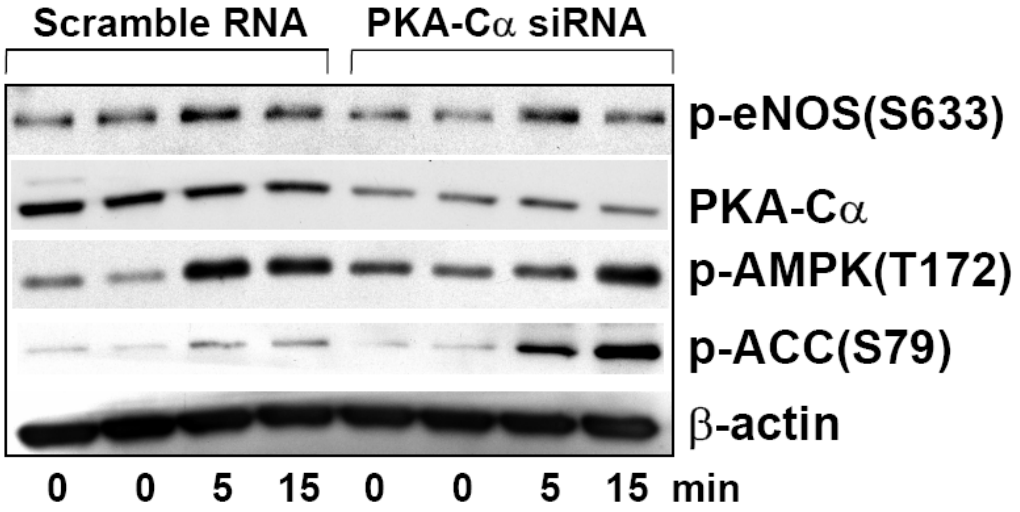

Fig. 2-9 PKA siRNA does not inhibit shear stress increased-eNOS Ser-633 phosphorylation. HUVECs were transfected with scramble or PKACα siRNA (10 pmol) for 48 h before subjected to laminar shear stress (12 dyne/cm^2) for 5 or 15 minutes. Cells kept in static condition were used as control. Whole cell proteins were extracted and resolved by SDS-PAGE, followed by Western blotting with various primary antibodies as indicated.

Table 2-1 The sequence, mass, and m/z for the phosphorylation of SAMS, S633, and S1177 peptides

Peptide	Sequence	Monoisotopic mass		Charge state	m/z [B]
		nonphosphorylated	phosphorylated		
SAMS	HMRSAMSGLHLVKRR[A]	1777.97	1857.93	4+	465.49
S633	PLVSSWRRKRKESSNTDSA	2203.15	2283.11	4+	571.79
S1177	RTQEVTSRIRTQSFSLQER	2321.22	2401.19	3+	801.40

[A] the putative Ser phosphorylation sites

[B] m/z, 3+ (801.40) represents phosphorylated S1177 whereas m/z 4+ (465.49 and 571.79) are those for phosphorylated SAMS and S633.

Chapter 3

Shear Stress, SIRT1, and Vascular Homeostasis

3.1 Abstract

Shear stress imposed by blood flow is crucial for maintaining vascular homeostasis. We examined the role of shear stress in regulating SIRT1, an NAD^+-dependent deacetylase, and its functional relevance *in vitro* and *in vivo*. The application of laminar flow increased SIRT1 level and activity, mitochondrial biogenesis, and expression of SIRT1-regulated genes in cultured endothelial cells (ECs). When the effects of different flow patterns were compared *in vitro*, SIRT1 level was significantly higher in ECs exposed to physiologically relevant pulsatile flow than pathophysiologically relevant oscillatory flow. These results are in concert with the finding that SIRT1 level was higher in the mouse thoracic aorta exposed to athero-protective flow than in the aortic arch under athero-prone flow. Since laminar shear stress activates AMP-activated protein kinase (AMPK), with subsequent phosphorylation of endothelial nitric oxide synthase (eNOS) at Ser-633 and Ser-1177, we studied the interplays of AMPK and SIRT1 on eNOS. Laminar flow increased SIRT1-eNOS association and eNOS deacetylation. By using the AMPK inhibitor and eNOS Ser-633 and -1177 mutants, we demonstrated that AMPK phosphorylation of eNOS is needed to prime SIRT1-induced deacetylation of eNOS to enhance NO production. To verify this finding *in vivo*, we compared the acetylation status of eNOS in thoracic aortas from $AMPK\alpha2^{-/-}$ mice and their $AMPK\alpha2^{+/+}$ littermates. Our finding that $AMPK\alpha2^{-/-}$ mice had a higher eNOS

acetylation indicates that AMPK phosphorylation of eNOS is required for the SIRT1 deacetylation of eNOS. These results suggest that athero-protective flow, via AMPK and SIRT1, increases NO bioavailability in endothelium.

3.2 Introduction

SIRT1, also known as Sirtuin 1 (silent mating type information regulator 2 homolog), contributes to the caloric restriction (CR)-induced increase in life span in species ranging from yeast to mammals (Lin et al. 2000; Bordone et al. 2007; Boily et al. 2008). Functioning as an NAD^+-dependent class III histone deacetylase (Imai et al. 2000), SIRT1 deacetylates multiple targets in mammalian cells, including tumor suppressor p53, Forkhead box O1 and 3 (FOXO1 and FOXO3), ***peroxisome proliferator-activated receptor*** γ (PPARγ) coactivator 1α (PGC-1α), liver X receptor, and hypoxia-inducible factor 2α (Luo et al. 2001; Vaziri et al. 2001; Brunet et al. 2004; Motta et al. 2004; Nemoto et al. 2005; Rodgers et al. 2005; Yang et al. 2005; Lagouge et al. 2006; Li et al. 2007; Ota et al. 2007; Dioum et al. 2009). By regulating these molecules involved in cell survival and in carbohydrate and lipid metabolism, SIRT1 functions as a master regulator of stress response and energy homeostasis.

SIRT1 is also an important modulator in cardiovascular functions in health and disease. The beneficial effects of SIRT1 on endothelial cell (EC) biology were demonstrated by several previous studies. Ota et al. showed that overexpression of SIRT1 prevented oxidative stress-induced endothelial senescence, whereas inhibition of SIRT1 led to premature senescence (Ota et al. 2007; Csiszar et al. 2009). Treatment of human coronary arterial ECs with resveratrol (RSV), an SIRT1 activator, increased the

mitochondrial mass and key factors mediating mitochondrial biogenesis, such as PGC-1α and nuclear respiratory factor 1 (NRF1) (Csiszar et al. 2009). Mattagajasingh et al. demonstrated that inhibition of SIRT1 in rat arteries attenuated endothelium-dependent vasodilation, which might be due to the enhanced acetylation of endothelial nitric oxide synthase (eNOS) (Mattagajasingh et al. 2007). In mice, RSV administration increased aortic eNOS activity (Orimo et al. 2009). Furthermore, EC-specific overexpression of SIRT1 decreased atherosclerosis in ApoE-knockout mice (Zhang et al. 2008).

The endothelium forms a bioactive interface between the circulating blood and the vessel wall. The constant exposure of ECs to shear stress maintains vascular tone, which is mediated in part through its regulation of eNOS. Depending on the flow pattern, the associated shear stress can be athero-protective or athero-prone. Steady pulsatile flow present in the straight parts of the arterial tree is athero-protective, which increases the eNOS-derived NO bioavailability and exerts anti-inflammatory and anti-oxidative effects. In bends and bifurcations, disturbed flow patterns induce the expression of molecules involved in atherogenesis and elevate the level of reactive oxygen species (ROS) in ECs (Chien 2008). Using the flow channel as a model system, we have shown that laminar flow causes activation of AMP-activated protein kinase (AMPK), which in turn phosphorylates eNOS at Ser-633 and -1177, thus leading to enhanced NO bioavailability (Zhang et al. 2006; Chen et al. 2009).

In hepatocytes, SIRT1 regulates lipid metabolism through AMPK (Hou et al. 2008). In skeletal muscles, however, AMPK regulates SIRT1 by modulating the activity of nicotinamide phosphoribosyl transferase (Fulco et al. 2008). A recent report by Canto

et al. (Canto et al. 2009) showed that the phosphorylation of PGC-1α by AMPK primes the PGC-1α deacetylation by SIRT1 in myocytes. These studies suggest that AMPK may crosstalk with SIRT1 to modulate downstream targets. Because shear stress regulates the endothelium in health and disease and both AMPK and SIRT1 play critical roles in endothelial biology, we investigated the effect of shear stress on SIRT1 in ECs and its functional consequences. Our results show that laminar flow elevates SIRT1 in ECs and that the laminar flow-activated SIRT1 acts synergistically with AMPK to increase NO bioavailability *in vitro* and *in vivo*.

3.3 Materials and Method

3.3.1 Antibodies and reagents

The antibodies used in the present study were anti-SIRT1 from Millipore Corp.; anti-pan-AMPKα, anti-phospho-AMPK Thr-172, anti-phospho-ACC Ser-79, anti-acetyl-p53 Lys-379/382, anti-p53, anti-PGC-1α, anti-eNOS, anti-acetylated lysine, anti-PARP-1, anti-α-tubulin, horseradish peroxide-conjugated anti-rabbit and anti-mouse antibodies from Cell Signaling Technology. Anti-phospho-eNOS Ser-633/635, anti-phospho-eNOS Ser-1177/1179, and anti-eNOS used in immunoprecipitation were from BD Transduction Laboratory.

3.3.2 Fluid shear stress experiments

The shear stress experiments were performed as previously described (Guo et al. 2007; Chen et al. 2009; Young et al. 2009). Various types of cells were exposed to laminar flow at 12 dyne/cm^2 for different times. In some experiments, a reciprocating

syringe pump was connected to the circulating system to introduce a sinusoidal component with a frequency of 1 Hz onto the shear stress. Pulsatile shear flow or oscillatory shear flow was applied to ECs with a shear stress of 12 ± 4 dyne/cm^2 or 1 ± 4 dyne/cm^2, respectively.

3.3.3 Cell culture, adenoviral infection, siRNA knockdown, and transient transfection

Human umbilical vein ECs (HUVECs) were cultured in medium M199 (Gibco Life Technology) supplemented with 15% fetal bovine serum (FBS) from Omega, 3 ng/mL β-EC growth factor (Sigma), 4 U/mL heparin (Sigma), and 100 U/mL penicillin-streptomycin. MEFs and HEK293 cells were cultured in DMEM containing 10% FBS.

Ad-AMPK-CA, a recombinant adenovirus expressing a constitutively active (CA) form of AMPKα2, was described previously (Foretz et al. 2005). MEFs at 70% confluency were seeded on 6-well plates and infected with Ad-null or Ad-AMPK-CA at 100 multiplicities of infection (MOI) and incubated for 24 hr before further experimentation.

Transient transfection was performed with Lipofectamine RNAiMAX (Invitrogen). In brief, HUVECs at 70% confluency were transfected with AMPKα1 and AMPKα2 at 10 nM each (Qiagen, SI02622235, SI02758595), and SIRT1 (Qiagen, SI00098434) or scramble (ctrl) siRNA, each at 20 nM, in Opti-MEM (Gibco). Four hours after transfection, the medium was changed to fresh M199, and cells were kept in culture for 48 hr before shear stress experiments.

Human embryonic kidney 293 (HEK293) cells were transiently transfected with 1 μg of respective DNA and 2.5 μl Lipofectamine 2000 (Invitrogen) per 10^6 cells, following a standard protocol. Twenty-four hours after transfection, cells were infected with Ad-SIRT1 or Ad-SIRT1-DN (Luo et al. 2001) for another 24 hr.

3.3.4 Western blot analysis and immunoprecipitation

Lysates from ECs, MEFs, HEK293 cells, or mouse aortas were resolved on 8% SDS-PAGE, and proteins were transferred to PVDF membrane. The immunoblotting with different antibodies followed instructions provided by various manufacturers. Immunoprecipitation for SIRT1 and eNOS was performed following the standard protocol provided by manufacturers (Millipore Corp. for SIRT1 and BD Biosciences for eNOS).

3.3.5 Quantitative RT-PCR

Total RNA was isolated with Trizol reagent (Invitrogen). Reverse transcription was carried out with 3 μg of total RNA by the Superscript II reverse transcriptase (Invitrogen). The synthesized cDNA was used to perform real-time quantitative PCR (qPCR) with the iQ SYBR Green supermix (Bio-Rad, Hercules, CA) on the iCycler real-time PCR detection system (Bio-Rad). The sequences of primer sets used were as follows: for PGC1α,

forward: GGAGCAATAAAGCGAAGA; reverse: GAGGAGTTGTGGGAGGAG;

for NRF1,

forward: ACTCTACAGGTCGGGGAAAA; reverse: AGTGAGACAGTGCCATCAGG; for COX4,

forward: GCAGTGGCGGCAGAATGT; reverse: GGCTAAGCCCTGGATGGG.

3.3.6 NAD^+ measurement and MTT assays

The cellular level of NAD^+ and was measured as previously described (Jacobson and Jacobson 1976). The cell extract was neutralized and centrifuged to collect the supernatant. 40 μl of supernatant was added to 80 μl of an NAD^+ reaction mixture and incubated for 5 min at 37°C. After measuring the basal absorbance at 570 nm, the reaction was initiated by adding 20 μl of alcohol dehydrogenase solution and then incubated at 37°C for 20 min. The absorbance of the reaction mixture was determined again at 570 nm. The NAD^+ level was obtained by subtracting the basal absorbance from the second reading.

3-(4,5-dimethylthiazol-2-yl)-2,5-diphenyltetrazolium Bromide (MTT, Molecular Probes) was used to assess mitochondrial activity with a protocol adapted from Xia et al. 2006 (Xia and Laterra 2006). HUVECs were incubated with 150 μg/ml MTT under normal growth conditions (5% CO_2, 37°C) for 2 hr. The medium was removed, the formazan product was dissolved in DMSO, and the solution was then incubated at 37°C for 10 min. The absorbance of formazan product from MTT was measured at 540 nm by using a spectrophotometer. After subtracting the background, the reading was normalized to total protein concentration.

3.3.7 NO bioavailability assays

The NO production from cells transfected with various plasmids was detected as the accumulated nitrite (NO_2^-), a stable breakdown product of NO, in cell culture media by using Griess reagent (Sigma). An aliquot of cell culture media was mixed with an equal volume of Griess reagent and then incubated at room temperature for 15 minutes. The azo dye production was analyzed by use of a spectrophotometer with absorbance set at 540 nm.

3.3.8 SIRT1 activity assay

SIRT1 activity was assessed as previously described (Fulco et al. 2008), with minor modification. Briefly, 10-20 μg of EC extracts were used in a deacetylation assay, with Fluor de Lys-SIRT1 as the substrate (Biomol). The deacetylation of the substrate was measured by use of a microplate-reading fluorimeter, with excitation set at 380 nm and emission at 460 nm.

3.3.9 Mitotracker and immunofluorescence staining

Mitotracker Green FM (Invitrogen) was used to stain mitochondria in HUVECs as previously described (Schulz et al. 2008). The cells were washed twice with PBS and then incubated with 20 nM Mitotracker Green FM for 30 min. After 3 washes with PBS, the cells were subjected to fluorescence detection (excitation, 490 nm; emission, 516 nm) by using a Leica SP2 confocal microscope.

For immunostaining, HUVECs were fixed with 4% paraformaldehyde in PBS (pH 7.4) for 30 min at room temperature. For *en face* staining, mouse aortas were perfused with 4% paraformaldehyde in PBS for 15 min, and the dissected specimens were fixed for another 60 min after the removal of tunica adventitia. Primary antibodies, i.e., rabbit

anti-SIRT1 and mouse anti-eNOS, were applied at 1:100 dilution to the specimens, which were incubated at 4°C overnight and then washed off with PBS and 0.1% Tween-20 (PBST), followed by the application of Alexa Fluor 488-conjugated chicken anti-rabbit or Alexa Fluor 555-conjugated chicken anti-mouse (Invitrogen). After PBST wash, coverslips were mounted with Prolong Gold Antifade Reagent (Invitrogen) and viewed with a Leica SP2 confocal microscope. For all immunofluorescence experiments, parallel groups of cells or aorta specimens were stained with only primary antibody or secondary antibody as a control. Multiple images were captured from 3-4 regions in the aortic arch and thoracic aorta of every mouse.

3.3.10 Animal experiments

The animal experimental protocols were approved by the Institutional Animal Care and Use Committee of University of California, Riverside. The thoracic aorta and aortic arch from male C57BL6 mice older than 20 weeks were isolated for both Western blot analysis and *en face* immunostaining as previously described (47,48). In addition, thoracic aortas were dissected from 20-week-old AMPK$\alpha 2^{-/-}$ mice and their AMPK$\alpha 2^{+/+}$ littermates. Tissue extracts from aortas were pooled for eNOS immunoprecipitation and immunoblotting.

3.3.11 Statistical analysis

The significance of variability was determined by Student's *t* test or one-way ANOVA. All results are presented as mean±SD from at least 3 independent experiments. Unless otherwise indicated, $p<0.05$ was considered statistically significant.

3.4 Results

3.4.1 Shear stress increases SIRT1 level/activity in ECs

To explore whether shear stress regulates SIRT1 and AMPK in ECs, we applied a laminar flow at 12 dyne/cm^2 to HUVECs for various durations. Western blot analysis revealed that laminar flow increased the SIRT1 level and AMPK phosphorylation at Thr-172 and that these elevations lasted for at least 16 hr (Fig. 3-1A). Concomitant with the increase in SIRT1 level, shear stress also augmented its deacetylase activity, as demonstrated by the decreased acetylation of Arg-His-Lys-Lys(ac) (Fig. 3-1B). Because p53 Lys-382 is an SIRT1 target site (Langley et al. 2002), the acetylation status of this Lys in ECs was examined. Shear stress decreased the acetylation of p53 Lys-382 in cells under shear stress, as compared to static controls (Fig. 3-1C). Because the enzymatic activity of SIRT1 depends on the cellular level of NAD^+ and shear stress has been shown to increase the activity of NAD(P)H oxidase, which converts NADH to NAD^+ (De Keulenaer et al. 1998), we compared the cellular level of NAD^+ in ECs under shear stress and in controls. Compared with static control conditions, laminar flow increased NAD^+ level by ~50% (Fig. 3-1D). Together, Fig. 3-1 suggests that laminar flow elevates SIRT1 level with an attendant increase in SIRT1 deacetylation activity.

3.4.2 Shear stress increases mitochondrial biogenesis in ECs

In several cell types, the elevation of SIRT1 is tightly correlated with increased mitochondrial biogenesis (Lagouge et al. 2006; Canto et al. 2009; Csiszar et al. 2009). In the present study, laminar flow indeed increased the mitochondrial mass (Fig. 3-2A), with attendant increase in the activity of mitochondrial reductase (Fig. 3-2B). Because

PGC-1α and NRF1 are key regulators of mitochondrial biogenesis and COX4 is involved in the mitochondrial respiratory chain (Hock and Kralli 2009), we examined whether laminar flow increases the expression of these molecules in ECs. As shown in Fig. 3-2C, laminar flow increased the mRNA level of PGC-1α, NRF1, and COX4 in a time-dependent manner. Importantly, SIRT1 knockdown by small interfering RNA (siRNA) abolished the flow-induced PGC-1α, NRF1, and COX4 (Fig. 3-2D,E). These results suggest that laminar flow increases mitochondrial biogenesis in ECs and that this effect is mediated through SIRT1.

3.4.3 Shear stress induction of SIRT1 is independent of AMPK

Depending on the stimuli, AMPK and SIRT1 can regulate each other reciprocally (Fulco et al. 2008; Hou et al. 2008). Because laminar flow concurrently activated AMPK and SIRT1, we investigated whether AMPK regulates SIRT1 or vice versa in ECs under shear stress. As shown in Fig. 3A, AMPKα knockdown by siRNA did not affect the laminar flow-induction of SIRT1, indicating that AMPK is not upstream of SIRT1. That the shear-induced increase in SIRT1 level is independent of AMPK was further verified by the finding that ablation of both AMPKα1 and α2 in MEFs had little effect on the shear induction of SIRT1 (Fig. 3-3C). Furthermore, the level of SIRT1 was comparable in wild-type MEFs infected with Ad-null or Ad-AMPK-CA expressing the constitutively activated form of AMPK (Fig. 3-3E). These experiments demonstrate that AMPK is neither necessary nor sufficient for the laminar flow-induced SIRT1. We also knocked down SIRT1 in ECs and used MEFs isolated from SIRT1-null mouse embryos to determine whether SIRT1 regulates AMPK. As shown in Fig. 3-3B,D, laminar flow was

still able to activate AMPK in EC with SIRT1 knocked down or in SIRT1$^{-/-}$ MEFs, indicating that SIRT1 is also not upstream to AMPK in our system. The results presented in Fig. 3-3 suggest that AMPK and SIRT1 are independently activated by laminar flow; neither is upstream to the other.

3.4.4 AMPK and SIRT1 synergistically activate eNOS

Although AMPK and SIRT1 were independently activated by laminar flow, there is the possibility that they may act synergistically on eNOS to increase NO bioavailability. Hence, we examined first whether laminar flow can increase the association of SIRT1 with eNOS. Following immunoprecipitation of SIRT1 from ECs, subsequent anti-eNOS immunoblotting showed an increase in the level of co-immunoprecipitated eNOS in lysates from ECs that had been subjected to laminar flow (Fig. 3-4A). The increased association between SIRT1 and eNOS in ECs exposed to laminar flow was further confirmed by double immunostaining (Fig. 3- 4B).

Next, we examined the functional consequence of the SIRT1-eNOS association. eNOS immunoprecipitation followed by immunoblotting with an antibody recognizing acetylated Lys revealed that acetylation of eNOS was decreased in ECs exposed to laminar flow (Fig. 3-4C). We have shown that the application of laminar flow causes AMPK activation before SIRT1 elevation ((Chen et al. 2009) and Fig. 3-1), suggesting that eNOS phosphorylation by AMPK may prime eNOS for deacetylation by SIRT1. This possibility was verified by the finding that the increase in eNOS phosphorylation and deacetylation induced by laminar flow were blocked by the AMPK-inhibitor

Compound C (Fig. 3-4C). In contrast, SIRT1 inhibition by nicotinamide (NAM in Fig. 3-4C) abolished eNOS deacetylation without affecting eNOS phosphorylation.

To further delineate the requirement of eNOS phosphorylation for SIRT1 deacetylation, we transfected HEK293 cells with plasmids overexpressing gain- or loss-of-function mutants of bovine eNOS (bovine eNOS Ser-635 and -1179 corresponds to human eNOS Ser-633 and -1177). S635D and S1179D (Asp replacing Ser) are the phosphomimetics that simulates the phosphorylation by AMPK, whereas S635A and S1179A (Ala replacing Ser) are the nonphosphorylatable mutants. As shown in Fig. 3-4D, eNOS S635A and S1179A were more acetylated than the wild-type, S635D, or S1179D. The transfected cells were also infected with adenovirus overexpressing the wild-type SIRT1 (Ad-SIRT1) to mimic the induction by flow (Fig. 3-4E). In parallel control experiments, cells were infected with a dominant negative mutant of SIRT1 (Ad-SIRT1-DN) (Fig. 3-4F). Overexpression of Ad-SIRT1, but not Ad-SIRT1-DN, increased NO production by cells overexpressing S635D or S1179D. In cells transfected with S635A or S1179A, the NO production was not changed by overexpressing SIRT1, nor by using SIRT1-DN (Fig. 3-4E,F).

3.4.5 Pulsatile and oscillatory flows have opposite effects on regulating SIRT1

To correlate the results obtained from flow channel experiments with physiological and pathophysiological flow conditions in arteries, we compared the SIRT1 level in ECs subjected to pulsatile flow (12 ± 4 dyne/cm^2) and oscillatory flow (1 ± 4 dyne/cm^2) representing steady flow that has a distinct direction and disturbed flow with little net direction, respectively. As shown in Fig. 3-5A, pulsatile flow but not oscillatory

flow increased the SIRT1 level in ECs. As a positive control, RSV treatment increased the SIRT1 level in ECs similar to that with pulsatile flow. Consistent with the increase in SIRT1 level, the NAD^+ level in ECs was higher under pulsatile than oscillatory flow (Fig. 3-5B). Mitochondrial mass, revealed by Mitotracker Green staining, was also increased by pulsatile but not oscillatory flow (Fig. 3-5C).

Poly(ADP-ribose) polymerase-1 (PARP-1), which is highly sensitive to ROS, consumes NAD^+ for catalysis of poly(ADP-ribosyl)ation on target proteins (Ha and Snyder 1999; Chiarugi 2002). Since oscillatory flow causes a sustained activation of NAD(P)H oxidase and a high level of intracellular ROS (De Keulenaer et al. 1998; Hwang et al. 2003), we considered the possibility that PARP-1 may be involved in the differential regulation of SIRT1 in ECs subjected to different flow patterns. Fig. 3-5D shows the level of PARP-1 was indeed higher under oscillatory than pusaltile flow.

3.4.6 Differential regulation of SIRT1-eNOS in the vessel wall

To determine whether SIRT1 is differentially regulated in athero-prone versus athero-protective areas in the arterial tree, we isolated the aortic arch and thoracic aorta from C57BL6 mice. These areas correspond to regions under disturbed and pulsatile flows, respectively (Suo et al. 2007). Western blot analysis showed that the SIRT1 level was higher in the thoracic aorta (under pulsatile flow) than in the aortic arch (under disturbed flow) (Fig. 3-6A). Because the isolated tissues were a mixture of ECs, vascular smooth muscle cells, and connective tissues, we performed *en face* staining on the mouse arterial tree. Confocal microscopy revealed that the level of SIRT1 in the endothelium of the thoracic aorta was significantly higher than that in the inner curvature of the aortic

arch (Fig. 3-6B). Furthermore, colocalization of SIRT1 and eNOS was noticeably higher in the thoracic aorta than aortic arch endothelium. To confirm the synergistic effect of AMPK and SIRT1 on eNOS *in vivo*, we compared the phosphorylation and acetylation of eNOS in thoracic aortas from AMPK$\alpha 2^{-/-}$ mice and their AMPK$\alpha 2^{+/+}$ littermates. As seen in Fig. 3-6C, D, acetyl-CoA carboxylase (ACC), the AMPK canonical target, and eNOS phosphorylations were lower, while eNOS acetylation level was higher in the thoracic aortas of AMPK$\alpha 2^{-/-}$ mice, as compared with their AMPK$\alpha 2^{+/+}$ littermates. However, the SIRT1 level was comparable between the two lines of mice. These results suggest that eNOS deacetylation by SIRT1 in the vessel wall requires AMPK.

3.5 Discussion

Dysfunctional ECs, signified by enhanced inflammation and oxidative stress, prelude atherosclerosis and other vascular impairments. The effects of shear stress on ECs can be athero-protective or athero-prone depending on the associated flow patterns. Because SIRT1 exerts anti-inflammatory and anti-oxidative effects on various cell types, including ECs, we studied the shear stress regulation of SIRT1 in ECs. Our results indicate that laminar flow causes a marked increase in SIRT1 level, and that AMPK and SIRT1 synergistically increase the eNOS-derived NO bioavailability in ECs responding to laminar flow.

Consistent with its effects of elevating the levels of SIRT1 and NAD^+, laminar flow increased the mitochondria mass and levels of PGC-1α, NRF1, and COX4. siRNA knockdown experiments presented in Fig. 3-2 showed that these key regulators of mitochondrial biogenesis are upregulated by the flow-elevated SIRT1 (Fig. 3-2C-E).

Increased mitochondrial biogenesis is implicated in the balance of the endothelial redox state (Davidson and Duchen 2007). By scavenging free radicals (e.g., ROS and reactive nitrogen species) through PGC-1α-induced ROS detoxifying enzymes (St-Pierre et al. 2006), the laminar flow-enhanced mitochondrial biogenesis may protect ECs against oxidative stress. We have previously shown that laminar flow activates endogenous PPARγ and its target genes in ECs and that these effects are ligand-dependent (Liu et al. 2004). Together with the ligand-activated PPARγ, the elevated PGC-1α, functioning as a transcriptional coactivator of PPARγ, may also contribute to the positive effects of PPARγ on EC biology, including reverse cholesterol transport, anti-inflammation, and anti-atherosclerosis (Tontonoz and Spiegelman 2008). In addition, laminar flow is known to arrest the EC cycle at the G0/G1 phase (Lin et al. 2000), which may explain the quiescence of ECs in the straight part of the arterial tree. Inhibition of SIRT1 by sirtinol or siRNA causes premature senescence-like growth arrest in ECs (Ota et al. 2007). The implication of this notion in the current study is that the elevated SIRT1 by laminar flow may ameliorate aging-related senescence of ECs, even if they are quiescent.

eNOS-derived NO bioavailability, which is critically important for EC physiological functions, is regulated by multiple mechanisms at transcriptional and post-translational levels (Sessa 2004). Among the various mechanisms, phosphorylations at Ser-633 and Ser-1177 enhance eNOS activity, and AMPK can phosphorylate both sites (Boo et al. 2006; Zhang et al. 2006; Chen et al. 2009). Although the shear stress activation of AMPK and SIRT1 seem to be independent processes, the activated AMPK and SIRT1 converge at eNOS in that AMPK phosphorylation may prime eNOS for

SIRT1 deacetylation (depicted in Fig. 3-6E). Such a model is supported by the following observations: eNOS was no longer deacetylated following inhibition of AMPK activity by Compound C (Fig. 3-4C); and eNOS S635A and S1179A were much more acetylated than eNOS S635D and S1179D (Fig. 3-4D). This mode of action is reminiscent of the synergistic effects of AMPK and SIRT1 on PGC-1α (Canto et al. 2009). By using AMPKα2$^{-/-}$ mice, we showed that this synergism occurs *in vivo*. Because shear stress appears to preferentially activate AMPKα2 in ECs (Fisslthaler and Fleming 2009) and AMPKα1 ablation caused anemia and severe splenomegaly in the knockout animals (Foller et al. 2009), AMPKα2$^{-/-}$ instead of AMPKα1$^{-/-}$ mice were used. AMPKα2 ablation resulted in a lower level of eNOS phosphorylation and a higher level of eNOS acetylation, even though SIRT1 was as abundant as in the wild-type (Fig. 3-6C, D). These results indicate that AMPK phosphorylation of eNOS is required for the deacetylation by SIRT1 in the mouse thoracic aorta. SIRT1 inhibition by nicotinamide resulted in superphosphorylation of eNOS (Fig. 3-4C). It seems that eNOS deacetylation is also correlated with its dephophorylation. Such a mechanism may restore the set point for eNOS activation. Despite that eNOS phosphorylation sites have been extensively studied, the acetylation sites remain unclear. Two potential residues are Lys-494 and Lys-504 (Mattagajasingh et al. 2007). The identification of SIRT1-targeted sites in eNOS and their interplay with phosphorylation sites warrant future research.

Cellular NAD^+ level can modulate SIRT1 activity and expression (Lin et al. 2004; Zhang et al. 2007). Thus, one possible mechanism by which laminar/pulsatile flow augments SIRT1 level and/or activity is through the elevated NAD^+ level. Such an

enhanced oxidized state in ECs may be caused by the increase in NAD^+ (Fig. 3-1D, 3-5B) resulting from an increased activity of NAD(P)H oxidase. Indeed, laminar flow induces a transient increase in the activity of NAD(P)H oxidase (De Keulenaer et al. 1998). Previously, Nisoli et al. found that the SIRT1 induction by CR involves eNOS-derived NO, as evidenced by the attenuated SIRT1 in white adipose tissue of the eNOS-null mice (Nisoli et al. 2005). However, laminar flow was able to increase SIRT1 level in eNOS-null MEFs and in HUVECs treated with the NOS inhibitor, nitro-L-arginine methyl ester (L-NAME) (Fig.3-7). These results suggest that the flow-induction of SIRT1 does not depend on eNOS. One possible explanation for this independency is that the moderate and transient increase in ROS by pulsatile flow is able to induce SIRT1. This is in line with the recent finding that oxidative stress generated by short-term H_2O_2 treatment enhanced SIRT1 (Nasrin et al. 2009). In contrast to pulsatile flow, oscillatory flow causes a sustained activation of NAD(P)H oxidase with an attendant strong elevation of ROS (De Keulenaer et al. 1998; Hwang et al. 2003; Hwang et al. 2003). This pathophysiological ROS level should induce or activate PARP-1 (Chiarugi 2002), which in turn depletes cellular NAD+ to diminish the expression or activity of SIRT1 as seen in Fig. 3-5A, B.

The differential effects of pulsatile vs. oscillatory flow on SIRT1 expression was verified in the mouse arterial tree (Fig. 3-6). SIRT1 level was higher, with increased eNOS co-localized in the athero-protective areas. It is known that endothelial dysfunction (which is signified by increased oxidative and inflammatory responses) predisposes the arteries to atherosclerosis. Hence, SIRT1 activation by pulsatile flow

may prevent EC dysfunction and counteract the risk factors associated with atherosclerosis. Compared with therapeutic interventions such as RSV and several small molecules developed for SIRT1 activation, shear stress would be more physiologically relevant. The molecular basis underlying the marked differences between pulsatile and oscillatory flows in the modulation of SIRT1 may provide new insights into the mechanism of regulation of EC biology by shear stress.

3.6 References

Boily, G, EL Seifert, L Bevilacqua, XH He, G Sabourin, C Estey, et al. (2008). "SirT1 regulates energy metabolism and response to caloric restriction in mice." PLoS One **3**(3): e1759.

Boo, YC, HJ Kim, H Song, D Fulton, W Sessa and H Jo (2006). "Coordinated regulation of endothelial nitric oxide synthase activity by phosphorylation and subcellular localization." Free Radic Biol Med **41**(1): 144-53.

Bordone, L, D Cohen, A Robinson, MC Motta, E van Veen, A Czopik, et al. (2007). "SIRT1 transgenic mice show phenotypes resembling calorie restriction." Aging Cell **6**(6): 759-67.

Brunet, A, LB Sweeney, JF Sturgill, KF Chua, PL Greer, Y Lin, et al. (2004). "Stress-dependent regulation of FOXO transcription factors by the SIRT1 deacetylase." Science **303**(5666): 2011-5.

Canto, C, Z Gerhart-Hines, JN Feige, M Lagouge, L Noriega, JC Milne, et al. (2009). "AMPK regulates energy expenditure by modulating NAD+ metabolism and SIRT1 activity." Nature **458**(7241): 1056-60.

Chen, Z, IC Peng, W Sun, MI Su, PH Hsu, Y Fu, et al. (2009). "AMP-activated protein kinase functionally phosphorylates endothelial nitric oxide synthase Ser633." Circ Res **104**(4): 496-505.

Chiarugi, A (2002). "Poly(ADP-ribose) polymerase: killer or conspirator? The 'suicide hypothesis' revisited." Trends Pharmacol Sci **23**(3): 122-9.

Chien, S (2008). "Effects of disturbed flow on endothelial cells." Ann Biomed Eng **36**(4): 554-62.

Csiszar, A, N Labinskyy, JT Pinto, P Ballabh, H Zhang, G Losonczy, et al. (2009). "Resveratrol induces mitochondrial biogenesis in endothelial cells." Am J Physiol Heart Circ Physiol **297**(1): H13-20.

Davidson, SM and MR Duchen (2007). "Endothelial mitochondria: contributing to vascular function and disease." Circ Res **100**(8): 1128-41.

De Keulenaer, GW, DC Chappell, N Ishizaka, RM Nerem, RW Alexander and KK Griendling (1998). "Oscillatory and steady laminar shear stress differentially affect human endothelial redox state: role of a superoxide-producing NADH oxidase." Circ Res **82**(10): 1094-101.

Dioum, EM, R Chen, MS Alexander, Q Zhang, RT Hogg, RD Gerard, et al. (2009). "Regulation of hypoxia-inducible factor 2alpha signaling by the stress-responsive deacetylase sirtuin 1." Science **324**(5932): 1289-93.

Fisslthaler, B and I Fleming (2009). "Activation and signaling by the AMP-activated protein kinase in endothelial cells." Circ Res **105**(2): 114-27.

Foller, M, M Sopjani, S Koka, S Gu, H Mahmud, K Wang, et al. (2009). "Regulation of erythrocyte survival by AMP-activated protein kinase." FASEB J **23**(4): 1072-80.

Foretz, M, N Ancellin, F Andreelli, Y Saintillan, P Grondin, A Kahn, et al. (2005). "Short-term overexpression of a constitutively active form of AMP-activated protein kinase in the liver leads to mild hypoglycemia and fatty liver." Diabetes **54**(5): 1331-9.

Fulco, M, Y Cen, P Zhao, EP Hoffman, MW McBurney, AA Sauve, et al. (2008). "Glucose restriction inhibits skeletal myoblast differentiation by activating SIRT1 through AMPK-mediated regulation of Nampt." Dev Cell **14**(5): 661-73.

Guo, D, S Chien and JY Shyy (2007). "Regulation of endothelial cell cycle by laminar versus oscillatory flow: distinct modes of interactions of AMP-activated protein kinase and Akt pathways." Circ Res **100**(4): 564-71.

Ha, HC and SH Snyder (1999). "Poly(ADP-ribose) polymerase is a mediator of necrotic cell death by ATP depletion." Proc Natl Acad Sci U S A **96**(24): 13978-82.

Hock, MB and A Kralli (2009). "Transcriptional control of mitochondrial biogenesis and function." Annu Rev Physiol **71**: 177-203.

Hou, X, S Xu, KA Maitland-Toolan, K Sato, B Jiang, Y Ido, et al. (2008). "SIRT1 regulates hepatocyte lipid metabolism through activating AMP-activated protein kinase." J Biol Chem **283**(29): 20015-26.

Hwang, J, MH Ing, A Salazar, B Lassegue, K Griendling, M Navab, et al. (2003). "Pulsatile versus oscillatory shear stress regulates NADPH oxidase subunit expression: implication for native LDL oxidation." Circ Res **93**(12): 1225-32.

Hwang, J, A Saha, YC Boo, GP Sorescu, JS McNally, SM Holland, et al. (2003). "Oscillatory shear stress stimulates endothelial production of O2- from p47phox-dependent NAD(P)H oxidases, leading to monocyte adhesion." J Biol Chem **278**(47): 47291-8.

Imai, S, CM Armstrong, M Kaeberlein and L Guarente (2000). "Transcriptional silencing and longevity protein Sir2 is an NAD-dependent histone deacetylase." Nature **403**(6771): 795-800.

Jacobson, EL and MK Jacobson (1976). "Pyridine nucleotide levels as a function of growth in normal and transformed 3T3 cells." Arch Biochem Biophys **175**(2): 627-34.

Lagouge, M, C Argmann, Z Gerhart-Hines, H Meziane, C Lerin, F Daussin, et al. (2006). "Resveratrol improves mitochondrial function and protects against metabolic disease by activating SIRT1 and PGC-1alpha." Cell **127**(6): 1109-22.

Langley, E, M Pearson, M Faretta, UM Bauer, RA Frye, S Minucci, et al. (2002). "Human SIR2 deacetylates p53 and antagonizes PML/p53-induced cellular senescence." EMBO J **21**(10): 2383-96.

Li, X, S Zhang, G Blander, JG Tse, M Krieger and L Guarente (2007). "SIRT1 deacetylates and positively regulates the nuclear receptor LXR." Mol Cell **28**(1): 91-106.

Lin, K, PP Hsu, BP Chen, S Yuan, S Usami, JY Shyy, et al. (2000). "Molecular mechanism of endothelial growth arrest by laminar shear stress." Proc Natl Acad Sci U S A **97**(17): 9385-9.

Lin, SJ, PA Defossez and L Guarente (2000). "Requirement of NAD and SIR2 for life-span extension by calorie restriction in Saccharomyces cerevisiae." Science **289**(5487): 2126-8.

Lin, SJ, E Ford, M Haigis, G Liszt and L Guarente (2004). "Calorie restriction extends yeast life span by lowering the level of NADH." Genes Dev **18**(1): 12-6.

Liu, Y, Y Zhu, F Rannou, TS Lee, K Formentin, L Zeng, et al. (2004). "Laminar flow activates peroxisome proliferator-activated receptor-gamma in vascular endothelial cells." Circulation **110**(9): 1128-33.

Luo, J, AY Nikolaev, S Imai, D Chen, F Su, A Shiloh, et al. (2001). "Negative control of p53 by Sir2alpha promotes cell survival under stress." Cell **107**(2): 137-48.

Mattagajasingh, I, CS Kim, A Naqvi, T Yamamori, TA Hoffman, SB Jung, et al. (2007). "SIRT1 promotes endothelium-dependent vascular relaxation by activating endothelial nitric oxide synthase." Proc Natl Acad Sci U S A **104**(37): 14855-60.

Motta, MC, N Divecha, M Lemieux, C Kamel, D Chen, W Gu, et al. (2004). "Mammalian SIRT1 represses forkhead transcription factors." Cell **116**(4): 551-63.

Nasrin, N, VK Kaushik, E Fortier, D Wall, KJ Pearson, R de Cabo, et al. (2009). "JNK1 phosphorylates SIRT1 and promotes its enzymatic activity." PLoS One **4**(12): e8414.

Nemoto, S, MM Fergusson and T Finkel (2005). "SIRT1 functionally interacts with the metabolic regulator and transcriptional coactivator PGC-1{alpha}." J Biol Chem **280**(16): 16456-60.

Nisoli, E, C Tonello, A Cardile, V Cozzi, R Bracale, L Tedesco, et al. (2005). "Calorie restriction promotes mitochondrial biogenesis by inducing the expression of eNOS." Science **310**(5746): 314-7.

Orimo, M, T Minamino, H Miyauchi, K Tateno, S Okada, J Moriya, et al. (2009). "Protective role of SIRT1 in diabetic vascular dysfunction." Arterioscler Thromb Vasc Biol **29**(6): 889-94.

Ota, H, M Akishita, M Eto, K Iijima, M Kaneki and Y Ouchi (2007). "Sirt1 modulates premature senescence-like phenotype in human endothelial cells." J Mol Cell Cardiol **43**(5): 571-9.

Rodgers, JT, C Lerin, W Haas, SP Gygi, BM Spiegelman and P Puigserver (2005). "Nutrient control of glucose homeostasis through a complex of PGC-1alpha and SIRT1." Nature **434**(7029): 113-8.

Schulz, E, J Dopheide, S Schuhmacher, SR Thomas, K Chen, A Daiber, et al. (2008). "Suppression of the JNK pathway by induction of a metabolic stress response prevents vascular injury and dysfunction." Circulation **118**(13): 1347-57.

Sessa, WC (2004). "eNOS at a glance." J Cell Sci **117**(Pt 12): 2427-9.

St-Pierre, J, S Drori, M Uldry, JM Silvaggi, J Rhee, S Jager, et al. (2006). "Suppression of reactive oxygen species and neurodegeneration by the PGC-1 transcriptional coactivators." Cell **127**(2): 397-408.

Suo, J, DE Ferrara, D Sorescu, RE Guldberg, WR Taylor and DP Giddens (2007). "Hemodynamic shear stresses in mouse aortas: implications for atherogenesis." Arterioscler Thromb Vasc Biol **27**(2): 346-51.

Tontonoz, P and BM Spiegelman (2008). "Fat and beyond: the diverse biology of PPARgamma." Annu Rev Biochem **77**: 289-312.

Vaziri, H, SK Dessain, E Ng Eaton, SI Imai, RA Frye, TK Pandita, et al. (2001). "hSIR2(SIRT1) functions as an NAD-dependent p53 deacetylase." Cell **107**(2): 149-59.

Xia, S and J Laterra (2006). "Hepatocyte growth factor increases mitochondrial mass in glioblastoma cells." Biochem Biophys Res Commun **345**(4): 1358-64.

Yang, Y, H Hou, EM Haller, SV Nicosia and W Bai (2005). "Suppression of FOXO1 activity by FHL2 through SIRT1-mediated deacetylation." EMBO J **24**(5): 1021-32.

Young, A, W Wu, W Sun, HB Larman, N Wang, YS Li, et al. (2009). "Flow activation of AMP-activated protein kinase in vascular endothelium leads to Kruppel-like factor 2 expression." Arterioscler Thromb Vasc Biol **29**(11): 1902-8.

Zhang, Q, SY Wang, C Fleuriel, D Leprince, JV Rocheleau, DW Piston, et al. (2007). "Metabolic regulation of SIRT1 transcription via a HIC1:CtBP corepressor complex." Proc Natl Acad Sci U S A **104**(3): 829-33.

Zhang, QJ, Z Wang, HZ Chen, S Zhou, W Zheng, G Liu, et al. (2008). "Endothelium-specific overexpression of class III deacetylase SIRT1 decreases atherosclerosis in apolipoprotein E-deficient mice." Cardiovasc Res **80**(2): 191-9.

Zhang, Y, TS Lee, EM Kolb, K Sun, X Lu, FM Sladek, et al. (2006). "AMP-activated protein kinase is involved in endothelial NO synthase activation in response to shear stress." Arterioscler Thromb Vasc Biol **26**(6): 1281-7.

Fig. 3-1

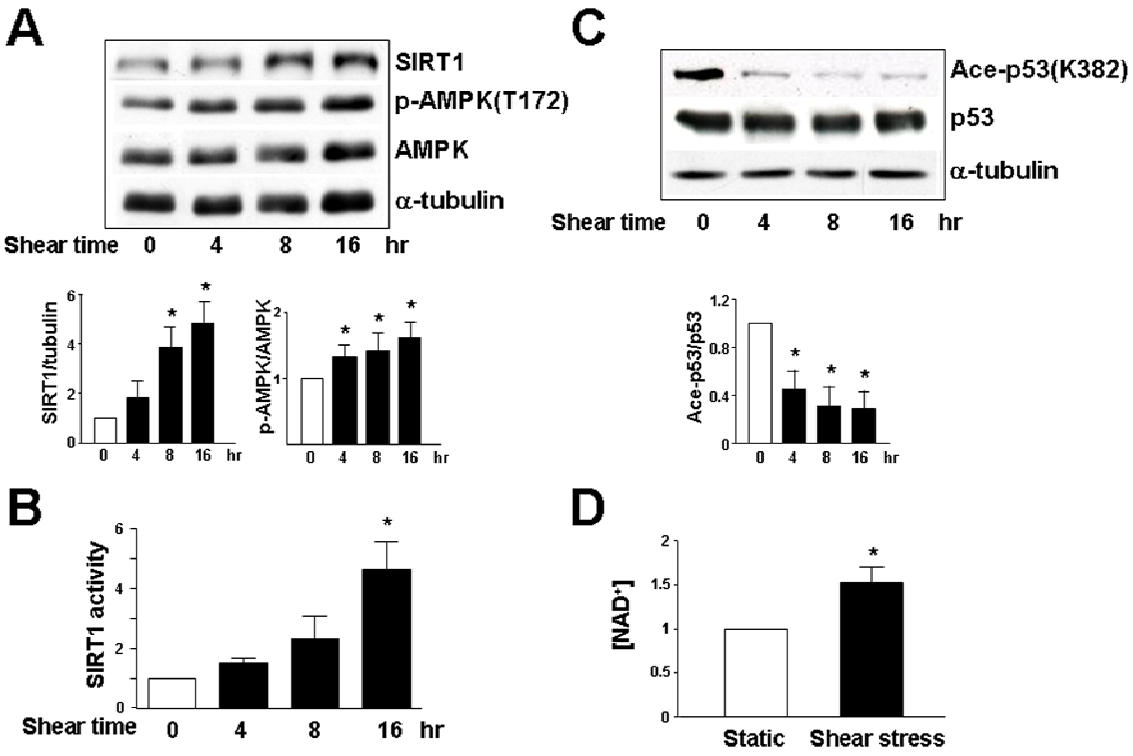

Fig. 3-1 Laminar shear stress increases SIRT1 level/activity in ECs. Confluent monolayers of HUVECs were subjected to laminar flow at 12 dyne/cm^2 for various times or kept as static controls represented as time 0. (A,C) Cell lysates were analyzed by Western blotting with anti-SIRT1, anti-phospho-AMPK (Thr-172; T172), anti-AMPK, anti-α-tubulin, anti-acetyl-p53 (Lys-382; K382), and anti-p53 antibodies. The bar graphs below are results of densitometry analyses of the ratios of SIRT1 to α-tubulin, phospho-AMPK to AMPK, and acetyl-p53 to p53. (B) SIRT1 deacetylase activity in HUVECs under shear stress or static conditions was assessed by using fluorogenic Arg-His-Lys-Lys (ac) as the substrate. The fluorescent intensities obtained from different groups were compared, with the value obtained at time 0 set as 1. (D) NAD^+ level in HUVECs under laminar flow or static condition for 16 hr was measured by spectrophotometry. The reading of the static group was set as 1. The bar graphs in all panels are mean±S.D. averaged from 3 independent experiments. **P*<0.05 vs. static control.

Fig. 3-2

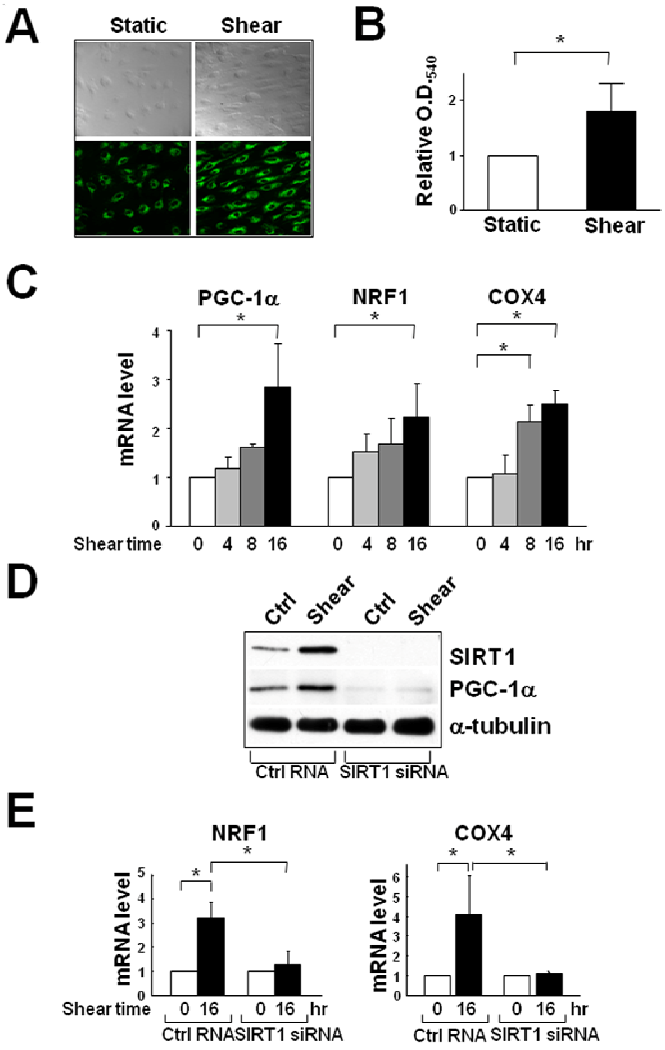

Fig. 3-2 Shear stress-increased mitochondrial biogenesis is mediated by SIRT1. Confluent monolayer of HUVECs were subjected to laminar flow for 16 hr or kept under static condition. (A) Mitotracker Green FM staining. (B) Quantification of mitochondrial reductase activity by MTT assay from absorbance at 540 nm. (C) Assay of levels of mRNA encoding PGC-1α, NRF1, and COX4 in HUVECs subjected to laminar flow for various durations by quantitative RT-PCR (qRT-PCR). (D, E) HUVECs were transfected with SIRT1 siRNA or control RNA (20 nM) and then exposed to laminar flow for 16 hr or were kept as static controls. SIRT1, PGC-1α, and α-tubulin levels were assessed by Western blot analysis in (D), and NRF1 and COX4 mRNA levels were analyzed by qRT-PCR in (E). Bar graphs are mean±S.D. from 3 independent experiments. *P<0.05 between indicated groups.

Fig. 3-3

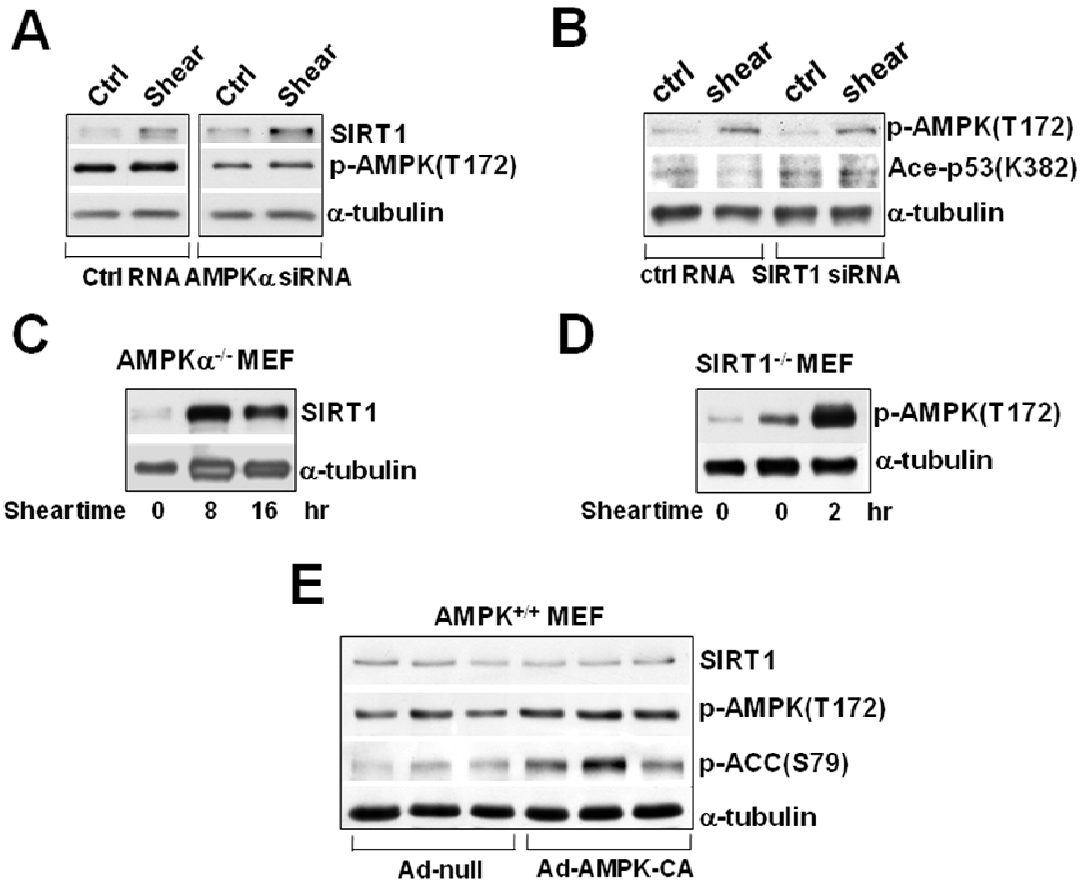

Fig. 3-3 Shear stress-increased SIRT1 is AMPK independent. (A,B) HUVECs were transfected with AMPK α1 and α2 siRNAs (10 nM each), SIRT1 siRNA (20 nM), or with control RNA (20 nM) before being subjected to laminar flow for 16 hr. (C,D) MEFs ablated with AMPKα or SIRT1 (i.e., AMPKα$^{-/-}$ and SIRT1$^{-/-}$) were subjectd to laminar flow, and cell extracts were collected at the indicated times. (E) Wild-type MEFs were infected with Ad-AMPK-CA (100 MOI) or Ad-null for 48 hr. Total cell proteins were then resolved by SDS-PAGE and subjected to Western blot analysis with various antibodies as indicated.

Fig. 3-4

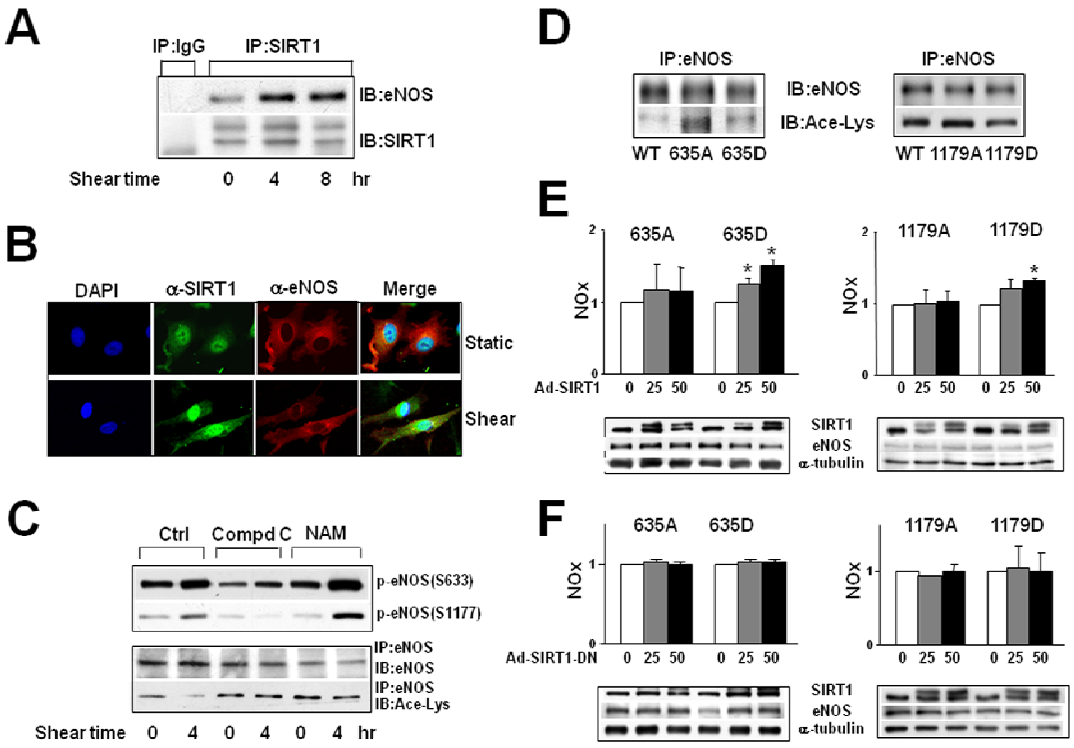

Fig. 3-4 Synergistic effects of AMPK and SIRT1 on eNOS. (A) HUVECs were exposed to laminar flow for the durations indicated or kept as static controls. SIRT1 was immunoprecipitated (IP) with anti-SIRT1, and immunoblotting (IB) was performed with anti-eNOS. In parallel, IgG was used as an IP control. The level of immunoprecipitated SIRT1 was also assessed by Western blot. (B) HUVECs under laminar flow or static condition for 4 hr were subjected to immunostaining with anti-SIRT1 and anti-eNOS, followed by conjugated secondary antibodies. The cell nuclei were counterstained with DAPI. The colocalization of SIRT1 and eNOS is demonstrated by the merging of pseudocolors. (C) HUVECs were pretreated with DMSO, Compound C (10 μM), or nicotinamide (NAM, 5 mM) for 30 min before being exposed to laminar flow for 4 hr. The phosphorylation of eNOS Ser-633 and Ser-1177 was probed in the input lysates. In addition, eNOS was immunoprecipitated from whole cell lysates and the acetylation of eNOS and total eNOS were assessed by immunoblotting with anti-Ace-Lys and anti-eNOS. (D-F) HEK293 cells were transfected with plasmids expressing bovine eNOS wild-type (WT), S635A, S635D, S1179A, or S1179D. In (D), eNOS was immunoprecipiated, and then examined by Western blot analysis with anti-eNOS and anti-Ace-Lys. In (E,F), transfected HEK293 cells were infected with Ad-(Flag)-SIRT1 or Ad-(Flag)-SIRT1-DN with various MOIs as indicated. Twenty-four hr post-infection, the NO bioavailability in the cells was determined by Griess assay and expressed as NOx. The expressions of SIRT1 and eNOS were examined by Western blot.

Fig. 3-5

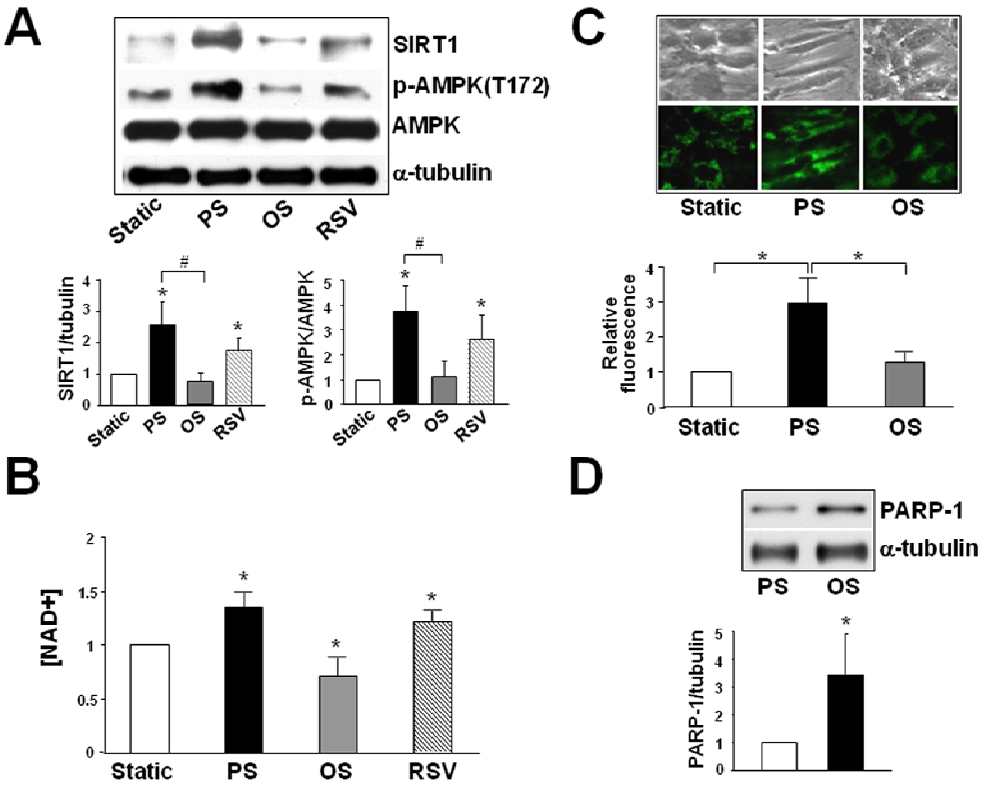

Fig. 3-5 SIRT1 is differentially regulated by pulsatile flow versus oscillatory flow. HUVECs were exposed to pulsatile flow (PS; 12±4 dyne/cm^2, 1 Hz) or oscillatory flow (OS; 1±4 dyne/cm^2, 1 Hz), treated with resveratrol (RSV; 100 μM), or kept under static condition for 16 hr. (A) The levels of SIRT1, phospho-AMPK (Thr-172), AMPK, and α-tubulin were assessed by Western blot analysis. * denotes P<0.05 compared to static control and # represents P<0.05 between PS and OS. (B) NAD^+ level was measured spectrophotometrically. * indicates P<0.05 compared to static control. (C) The mitochondria in static cells and those exposed to pulsatile or oscillatory flow were stained with Mitotracker Green FM. *P<0.05 between indicated groups. (D) PARP-1 expression in HUVECs exposed to pulsatile or oscillatory flow was revealed by Western blot analysis. * denotes P<0.05 compared to PS. Bar graphs represent densitometry analysis of 3 independent experiments, with the static group set as 1 in (A) (B) and (C). In (D), the level of PARP-1/α-tubulin in ECs exposed to pulsatile flow was set as 1.

Fig. 3-6

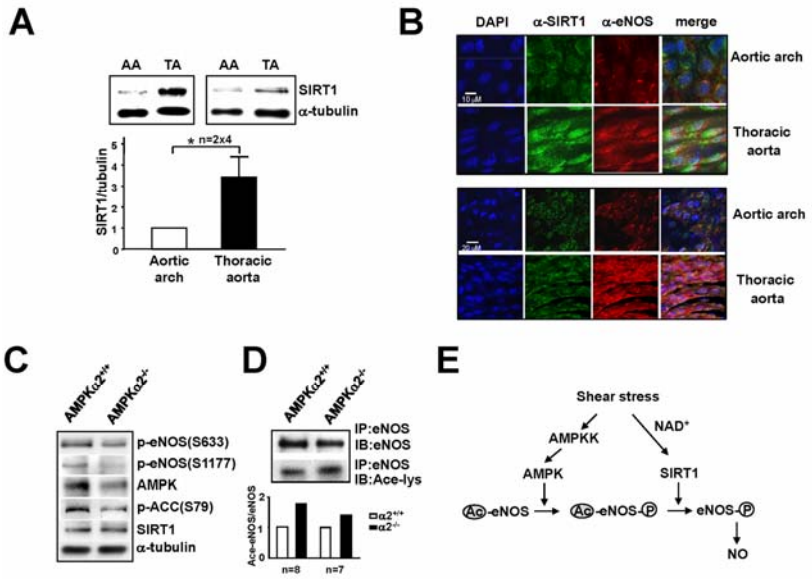

Fig. 3-6 Differential regulation of SIRT1/eNOS in the vessel wall *in vivo*. (A) Tissue extracts of the aortic arch (AA) and thoracic aorta (TA) from two C57BL6 male mice were pooled and subjected to Western blot analysis with anti-SIRT1 and α-tubulin antibodies. Data shown represent results from a total of 8 mice. (B) Confocal microscope images of *en face* immunostaining of SIRT1 and eNOS in the endothelium of the aortic arch and thoracic aorta of C57BL6 mice. The primary antibodies were anti-SIRT1 and anti-eNOS, and secondary antibodies were Alexa Fluor 488-conjugated chicken anti-rabbit or Alexa Fluor 555-conjugated chicken anti-mouse, respectively. Nuclei were counterstained with DAPI. Shown are representative images from 6 animals. (C, D) Tissue extracts were isolated from the thoracic aorta of AMPKα2$^{-/-}$ and their AMPKα2$^{+/+}$ littermates. In (C), the level of phospho-eNOS Ser-633, Ser-1177, AMPKα, phosphorylated ACC, SIRT1, and α-tubulin was determined by Western blot. In (D), eNOS was immunoprecipitated and the acetylation of eNOS in the immunoprecipitates was determined by immunoblotting with anti-Ace-Lys. After stripping, the blot was reprobed with anti-eNOS. The presented results on AMPKα2$^{-/-}$ and AMPKα2$^{+/+}$ mice were pooled from 8 aortas in each group. The experiments were repeated with another group of seven animals per mouse line. Bargraphs below are densitometry analysis of the ratios of acetyl-eNOS to eNOS from the two experiments. (E) A schematic model of the synergistic effects of AMPK and SIRT1 on eNOS activity. Laminar/pulsatile shear stress increases the NAD$^+$ level in ECs, thus leading to elevation of SIRT1. Concomitantly, AMPK is activated by upstream AMPK kinase (AMPKK), which in turn phosphorylates eNOS. The phosphorylated eNOS enhances its affinity toward SIRT1 so that eNOS is deacetylated. Such a synergism between AMPK and SIRT1 augments the eNOS-derived NO bioavailability.

Fig. 3-7

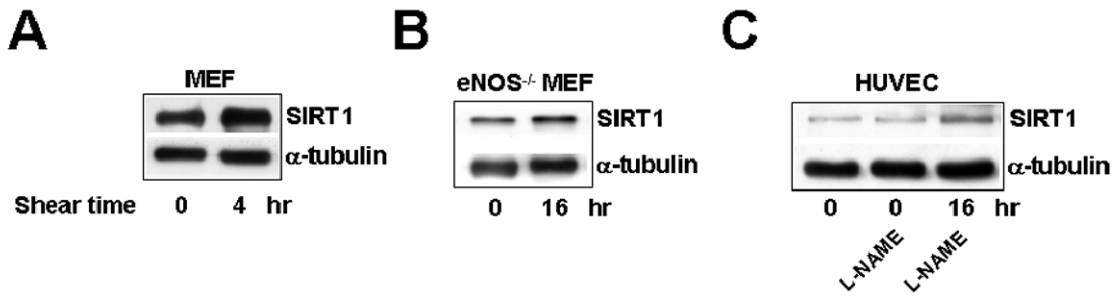

Fig. 3-7 Genetic ablation or pharmacological inhibition of eNOS does not inhibit shear stress-induced SIRT1. Confluent monolayer of the wild-type MEF (A) and $eNOS^{-/-}$MEF (B) were subjected to a laminar flow for the time as indicated or kept under static condition (time 0). In (C), HUVECs were treated with L-NAME (100 μM) 30 min prior to the exposure to the laminar flow for 16 hr. In parallel static controls, HUVECs were incubated with or without L-NAME. The collected lysates were analyzed by Western blot with anti-SIRT1 and anti-α-tubulin.

Chapter 4

Conclusions and Perspectives

4.1 Introduction

The study of the mechanisms by which physiological stimuli and pharmacological interventions modulate eNOS-derived NO by upstream kinases and deacetylases can facilitate our understanding of endothelial biology in health and disease. In this study, I explored the regulation of eNOS phosphorylation by AMPK and deacetylation by SIRT1 and the interplay between these two modifications. The major findings are as follows: (1) AMPK phosphorylates eNOS Ser-633 in ECs under various stimuli, thus leading to enhanced eNOS activity and NO bioavailability (as described in Chapter 2); (2) elevated SIRT1 by atheroprotective shear stress causes eNOS deacetylation; and (3) AMPK-mediated phosphorylation coordinates with SIRT1-modulated deacetylation of eNOS, through AMPK phosphorylation priming SIRT1 deacetylation. These findings suggest a model in which two metabolic regulators, AMPK and SIRT1, by converging on the target eNOS, play an essential role in endothelial biology. Noticeably, such synergistic effects were observed only under atheroprotective flow, such as laminar and pulsatile flow, but not under atherogenic oscillatory/disturbed flow. Therefore, the studies summarized in this dissertation also provide a novel explanation for the differential effects of flow patterns imposed on different regions of vasculature.

Table 4-1 Posttranlational modifications of eNOS

	Modification site	Modifying enzymes	Unmodifying enzymes	Stimulators of modification	Functions of modification	
phosphorylation	Ser-114	PKC (?)	PP2B	shear stress, HDL	?	
	Ser-495	PKC, AMPK (?)	PP1, PP2A, PP2B (?)	*shear stress, bradykinin, VEGF, H_2O_2 dephosphorylates it.	inhibition	
	Ser-615	Akt, PKA (?)		Bradykinin, ATP, VEGF, statins	?	
	Ser-633	AMPK, PKA		shear stress, VEGF, bradykinin, RSV, statins, ATP, 8-Br-cAMP, IBMX, etc.	activation (Ca^{2+}-dependent and independent)	
	Ser-1177	AMPK, PKA, Akt, PKG, CaMKII	PP2A	shear stress, VEGF, IGF-1, bradykinin, insulin, H_2O_2, estrogen, adiponectin, histamine, thrombin, ischemia, statins, RSV, ATP, 8-Br-cAMP, IBMX, etc.	activation (Ca^{2+}-dependet)	
	Tyr-83	Src	PTP	H_2O_2	activation	
deacetylation	Lys (494, 504?)	SIRT1	nonhistone lysine acetyltransferases (?)	CR, shear stress, RSV	Activation	
acylation	Gly-2 Myristoylation	N-myristoyl transferase (?)	thioesterases (?)		localization to Golgi complex	
	Cys-15, Cys-26 palmitoylation	palmitoyl acyl transferase (?)	thioesterases (?)		localization to caveolae and lipid rafts	

Abbreviations: PKC-protein kinase C, PKG-protein kinase G, CaMKII, calmodulin-dependant protein kinase II, PP2B-protein phosphatase 2B (calcineurin), PP1-protein phosphatase 1, PP2A-protein phosphoatase 2A, PTP-protein tyrosine phosphatase. VEGF-vascular endothelial growth factor. RSV-resveratrol, 8-Br-cAMP, 8-bromoadenosine-3',5'-cyclic monophosphate, IBMX-isobutylamethalxanthine. CR-caloric restriction. Adapted from Mount et al. 2007.

4.2 The role of AMPK and other protein kinases in eNOS phosphorylation

As summarized in Table 4-1, a number of protein kinases are involved in the eNOS phosphorylation at multiple sites and exert differential effects on the eNOS activity. AMPK, PKA, Akt, PKG, and CaMKII have all been implicated in phosphorylating Ser-633 and/or Ser-1177 (Fulton et al. 1999; Butt et al. 2000; Fleming et al. 2001; Boo et al. 2002; Boo et al. 2002). In addition to Ser/Thr residues, Tyr-83 of eNOS may also be phosphorylated by Src, thus resulting in eNOS activation (Fulton et al. 2005). PKA was suggested to be the major kinase that phosphorylates Ser-633 by shear stress or statins. The experimental evidence in these previous studies was that H89, a PKA inhibitor, abolished eNOS Ser-633 phosphorylation. Nevertheless, the pharmacological inhibitors always need to be thoroughly examined for effective concentrations, their inhibitory mechanisms, and off-target effects. For instance, a study evaluating the specificity of a panel of commonly used protein kinase inhibitors determined that when H89 was used at 10 μM, 80% of AMPK activity was also hindered (Davies et al. 2000). Indeed, when ECs were treated with H89 at this concentration, the phospho-ACC at Ser-79 was greatly ablated, which implies the non-specific inhibition of AMPK (Thors et al. 2004).

To address whether AMPK phosphorylates eNOS Ser-633, I used various approaches, including adenovirus-driven AMPKα-CA to overexpress the catalytic α subunit in ECs, siRNA against AMPKα to knock down AMPK expression, and MEFs with genetically ablated AMPKα. Furthermore, to verify that the AMPK phosphorylation of eNOS Ser-633 occurs *in vivo*, I used AMPKα2 knockout mice.

Collectively, these findings demonstrated that AMPK, rather than PKA, is the major kinase that phosphorylates eNOS Ser-633 responding to physiological (shear stress and adiponectin) and pharmacological stimuli (statins) (comment by Schulz et al, 2009).

The previously identified Ser-633 phosphorylation and the associated kinase mainly relied on the purified protein and a cell-free system. These simplified assays may introduce artifacts. For example, although PKG may phosphorylate eNOS at Ser-633 in a kinase reaction assay (Butt et al. 2000), this pathway does not seem to occur in ECs. LC/MS/MS was used for the first time to identify the phosphorylation of both Ser-1177 and Ser-633 in AICAR-treated ECs (Fig. 2-7, Chapter 2). I demonstrated that peptides containing these two phosphorylation sites could compete with ACC (Fig. 2-6, Chapter 2). This result indicates that peptide sequences flanking eNOS Ser-633, Ser-1177, and ACC Ser-79 share conformational similarity for phosphorylation by AMPK. Chapter 2 presents results of a comprehensive examination combining biochemistry, cellular biology, and an *in vivo* animal model of a functional phosphorylation pathway.

Despite ample evidence indicating that AMPK plays a major role in phosphorylating eNOS, the crosstalk between AMPK and Akt in activating eNOS in ECs remains to be investigated. Recent reviews suggest an independent and interdependent association of the two kinases in activating eNOS. Numerous stimuli, including shear stress and adiponectin, cause the activation of both AMPK and Akt in ECs (Ouchi et al. 2004; Guo et al. 2007). Study in our lab demonstrated that laminar shear stress caused a transient activation of both AMPK and Akt. Acting on distinct sites of mTOR, AMPK counteracts Akt to keep EC quiescent, which may prevent a dysfunctional endothelium

and the associated atherogenesis. In my study, the shear stress-induced eNOS Ser-633 phosphorylation was not affected with use of Akt-DN (Fig. 2-8, Chapter 2). In the aortas of AMPK$\alpha 2^{-/-}$ mice, the levels of both AMPK and eNOS phosphorylation were significantly lower than those in wild-type controls. However, Akt activity appears to be similar in the aortas of AMPK$\alpha 2^{-/-}$ and wild-type mice (Fig. 2-4, Chapter 2). These observations indicate that Akt seems not to be a major kinase in regulating eNOS phosphorylation of Ser-633 and its resulting NO production.

Another important issue involved in the elucidation of AMPK phosphorylation of eNOS is to delineate the role of the two isoforms of AMPKα subunit. The two α isoforms ($\alpha 1$ and $\alpha 2$) are differentially expressed in different tissues. AMPK$\alpha 2$ is predominant in adipose tissue and skeletal muscle, whereas AMPK$\alpha 1$ is the major isoform expressed in cardiomyocytes. AMPK$\alpha 1$ has been reported to be exclusively cytosolic, whereas the activated AMPK$\alpha 2$ can translocate into the nucleus, presumably to regulate gene expression. The expression of AMPKα subunit was found to be highly variable in HUVECs from different donors. Thus, whether AMPK$\alpha 1$ or AMPK$\alpha 2$ is the major form in endothelium and their functional role need further research (Fisslthaler and Fleming 2009).

As discussed earlier, many previous studies used pharmacological activators or inhibitors. Dissecting the effects attributable to individual AMPKα isoforms from results with these approaches is difficult. By using siRNAs specifically targeting $\alpha 1$ or $\alpha 2$, we showed that $\alpha 2$ seems to be the major form that mediates eNOS Ser-633 phosphorylation

in ECs (Fig. 2-3, Chapter 2), which justifies the use of AMPK$\alpha 2^{-/-}$ mice in the *in vivo* studies. Indeed, when AMPKα2 was genetically ablated, eNOS Ser-633 phosphorylation in the aortas was lower in statin-administered mice, whereas eNOS acetylation was higher, which confirms the indispensable role of AMPKα2 in eNOS modulation *in vivo*. Further research may involve pathways specifically activating α1 versus α2 and consequences of the activation of each of the isoforms in the vasculature. Knowledge obtained from these future studies may provide information on targeting a specific AMPK α isoform in therapeutic intervention of cardiovascular diseases.

4.3 Post-translational modifications of eNOS, an intricate but coordinated network

eNOS, a key player in NO bioavailability and endothelial homeostasis, is now known to be regulated by a network of post-translational modifications. These modifications include protein–protein interaction, (de)phosphorylation, (de)acetylation, and acylation (See Table 4-1 for summary). When inactivated, eNOS binds to caveolin-1 (Cav-1) in caveolae, the lipid raft in the EC membrane. When ECs are exposed to stimulation such as shear stress and VEGF, heat shock protein 90 (Hsp90) becomes associated with eNOS, which facilitates the binding of CaM to enhance the eNOS activity. Phosphorylation/dephosphorylation also plays an important role in eNOS activation, as evidenced by previous studies and results from research included in this dissertation. For example, by using eNOS Ser-633 loss-of-function mutants, I showed that the stimulation of eNOS by AICAR was abolished (Fig. 2-5, Chapter 2), which indicates the essentiality of Ser-633 phosphorylation for eNOS activation. Moreover, as

shown in Chapter 3 (Fig. 3-4), eNOS deacetylation by SIRT1 seems also crucial for eNOS activation.

Despite the knowledge of the diverse mechanisms by which eNOS is modified, questions remain on how these multiple modifications are integrated with protein–protein interactions and the subcellular localization of eNOS. One question is whether eNOS is first phosphorylated at the stimulatory sites (i.e., Ser-1177 and/or Ser-633), then dissociates from Cav-1 or needs to be exported to the cytosol and interact with Hsp90 before it can be phosphorylated/dephosphorylated at respective sites for activation. With either scenario, eNOS may be regulated differently in distinct subcellular locations, namely, caveolae, the Golgi complex, or cytoplasm. Answering these questions must consider acylation of eNOS, which is closely associated with the subcellular targeting of this protein. In fact, eNOS can also be myristoylated at Gly-2 (Pollock et al. 1992) and palmitoylated at Cys-15 and Cys-26 (Michel et al. 1993; Robinson and Michel 1995). The study by Boo et al. provided a clue that the cytosolic eNOS mutant did not respond to cAMP, which indicates that membrane association may be required for eNOS activation (Boo et al. 2006). Seemingly controversial, Erwin et al. found that the acylation-deficient eNOS mutant does not undergo *S*-nitrosylation, an inhibitory modification for eNOS activation (Erwin et al. 2005). These findings shed light on an emerging paradigm of eNOS activation hierarchy, which warrants further study.

eNOS Ser-633 and Ser-1177 phosphorylation occurs within minutes after the application of laminar shear stress (Fig. 2-1, Chapter 2), but eNOS deacetylation (Fig. 3-4, Chapter 3) is a much later event and takes hours to occur. Thus, the deacetylation by

SIRT1 is expected to occur after eNOS is transported into cytoplasm. This event would be consistent with the time-dependent activation of AMPK and SIRT1 (AMPK phosphorylation was increased within minutes and SIRT1 within hours). In the context of the temporal response to the applied shear stress, the immediate activation of AMPK leads to eNOS phosphorylation, which subsequently primes eNOS for deacetylation by SIRT1. This notion was supported by the following results: (1) AMPK inhibitor blocked eNOS phosphorylation, as well as deacetylation, in response to laminar shear stress, whereas the SIRT1 inhibitor attenuated only eNOS deacetylation (Fig. 3-4C); (2) as compared with wild-type eNOS, S633/1177A mutants displayed a higher acetylation status, which could not be further enhanced by SIRT1 overexpression to produce NO; and (3) eNOS S633/1177D mutants demonstrated a higher NO productivity with co-expression of SIRT1 (Fig. 3-4D,E). Such a synergistic action can be further examined by using the specific mutants mimicking constitutive deacetylation and acetylation forms of eNOS (e.g., Lys/Arg and Lys/Gln mutations). Presumably, these mutants would not affect the phosphorylation status of Ser-633/1177. However, a feedback loop may exist in the phosphorylation-deacetylation cycle. As seen in Fig. 3-4C, Chapter 3, NAM, the SIRT1 inhibitor, seems to cause a hyperphosphorylation of eNOS at Ser-633 and Ser-1177. Such a sustained and high level of phosphorylation may impair the re-sensitization of eNOS that is required for the subsequent activation. If true, phosphorylation and deacetylation may reciprocally regulate each other. Phosphorylation primes deacetylation for the maximal eNOS activity, but deacetylation may be necessary for eNOS dephosphorylation by phosphatases, which initiates a new setpoint for eNOS activation.

To further elucidate the functional consequences of eNOS deacetylation, one must inevitably identify the specific (de)acetylation sites responding to various stimuli. Although Lys-494 and Lys-504 are the two putative sites proposed to be targeted by SIRT1 (Mattagajasingh et al. 2007), further research is needed to identify the acetylation/deacetylation sites in cells or *in vivo*. Fig. 4-1 illustrates the possible eNOS modifications in its inactive and active forms.

LC/MS/MS, used in studies in Chapter 2 to identify eNOS Ser-633 phosphorylation in ECs, would be a useful approach for identification of eNOS (de)acetylation sites. With the information obtained from eNOS (de)acetylation mapping, the site-specific modification, their functional relevance, and their interrelation with phosphorylation can then be explored comprehensively.

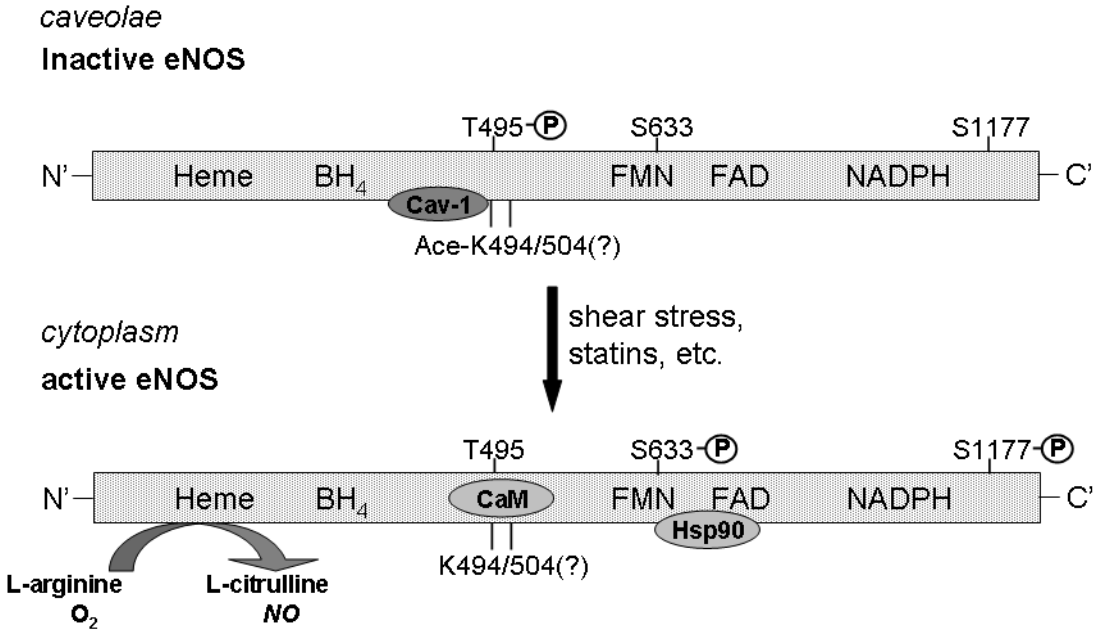

Fig. 4-1 Proposed scheme of multiple modifications on inactive and active eNOS. When inactive, Cav-1 is bound to eNOS, which is phosphorylated at Thr-495, dephosphorylated at Ser-633 and Ser-1177, and acetylated at putative lysine sites. This form would be present in caveolae. In the cytoplasm, the active form is associated with Hsp90, dephosphorylated at Thr-495, phosphorylated at Ser-633 and Ser-1177, and the putative lysine residues are deacetylated. Such modified status renders eNOS active in generating NO.

4.4 The regulating network of AMPK, SIRT1, eNOS and NO

AMPK and SIRT1 respond to cellular energy status by sensing the ratios of AMP/ATP and NAD^+/NADH, respectively. Through these regulations, AMPK and SIRT1 play key roles in maintaining cellular energy homeostasis, cell cycle progression/arrest, and anti-/pro-aging processes. Despite the restricted tissue expression, eNOS is essential in cardiovascular functions and facilitates the transport of oxygen and nutrient to various tissues/organs via circulation. Mounting evidence demonstrates a

complex network in which AMPK, SIRT1, and eNOS are interrelated in different ways to respond to different physiological and pathophysiological cues.

In metabolic-active tissues such as skeletal muscles, AMPK regulates SIRT1 activity by controlling nicotinamide phosphoribosyltransferase, the rate-liming enzyme of the NAD^+-salvage pathways (Fulco et al. 2008; Canto et al. 2009; Canto et al. 2010). This pathway not only activates SIRT1 but also accounts for the NAD^+ utilization in the cell. This finding supports the notion that AMPK may be upstream of SIRT1. However, this scenario seems to be reversed in the rat liver following starvation, where activated SIRT1 was shown to deacetylate LKB1 and hence activate AMPK (Lan et al. 2008). Considering that AMPK and SIRT1 have a common role functioning as "energy gauges," it is not surprising that they cross-talk with each other. Interestingly, eNOS has also been shown to act upstream of AMPK and/or SIRT1. For example, the shear stress-induced activation of AMPK was markedly attenuated in ECs from $eNOS^{-/-}$ mice, and the bradykinin-activated AMPK level was reported to be significantly lower in the aortas of eNOS-deficient mice than in those of the wild type (Fisslthaler et al. 2007; Zhang et al. 2008; Canto et al. 2009). Hence, NO has been proposed to act as an endogenous activator of AMPK (Zhang et al. 2008). Moreover, the eNOS-derived NO may enhance the expression of SIRT1 mRNA and protein by an as yet unidentified mechanism (Ota et al. 2008). Indeed, Nisoli et al. (2005) addressed the requirement of eNOS-derived NO in CR-induced SIRT1 and mitochondrial biogenesis in white adipose tissue by using $eNOS^{-/-}$ mice (Nisoli et al. 2005).

Data presented in Chapter 3 show that AMPK and SIRT1 appear to be activated independently, but they can synergistically activate eNOS, which in turn enhances NO bioavailability, particularly by atheroprotective flow. I used L-NAME, wild-type MEFs (little eNOS expression), or $eNOS^{-/-}$ MEFs and observed no obvious change in basal level of SIRT1 nor change in level induced by shear stress (Fig. 3-3 and 3-7, Chapter 3), which suggests that eNOS is not upstream of SIRT1 in ECs under shear stress. To strengthen this finding, more approaches should be used in future studies, including the use of siRNA against eNOS to evaluate the consequent AMPK and SIRT1 activation/induction. Similar experiments can be performed with the use of $eNOS^{-/-}$ mice. If AMPK and SIRT1 are upstream of eNOS in ECs, we would anticipate a similar level of AMPK phosphorylation and SIRT1 expression in the aortas from $eNOS^{-/-}$ and the wild-type mice. Meanwhile, we are creating the EC-specific SIRT1-KO mice to investigate eNOS acetylation and activity and endothelium-dependent vasodilation. Supposedly, we would observe a higher acetylation status and lower activity and an attenuated endothelium-dependent vasodilation in both basal and treated (e.g., statins) conditions in SIRT1-KO aortas.

4.5 Conclusions: the pleotropic effects of shear stress, CR, statins and resveratrol

The stimuli shear stress, CR, statins, and RSV all have generated interest because of their effects in anti-oxidative stress, anti-aging, anti-atherosclerosis, and cholesterol lowering, for example. Mechanistically, these beneficial effects may be attributed to AMPK and SIRT1. Under restricted nutrient or energy deficiency, such as in CR and exercise, the activity of AMPK and SIRT1 is increased, and the two coordinately regulate

a number of common targets, such as PGC1α, to promote mitochondrial biogenesis. In this dissertation, I demonstrated that AMPK and SIRT1 may synergistically activate eNOS in ECs responding to shear stress. Since statins exert pleotropic effects via AMPK, we also examined whether these drugs alter SIRT1 in ECs. To our surprise, ECs treated with statins showed a time- and dose-dependent reduction of SIRT1 (Fig. 4-2). Despite the unknown mechanism of this negative effect, this observation may be consistent with one of the side effects of statins, causing myofiber apoptosis (Dirks and Jones 2006), possibly through p53. Hence, the synergistic effects of AMPK and SIRT1 on eNOS are not likely to be elicited by statins.

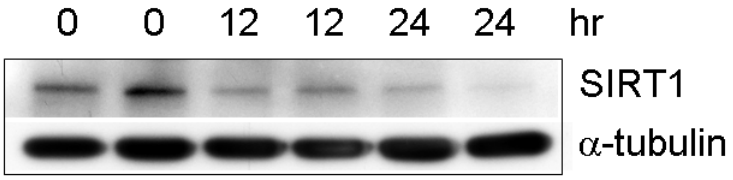

Fig. 4-2 The effect of atorvastatin in endothelial SIRT1. HUVECs were treated with atorvastatin (1 μM) for various times. The cell lysates were then collected and examined by SDS-PAGE and Western blotting for SIRT1. α-tubulin was detected as a loading control. (Courtesy of Dr. Wei Sun)

RSV, a polyphenol extracted from grapes and red wine, has rendered great promise in treating metabolic syndromes and lowering cardiovascular risks because of its putative effects on SIRT1 and AMPK. RSV activates AMPK and mediates mitochondrial protection against oxidative stress (Shin et al. 2009). As well, RSV was suggested to exert an anti-oxidative stress effect through activating SIRT1 (Csiszar et al. 2008). RSV-activated SIRT1 may account for the longevity effects in mammals (Baur et al. 2006). This study was initiated from using a fluo-de-lys SIRT1 substrate, a peptide

with a fluorophore tag modified from p53 Lys-379-382 to measure SIRT1 activity. The SIRT1 assay kit, based on the fluorescence emitted from this peptide, which "reflects the degree of deacetylation by SIRT1", was manufactured by BIOMOL International and became widely used in SIRT1-related studies. With the use of this assay, RSV was believed to be an SIRT1 direct activator (Howitz et al. 2003). Since then, a set of compounds with "1,000 times more potency than RSV" was developed, and their effects were demonstrated in improving whole-body glucose homeostasis and insulin sensitivity in adipose tissue, skeletal muscle, and the liver (Milne et al. 2007).

The basis of this assay kit was recently shown to be problematic, which challenges the effect of RSV in activating SIRT1 (Ledford 2010). In two studies, RSV was found to boost the SIRT1 activity only when the peptide substrate contained the fluorescent tag (Borra et al. 2005; Kaeberlein et al. 2005). More convincingly, using nuclear magnetic resonance, surface plasmon resonance and isothermal calorimetry techniques, Pacheloc et al. demonstrated that RSV interacts directly with the fluorophore of the fluo-de-lys SIRT1 substrate (Pacholec et al. 2010). This unexpected finding raises questions about all interpretations of RSV-activated SIRT1 and its effects. Nonetheless, in our study, we observed that RSV induced SIRT1 protein level (Fig. 3-5, Chapter 3), regardless of its pharmacological activating effect.

Although the same BIOMOL assay kit was used for SIRT1 activity in this study (Fig. 3-1, Chapter 3), only the components including the fluorophore-tagged substrate and the reaction buffer were used, without the addition of a small molecule, such as RSV. As clarified in Pacholec et al. (2010), without any addition of RSV or related compound,

the substrate does reflect SIRT1 activity in a SIRT1 dose-dependent manner. Therefore, the difference detected from the EC lysates subjected to shear stress or static conditions should be mostly, if not all, attributable to the single variable in this experiment (i.e. different times of shear stress application). Additionally, p53 Lys-382 acetylation in ECs was detected using Western blot analysis, and the shear stress-induced deacetylation of this site was attenuated when SIRT1 was knocked down in ECs (Fig. 3-1 and Fig. 3-3, Chapter 3). Therefore, the shear stress-enhanced SIRT1 activity and deacetylation of SIRT1 targets was reliable, even though the nature of the assay kit remains to be re-examined.-

Considering the key role of SIRT1 and AMPK in endothelial biology, a number of important questions remain to be answered. First, although the upstream kinases of AMPK have been identified, the upstream molecules that regulate SIRT1 in response to various stimuli are still unclear. Specifically, the mechanisms by which various flow patterns regulate SIRT1 expression and activity deserve further examination and may involve modifications at both translational and post-translational levels. Second, the interplay between AMPK phosphorylation and SIRT1 deacetylation on their common targets, including eNOS and PGC1α, need further study. Biochemical structure-based analysis would be valuable to reveal a mechanistic model of these synergistic actions, which may help to predict additional targets likely to be regulated in a similar fashion. Finally, more comprehensive study is necessary to understand other functional consequences of flow-enhanced SIRT1 and its co-regulation with AMPK. Such

investigation would explore the anti-oxidative stress, anti-inflammation, anti-aging, and anti-atherosclerotic effects of these pathways.

4.6 References

Boo, YC, J Hwang, M Sykes, BJ Michell, BE Kemp, H Lum, et al. (2002). "Shear stress stimulates phosphorylation of eNOS at Ser(635) by a protein kinase A-dependent mechanism." Am J Physiol Heart Circ Physiol **283**(5): H1819-28.

Boo, YC, HJ Kim, H Song, D Fulton, W Sessa and H Jo (2006). "Coordinated regulation of endothelial nitric oxide synthase activity by phosphorylation and subcellular localization." Free Radic Biol Med **41**(1): 144-53.

Boo, YC, G Sorescu, N Boyd, I Shiojima, K Walsh, J Du, et al. (2002). "Shear stress stimulates phosphorylation of endothelial nitric-oxide synthase at Ser1179 by Akt-independent mechanisms: role of protein kinase A." J Biol Chem **277**(5): 3388-96.

Butt, E, M Bernhardt, A Smolenski, P Kotsonis, LG Frohlich, A Sickmann, et al. (2000). "Endothelial nitric-oxide synthase (type III) is activated and becomes calcium independent upon phosphorylation by cyclic nucleotide-dependent protein kinases." J Biol Chem **275**(7): 5179-87.

Davies, SP, H Reddy, M Caivano and P Cohen (2000). "Specificity and mechanism of action of some commonly used protein kinase inhibitors." Biochem J **351**(Pt 1): 95-105.

Dirks, AJ and KM Jones (2006). "Statin-induced apoptosis and skeletal myopathy." Am J Physiol Cell Physiol **291**(6): C1208-12.

Fleming, I, B Fisslthaler, S Dimmeler, BE Kemp and R Busse (2001). "Phosphorylation of Thr(495) regulates Ca(2+)/calmodulin-dependent endothelial nitric oxide synthase activity." Circ Res **88**(11): E68-75.

Fulton, D, JE Church, L Ruan, C Li, SG Sood, BE Kemp, et al. (2005). "Src kinase activates endothelial nitric-oxide synthase by phosphorylating Tyr-83." J Biol Chem **280**(43): 35943-52.

Fulton, D, JP Gratton, TJ McCabe, J Fontana, Y Fujio, K Walsh, et al. (1999). "Regulation of endothelium-derived nitric oxide production by the protein kinase Akt." Nature **399**(6736): 597-601.

Lan, F, JM Cacicedo, N Ruderman and Y Ido (2008). "SIRT1 modulation of the acetylation status, cytosolic localization, and activity of LKB1. Possible role in AMP-activated protein kinase activation." J Biol Chem **283**(41): 27628-35.

Ledford, H (2010). "Ageing: Much ado about ageing." Nature **464**(7288): 480-1.

Mattagajasingh, I, CS Kim, A Naqvi, T Yamamori, TA Hoffman, SB Jung, et al. (2007). "SIRT1 promotes endothelium-dependent vascular relaxation by activating endothelial nitric oxide synthase." Proc Natl Acad Sci U S A **104**(37): 14855-60.

Mount, PF, BE Kemp and DA Power (2007). "Regulation of endothelial and myocardial NO synthesis by multi-site eNOS phosphorylation." J Mol Cell Cardiol **42**(2): 271-9.

Nisoli, E, C Tonello, A Cardile, V Cozzi, R Bracale, L Tedesco, et al. (2005). "Calorie restriction promotes mitochondrial biogenesis by inducing the expression of eNOS." Science **310**(5746): 314-7.

Pollock, JS, V Klinghofer, U Forstermann and F Murad (1992). "Endothelial nitric oxide synthase is myristylated." FEBS Lett **309**(3): 402-4.

Shin, SM, IJ Cho and SG Kim (2009). "Resveratrol protects mitochondria against oxidative stress through AMP-activated protein kinase-mediated glycogen synthase kinase-3beta inhibition downstream of poly(ADP-ribose)polymerase-LKB1 pathway." Mol Pharmacol **76**(4): 884-95.

Thors, B, H Halldorsson and G Thorgeirsson (2004). "Thrombin and histamine stimulate endothelial nitric-oxide synthase phosphorylation at Ser1177 via an AMPK mediated pathway independent of PI3K-Akt." FEBS Lett **573**(1-3): 175-80.